NPL Report MATC(A)101

October 2002

Microstructure and Toughness of Various Baseline and Wide Grained Hardmetals

B Roebuck and E G Bennett
Materials Centre
National Physical Laboratory
Teddington, Middlesex TW11 0LW, UK

ABSTRACT

Over twenty baseline hardmetals supplied by industry were characterised for their microstructure and mechanical properties. The measurements were used to validate methods for the measurement of WC grain size and mechanical properties of hardmetals. The mechanical properties included measurements of Palmqvist toughness. These tests were used to compare the toughness of a series of wide grained hardmetals with the baseline hardmetals.

© Crown copyright 2002
Reproduced by permission of the Controller, HMSO

ISSN 1473 2734

National Physical Laboratory
Teddington, Middlesex TW11 0LW, UK

Extracts from this report may be reproduced provided
that the source is acknowledged

Approved on behalf of Managing Director, NPL,
by Dr C Lea, Head, NPL Materials Centre

CONTENTS

1 INTRODUCTION **1**
1 1 WIDE GRAINED HARDMETALS 1

2 MATERIALS AND MEASUREMENT **1**
2.1 CPM MATERIALS 1
2.2 MEASUREMENTS 2
2.3 WIDE GRAINED HARDMETALS 2

3 RESULTS AND DISCUSSION **2**
3.1 CHEMICAL ANALYSES 2
3.2 DENSITY MEASUREMENTS 2
3.3 MAGNETIC MEASUREMENTS 3
3.4 STRUCTURE AND GRAIN SIZE MEASUREMENTS 3
3.5 MECHANICAL PROPERTIES 11
3.5.1 Abrasion Tests – Baseline Hardmetals 11
3.5.2 Abrasion Tests – Wide Grain Hardmetals 11
3.5.3 Hardness and Palmqvist Toughness Tests – Baseline Hardmetals 11
3.5.4 Comparison of hardness values 12
3.5.5 Toughness Tests – Wide Grained Hardmetals 12

4 SUMMARY **13**
4.1 BASELINE HARDMETALS 13
4.2 WIDE GRAINED HARDMETALS 13

5 REFERENCES **13**

6 ACKNOWLEDGEMENTS **14**

1 INTRODUCTION

New and improved hardmetals need to be benchmarked against conventional materials for basic mechanical properties such as hardness, wear resistance and toughness. Microstructures also need to be quantified and there are no standardised techniques for WC grain size measurement. For this reason the UK hardmetal industry, through the Research Group of the British Hardmetal Industry, has worked in partnership with the Materials Centre at NPL to characterise a range of conventional hardmetals for this baseline purpose. The UK DTI provided support for NPL for this activity through projects CPM5.4 and CPM5.5 in the Characterisation and Performance Materials Measurement and also through a Studio project in the CPM programme that included work on the toughness of wide grained hardmetals.

The materials for investigation were chosen to complement a number of hardmetals investigated previously [1]. They included a range of grain sizes and Co contents from 3-25 wt%. They also included materials with binder phases other than Co, i.e. Ni, Co/Ni and Fe/Co/Ni.

The structural characterisation exercise consisted of a measurement of WC grain size and size distribution. The property characterisation exercise consisted of a measurement of hardness, toughness (by the Palmqvist method) and abrasion resistance.

1 WIDE GRAINED HARDMETALS

In previous work [2] a series of hardmetals had been prepared with a WC grain size distribution that was wider than that in a conventional WC/Co hardmetal. Palmqvist toughness measurements were also made on this hardmetal and compared with baseline data. Because of the difficulty in precracking some of the lower hardness materials an alternative method of precracking the wide grained hardmetals, based on the use of a razor blade with diamond powder, was tried. The results of these toughness tests and comparison of the data with previous work on property models [1] is included in this report.

2 MATERIALS AND MEASUREMENT

2.1 CPM MATERIALS

Twenty-one hardmetals were supplied by industry. The codes and source details are given in Table 1 together with a chemical analysis. The chemical analyses were provided by Sandvik Hard Materials and H C Starck except for sample cwfnc20 (values given are nominal). Additional comments on individual sources are as follows:

Cerametal UK:

Sample cwn8 contains Ni and cwfnc20 sample contains a 20% binder as a mixture of Fe, Ni and Co (14/4/2).

Marshalls Hardmetals:

Sample macn9 contains a Co/Ni binder and significant amounts of Cr and V.

Sandvik HM:

Sample shmcn5 contains Co/Ni in the approximate ratio of 3/1 It also contains significant amounts of Cr and Mo. Sample shm3 contains some V.

Kennametal:

Sample x160 contains a significant amount of Cr.

2.2 MEASUREMENTS

Magnetic coercivity measurements were performed at Marshalls Hardmetals Ltd. Magnetic moment data (expressed as $\mu T\ m^3\ kg^{-1}$ of hardmetal) were obtained using the LDJ equipment at NPL.

Grain size measurements were made using the linear intercept method from scanning electron micrographs. Testpieces for Palmqvist toughness tests were polished and annealed at 800 °C for 1h in a vacuum. Tests were performed at applied loads of 30 and 100 kgf due to the difficulty in obtaining cracks on some of the materials at the lower loads. Abrasion tests were performed on testpieces that had been diamond ground at NPL. Al_2O_3 abrasives were used, following the ASTM B611 procedure.

2.3 WIDE GRAINED HARDMETALS

Nine hardmetals were selected from a large population previously described [2]. These were coded FH15C2, FH15D2, FD15B5, FD15B2, FD15C2, CD15D2, FD15K2, FD15M2 and FD15T2. In the code the final letter corresponds to the different organisations responsible for sintering and the second letter (D or H) corresponds to Dymet or Hydra where the samples were presintered.

Palmqvist tests were conducted at HV30 as described above. In addition a razor blade method [3] of notching rectangular beams (40 × 2 × 5 mm) was tried. However, it proved difficult to reliably cut notches with radii less than 10 μm with the current test rig and only two samples were successfully notched. Success was judged by the notch radius measured on the side face of the testpiece. This was considered to be satisfactory if less than 10 μm.

3 RESULTS AND DISCUSSION

3.1 CHEMICAL ANALYSES

The results of chemical analyses are given in Table 1

3.2 DENSITY MEASUREMENTS

The density values are plotted in Fig 1 for each group of materials and compared with previous data [1]. Theoretical bounds are shown for hardmetals manufactured from pure WC (with assumed densities of either 15.55, 15.65 or 15.75 $Mg\ m^{-3}$) and pure Co (density of 8.9 $Mg\ m^{-3}$).

3.3 MAGNETIC MEASUREMENTS

The results of magnetic moment and coercivity measurements are given in Table 1 and Figs 2-3 and compared with previous data. The scatter in Fig 3 is probably caused by the variation in WC grain size at any given Co content.

The chemical analyses, density and magnetic measurements can be used to estimate the approximate carbon content of the materials, i.e. the position within the two-phase field.

3.4 STRUCTURE AND GRAIN SIZE MEASUREMENTS

SEM and optical micrographs of the materials are shown in Figs 4-45. The optical micrographs are at x1000 and x1600. All the materials were nominally two-phase except for sample h10. This material contained significant amounts of graphite. Sample ma6 also contained traces of graphite.

Figs 46-48 show plots of the number distributions of the intercept data. Fig 46 is for all the materials. Figures 47-48 are for groups of materials to allow the individual data to be seen more clearly. There is a very wide range of grain sizes in the materials from sample shm9 with an arithmetic mean linear intercept (amli) of about 0.15 μm to uc9 with an amli of about 5 μm.

The results of the grain size measurements are given in Table 2. This table includes the number of intercepts measured to obtain the arithmetic mean linear intercept. It also includes columns for the inverse of the mean linear intercept and the inverse of the square root of the mean linear intercept as these parameters are used for analysing the data and developing property maps.

Figures 49-51 show plots of the size distributions of the intercept data where size probability was calculated from squaring the intercepts to give estimated values of area [4]. Figure 49 is for all the materials. Figures 50-51 are for groups of materials to allow individual data to be seen more clearly. It can be seen that sample k801 in particular has a very wide grain size distribution. In addition some of the other materials had size distributions that were significantly different to those of the majority, e.g. cwn8, d10 and ma6. Measurements of the WC size distribution of the very wide grained hardmetal, k801, were compared with size distribution data from material F15 (a previously manufactured wide grained material [2]) in Fig 52. The plot shows that k801 had the widest size distribution of any hardmetal yet investigated.

Table 1
CPM 5.4/5.5 MATERIALS INVENTORY and PROPERTIES

Material Code	Source	Number		Nominal binder content (Co, wt%)	Density Mg m^{-3}	Hardness, HV30
		Wear 40x20x5 mm	Bend 40x5x2 mm		Source	Source
cw3	CW Carbides	10	60	3	15.30	1950
cwn8	CW Carbides	6	20**	8++		1320
cwfnc20	CW Carbides	-	40**	20+++		1264***
ma6	Marshalls	7	72	6	14.96	1448
ma11	Marshalls	7	72	11	14.41	912
ma14	Marshalls	7	72	14	14.23	1165
macn9	Marshalls	8	60	9++	14.36	1661
n15	Neepsend	10	52	15		
t25	Teco	10	70	25	13.31	83.5-84.5+
h10	Hoybide	11	71	10	14.51	1535
shm3	Sandvik HM	10	80	3.3		2000
shmcn5	Sandvik HM	10	35**	5.3++		1950
shm9	Sandvik HM	-	6*	9		2000
d10	Dymet	10	70	10		
uc9	Hydra	12	75	9	14.52	966-974
t	Hydra	12	75	9	14.6-14.68	1226-1274
b9	Boart			9		
x160	Kennametal	10	60	10		1549
k322	Kennametal	10	60	9.75		1374
k801	Kennametal	10	30**	6++		1022
k3520	Kennametal	10	60	20		846

* round testpieces, 3.25 mm diameter
** ETMT testpieces, 40×1×2 mm
*** HV10
\+ Rockwell hardness
++ Ni or Co-Ni alloy
+++ Fe, Ni, Co alloy

CPM 5.4/5.5 INVENTORY (Continued)

Material Code	Source	Coercivity				Magnetic moment μT m3 kg^{-1}		
		Marshalls		Source		NPL	NPL	Source
		Oersteds	kA m^{-1}	Oersteds	kA m^{-1}	40x20x5mm	40x5x2mm	
cw3	CW Carbides	353	28.1	350	27.8	-	0.42-0.45	
cwn8	CW Carbides	0	0	0	0	0.04	0.2	
cwfnc20	CW Carbides			170	13.5	-	2.93	-
ma6	Marshalls	158	12.6	155	12.3	0.87	0.87	
ma11	Marshalls	49	3.9	47	3.7	1.64	1.64	
ma14	Marshalls	112	8.9	113	9.0	1.88	1.98	
macn9	Marshalls	367	29.2	372^{+}	29.6^{+}	0.83	0.83-0.95	
n15	Neepsend	185	14.7			1.9-2.0	1.8-2.0	
t25	Teco	85	6.8	120-130	9.5-10.3	3.0	2.82	
h10	Hoybide	229	18.2	222		1.48	1.49	89%
shm3	Sandvik HM	402	32.0		33.5	0.45	0.45	
shmcn5	Sandvik HM	345	27.4		30.5	0.45	0.45	
shm9	Sandvik HM	491	39.1	503	40.0	-	1.13	75%
d10	Dymet	123	9.8			1.32-1.4	1.35	
uc9	Hydra	51	4.1	46-48	3.7	1.38-1.41	1.35	
t	Hydra	106	8.4	104-106	8.4	0.95-0.99	1.1	
b9	Boart	145	11.6			1.13	1.15-1.18	
x160	Kennametal	232	18.5				1.26	
k322	Kennametal	181	14.4				1.26	
k801	Kennametal	53.9	4.3				0.18	
k3520	Kennametal	64.1	5.1				2.88	

$^{+}$macn9 – 4×5×2 mm samples : 40×20×5 mm samples – 355 Oesteds/28.2 kA m^{-1}

CPM 5.4/5.5 INVENTORY (Continued)

Material code	Source	Composition, wt%								
		Co	Ni	Ta	Nb	Ti	Cr	V	Fe	Mo
cw3	CW Carbides	3.0	0.0	0.4	0.0	0.0	0.00	0.00	0.03	0
cwn8	CW Carbides	0.5	7.6	0.3	0.1	0.0	0.00	0.00	0.04	0
cwfnc20	CW Carbides	2.0	4.0	-	-	-	-	-	14.0	-
ma6	Marshalls	5.9	0.0	0.0	0.1	0.0	0.00	0.00	0.02	0
ma11	Marshalls	11.7	0.0	0.0	0.0	0.0	0.00	0.00	0.03	0
ma14	Marshalls	14.0	0.0	0.0	0.0	0.0	0.00	0.00	0.06	0
macn9	Marshalls	6.0	3.0	0.0	0.0	0.0	0.58	0.17	0.03	0
n15	Neepsend	14.5	0.0	0.0	0.0	0.0	0.00	0.00	0.00	0
t25	Teco	24.2	0.0	0.0	0.0	0.0	0.00	0.00	0.03	0
h10	Hoybide	10.1	0.0	0.2	0.1	0.0	0.21	0.00	0.07	0
shm3	Sandvik HM	3.3	0.0	0.0	0.0	0.0	0.00	0.12	0.04	0
shmcn5	Sandvik HM	3.3	1.1	0.0	0.0	0.0	0.50	0.00	0.05	0.09
shm9	Sandvik HM	9.0	-	-	-	-	0.39	0.24	-	-
d10	Dymet	10.0	0.0	0.0	0.0	0.0	0.00	0.00	0.00	0
uc9	Hydra	9.8	0.0	0.0	0.0	0.0	0.00	0.00	0.00	0
t	Hydra	9.1	0.0	0.0	0.0	0.0	0.00	0.00	0.11	0
b9	Boart	8.3	0.0	0.0	0.0	0.0	0.00	0.00	0.07	0
x160	Kennametal	10.0	< 0.1	< 0.05	< 0.01	-	0.54	-	0.10	-
k322	Kennametal	9.9	< 0.1	< 0.05	< 0.01	-	< 0.01	-	0.02	-
k801	Kennametal	0.4	5.5	0.06	< 0.01	-	< 0.01	-	0.06	-
k3520	Kennametal	20.3	< 0.1	0.1	0.06	-	< 0.01	-	0.16	-

Table 2 Grain Size

Material code	Arithmetic mean linear intercept μm	Inverse intercept μm^{-1}	Inverse square root intercept, $\mu m^{-0.5}$	Number of intercepts
shm9	0.15	6.67	2.58	287
macn9	0.23	4.35	2.09	254
shm3	0.31	3.23	1.80	288
shmcn5	0.37	2.70	1.64	264
cw3	0.4	2.50	1.58	290
h10	0.41	2.44	1.56	290
n15	0.49	2.04	1.43	266
cwfnc20	0.50	2.00	1.41	279
x160	0.64	1.56	1.25	178
k322	0.71	1.41	1.19	175
t25	0.77	1.30	1.14	264
b9	0.82	1.22	1.10	254
cwn8	0.85	1.18	1.08	259
ma14	0.91	1.10	1.05	268
ma6	1.03	0.97	0.98	287
d10	1.05	0.95	0.98	251
t	1.68	0.60	0.77	253
k3520	2.30	0.43	0.66	249
k801	2.70	0.37	0.61	248
uc9	4.97	0.20	0.45	289
ma11	5.16	0.19	0.44	267

Table 3
Abrasion Results

Material Code	Hardness HV30		Abrasion Resistance, vol loss cm^3			Density $Mg\ m^{-3}$	
	Source	NPL	1	2	mean	Source	NPL
cw3	1950	1918	0.010	0.011	0.011	15.30	15.26
cwn8	1320	1301	0.069	0.075	0.072	14.85	14.73
ma6	1448	1518	0.058	0.060	0.059	14.96	14.91
ma11	912	955	0.313	0.293	0.303	14.41	14.35
ma14	1165	1206	0.201	0.217	0.209	14.23	14.20
macn9	1661	1683	0.0173	0.0170	0.0171		14.33
n15		1248	0.200	0.192	0.196		14.11
t25	83.5-84.5*	980	0.487	0.489	0.488	13.31	13.28
h10	1535	1367	0.049	0.041	0.045	14.51	14.41
shm3	2000	2071	0.0047	0.0046	0.0047		15.32
shmcn5	1950	1953	0.0082	0.0081	0.0082		15.01
d10		1336	0.113	0.104	0.109		14.54
uc9	966-974	996					
t	1226-1274	1344	0.120	0.118	0.119		14.48
b9		1438	0.074	0.070	0.072		14.72
x160	1549	1626	0.035	0.035	0.035		14.41
k322	1374	1451	0.069	0.066	0.068		14.58
k801	1022	1063	0.481	0.523	0.502		14.92
k3520	846	883	0.412	-	0.412		13.50

* Rockwell Hardness

Table 4 Palmqvist Toughness – HV30

Material code	Diagonal µm	HV30	Total crack length µm	HV30 mean	Mean crack length µm	Mean K $MNm^{-3/2}$	Arithmetic mean linear intercept µm	Number of intercepts
macn9	182.4	1673	409.4					
	179.7	1722	424.9					
	183.4	1653	443.3	1683	426	9.5	0.23	254
shm3	163.1	2092	688.1					
	163.7	2075	703.1					
	164.9	2047	703.3	2071	698	8.2	0.31	288
shmcn5	168.7	1954	508.1					
	168.7	1956	514.0					
	168.9	1950	536.2	1953	519	9.2	0.37	264
cw3	171.0	1903	714.8					
	169.8	1929	713.2					
	170.1	1922	749.6	1918	726	7.7	0.4	290
h10	200.0	1391						
	201.8	1366						
	203.5	1344	shattered	1367			0.41	290
n15	209.7	1266	100.2					
	211.5	1243	74.8					
	212.2	1236	27.7	1248	68	20.5	0.49	266
t25	239.0	974						
	237.4	987						
	238.3	979	no cracks	980			0.77	264
b9	196.8	1437	248.5					
	196.7	1437	213.3					
	196.7	1438	203.1	1438	222	12.1	0.82	254
cwn8	205.9	1312	166.5					
	206.5	1305	174.9					
	208.0	1286	173.2	1301	172	13.1	0.85	259
ma14	213.4	1222	72.2					
	214.7	1207	73.8					
	216.4	1188	37.6	1206	61	21.1	0.91	268
ma6	191.9	1511	278.4					
	192.2	1506	316.7					
	190.2	1538	305.3	1518	300	10.7	1.03	287
d10	204.4	1332	183.1					
	203.2	1347	137.4					
	204.5	1330	172.0	1336	164	13.6	1.05	251
t	202.8	1353	131.2					
	204.8	1326	160.4					
	202.8	1353	109.8	1344	134	15.1	1.68	253
uc9	236.2	997						
	237.7	985						
	235.3	1005	no cracks	996			4.97	289
ma11	240.0	966						
	241.7	952						
	242.4	947	no cracks	955			5.16	267
x160	185.0	1625	249					
	184.5	1634	279					
	185.5	1617	258	1626	262	11.9	0.64	178
k322	195.0	1463	233					
	195.5	1456	237					
	197.0	1433	248	1451	239	11.7	0.71	175
k801	231.5	1038	no cracks					
	227.5	1075						
	227.5	1075		1063			2.70	248
k3520	252.0	876	no cracks					
	250.0	890						
	251.0	883		883			2.30	249

Table 5 Palmqvist Toughness – HV100

Material code	Diagonal µm	HV30	Total crack length µm	HV100 mean	Mean crack length µm	Mean K $MNm^{-3/2}$
macn9	332	1682	1530			
	325	1756	1166			
	326	1745	1189	1728	1295	10.0
shm3						
					0	
shmcn5	317	1845	1791			
	315	1869	1437			
	316	1857	1395	1857	1541	9.5
cw3						
cwfnc20	389	1225	343			
	387	1235	468			
	392	1204	362	1221	391	15.4
n15						
t25	439	962	0.0			
	438	967	75			
	440	958	70	962	48	38.8
b9	366	1384	1039			
	365	1392	1109			
	367	1377	904	1384	1017	10.1
cwn8						
ma14	399	1165	402			
	399	1165	362			
	400	1159	358	1163	374	15.3
ma6	347	1540	1082			
	347	1540	1166			
	347	1540	1061	1540	1103	10.3
d10						
t						
uc9	443	945	0.0			
	438	967	146			
	439	962	269	958	138	22.9
ma11	438	967	0.0			
	437	971	46			
	437	971	52	970	33	47.3
x160	341	1595	881			
	340	1609	834	1603		
	340	1604	867		861	11.9
k322	362	1415	815			
	364	1400	764			
	358	1443	800	1419	793	11.6
k801	422	1044	181			
	418	1064	0.0			
	426	1024	265	1044	223	18.8
k3520	461	874	38			
	455	898	106			
	456	892	60	888	102	25.6

3.5 MECHANICAL PROPERTIES

Abrasion Tests – Baseline Hardmetals

The results of the abrasion tests are given in Table 3. The abrasion resistance is expressed as volume loss in units of cm^3. Hardness and density measurements are also included in Table 3.

The abrasion results are plotted against hardness in Fig 53, compared with tests on hardmetals reported previously. It must be noted that the hardness values were those measured at NPL. It was observed that the NPL measurements of HV30 for the most part were slightly higher than the source data. Samples uc9, shm9 and cwfnc20 were not tested because of geometrical constraints on the sample size. It can be seen that the abrasion results for the CPM materials generally fall on the trend line for the baseline materials investigated previously except for two hardmetals, cwn8 and k801. Both these hardmetals had a wider grain size distribution than normal, especially k801, and both had nickel binder phases, yet one was better than the trend line and one was poorer with respect to abrasion resistance at a given value of hardness. The reason for this discrepancy is not known. The linear fit in Fig 53 is to all the data for HV30 > 1000 (NB: y axis is to a logarithmic base).

The abrasion data for the CPM materials are plotted as microstructure property maps, as abrasion plotted against inverse square root of the intercept, in Figs 54 and 55. In Fig 54 the CPM data show good agreement with previous work and the expressions developed for these property maps. In Fig 55 the data for the CPM materials with low binder phase content, alternative binders and wide grain size (k801) are shown superimposed on the derived property map expressions. Generally these materials have higher abrasion loss values than would be expected from the property maps.

Abrasion Tests – Wide Grain Hardmetals

Abrasion data from tests on two batches of wide grained material F13 (6wt% Co) and F15 (10wt% Co) are also plotted on the abrasion/grain size property map in Fig 56. This graph shows that for the Co bonded wide grained materials that abrasion loss is less than would be predicted by the arithmetic mean linear intercept.

Hardness and Palmqvist Toughness Tests – Baseline Hardmetals

Hardness and Palmqvist toughness test results are given in Tables 4 and 5. The results include data from tests at HV30 and HV100. The higher load was used because in some of the materials no cracks could be observed for the HV30 indents. The Palmqvist toughness data are plotted against hardness in Fig 57. Figure 57 shows a comparison with previous data on 6% and 10% Co baseline materials. For those materials that were tested at both HV30 and HV100 there is reasonable agreement in the Palmqvist toughness values for hardmetals with HV30 > 1200. One hardmetal, ma14, did not have such a good correlation, but still fell within the scatterband of previously tested baseline materials. One hardmetal, ×160, had a toughness value that was slightly higher than the trend line. This material had the most uniform grain size distribution.

An empirical fit was derived for the trend in Palmqvist toughness with hardness given by the following algebraic expression:

$$(T - p) = \frac{Q}{(H - r)} \qquad \text{for } 2000 > H > 850$$

where T and H are the Palmqvist toughness and Vickers Hardness respectively and the values for the coefficients p, Q and r were 3.35, 5247 and 806 respectively. Thus

$$T = (Q/(H-r)) + p$$
$$= (5247/(H-806)) + 3.35$$

The expression is plotted in Fig 58 together with data from the property map derived previously [1].

The Palmqvist toughness data are plotted in microstructure property maps in Figs 59 and 60. In Fig 59 toughness is plotted against WC intercept value. The agreement with previous data is not as good as the abrasion results plotted in Fig 54. This could be due to a variation in properties or uncertainty in the Palmqvist results, especially in the tougher materials. In Fig 60 toughness is plotted against WC intercept value for the CPM materials with low binder phase content, alternative binders and wide grain size (k801) compared with property models derived previously [1].

Comparison of hardness values

It was noted that there appeared to be a consistent trend of NPL HV30 values being higher, by about 40-50 HV30, than values reported from material sources. This is clearly demonstrated in Fig 61, where the NPL HV30 values for the CPM materials are plotted against source HV30 values. The reason for this difference is not known, although the NPL indentation diameters were measured at high magnification using an optical microscope. This method may give rise to a systematic difference in indentation diagonal. It should be noted that NPL HV30 values only are used for deriving the property maps.

Toughness Tests – Wide Grained Hardmetals

The results of the two successful razor blade notching experiments are shown in Fig 62, where the values obtained using this method are compared with those obtained using the Palmqvist technique. The agreement was good, indicating that the razor blade technique has potential if a reliable method for its application could be developed.

A property map showing abrasion results against Palmqvist toughness is shown in Fig 63 in which the F15 wide grained hardmetals investigated in the studio project are compared with baseline hardmetals (CPM and CAM projects) and the property models derived previously [1]. The graph indicates that the wide grained materials, as a group, are similar to the conventional materials in their combination of toughness and abrasion resistance.

4 SUMMARY

4. BASELINE HARDMETALS

Over 20 hardmetals have been characterised in work at NPL and through industrial contributions for:

• Composition	Industry
• WC grain size and distribution	NPL
Coercivity	Industry
Magnetic moment	NPL/Industry
Density	NPL/Industry
• Hardness	NPL/Industry
• Abrasion resistance (ASTM B611)	NPL
• Palmqvist toughness	NPL

The majority of the hardmetals were based on WC/Co but a few contained Ni or Co/Ni as a binder-phase. Analysis of the mechanical property data showed that for the standard hardmetals with > 6wt% Co binder phase the CPM data agreed very well with the property map expressions derived previously [1]. However, for the lower Co materials there was evidence of deviation from these trends and more work is needed to study this aspect of structure/property relations in hardmetals. It was noted that NPL HV30 values were systematically higher than source values.

The results of the measurements combined with data from previous work on 6 and 10% Co hardmetals form a baseline data set that can be used for reference, to evaluate new materials, or to benchmark current products for quality and consistency.

4.2 WIDE GRAINED HARDMETALS

Within the hardness and microstructure ranges examined it has been shown that hardmetals with a wider grain distribution than conventional materials have similar combinations of abrasion resistance and toughness. This contrasts with earlier work [2] which has indicated that the hardmetals with a wider grain size distribution have better abrasion resistance for the same hardness.

5 REFERENCES

1 B Roebuck, E G Bennett, W P Byrne and M G Gee. Characterisation of Baseline Hardmetals using Property Maps. NPL Report CMMT(A)172, April 1999.

B Roebuck and E G Bennett. Widely Distributed WC Grain Size in a 10% Co Hardmetal, NPL Report CMMT(D)150, September 1998.

3. J Kuebler. Fracture Toughness of Ceramics using the SEVNB Method: From a Preliminary Study to a Standard Test Method, Fracture Resistance Testing of Monolithic and Composite Brittle Materials, ASTM STP 1409, J A Salem, M G Jenkins and G D Quinn, eds., American Society for Testing and Materials, West Conshohocken, PA 2001.

4. B Roebuck. Measuring WC Grain Size Distribution, Metal Powder Report, April 1999, 20-24.

5. B Roebuck and M G Gee. Abrasion Resistance of Wide Grained WC/Co Hardmetals. EUROMET 2002, Oct 2002, Lausanne.

6 ACKNOWLEDGEMENTS

The work reported in this document on baseline materials was performed as part of the MTS Programme on Characterisation and Performance of Materials (CPM), a programme of underpinning research financed by the UK Department of Trade and Industry. The measurements of toughness of the wide grained hardmetals were supported within a Studio Project in the CPM programme. Members of the British Hardmetal Association Research Group are thanked for the supply of materials and the results of in-house characterisation tests for the baseline materials and for a financial contribution, as well as materials and in-kind support for the Studio Project. Colleagues Tom May, Andrew Gant and Mark Gee provided the abrasion data and comments on the results.

LIST OF CAPTIONS

Density measurements

Magnetic moment measurements

Coercivity measurements

Fig 4 SEM micrographs of cw3

Optical micrographs of cw3

SEM micrographs of cwn8

Optical micrographs of cwn8

SEM micrographs of cwfnc20

Optical micrographs of cwfnc20

Fig 10 SEM micrographs of ma6

Fig 1 Optical micrographs of ma6

Fig 12 SEM micrographs of ma11

Fig 13 Optical micrographs of ma11

Fig 14 SEM micrographs of ma14

Fig 15 Optical micrographs of ma14

Fig 16 SEM micrographs of macn9

Fig 17 Optical micrographs of macn9

Fig 18 SEM micrographs of n15

Fig 19 Optical micrographs of n15

Fig 20 SEM micrographs of t25

Fig 21 Optical micrographs of t25

Fig 22 SEM micrographs of h10

Fig 23 Optical micrographs of h10

Fig 24 SEM micrographs of shm3

Fig 25 Optical micrographs of shm3

Fig 26 SEM micrographs of shmcn5

Fig 27 Optical micrographs of shmcn5

Fig 28 SEM micrographs of shm9

Fig 29 Optical micrographs of shm9

Fig 30 SEM micrographs of d10

Fig 31 Optical micrographs of d10

Fig 32 SEM micrographs of uc9

Fig 33 Optical micrographs of uc9

Fig 34 SEM micrographs of t

Fig 35 Optical micrographs of t

Fig 36 SEM micrographs of b9

Fig 37 Optical micrographs of b9

Fig 38 SEM micrographs of x160

Fig 39 Optical micrographs of x160

Fig 40 SEM micrographs of k322

Fig 41 Optical micrographs of k322

Fig 42 SEM micrographs of k801

Fig 43 Optical micrographs of k801

Fig 44 SEM micrographs of k3520

Fig 45 Optical micrographs of k3520

Fig 46 Cumulative number distribution of intercept data for all the materials

Fig 47 Cumulative number distributions for shm9, shm3, shmcn5, n15, b9, ma6, cwn8, uc9, k322 and x160

Fig 48 Cumulative number distributions for macn9, cw3, h10, t25, ma14, d10, t, ma11, k3520 and k801

Fig 49 Size distribution of intercept squared data plotted against normalised intercepts for all the materials

Fig 50 Cumulative size distributions for shm9, shm3, shmcn5, n15, b9, ma6, cwn8, uc9, k322 and x160

Fig 51 Cumulative size distributions for macn9, cw3, h10, t25, ma14, d10, t, ma11, k3520 and k801

Fig 52 Comparison of WC size distribution data for k801 and material F15

Fig 53 Abrasion test results

Fig 54 Abrasion (volume loss)/inverse square root grain size for CPM materials

Fig 55 Abrasion property map for non-standard CPM materials

Fig 56 Abrasion property map for the wide grained hardmetals

Fig 57 Palmqvist test results compared with previous data

Fig 58 Empirical fit to Palmqvist toughness/Hardness results

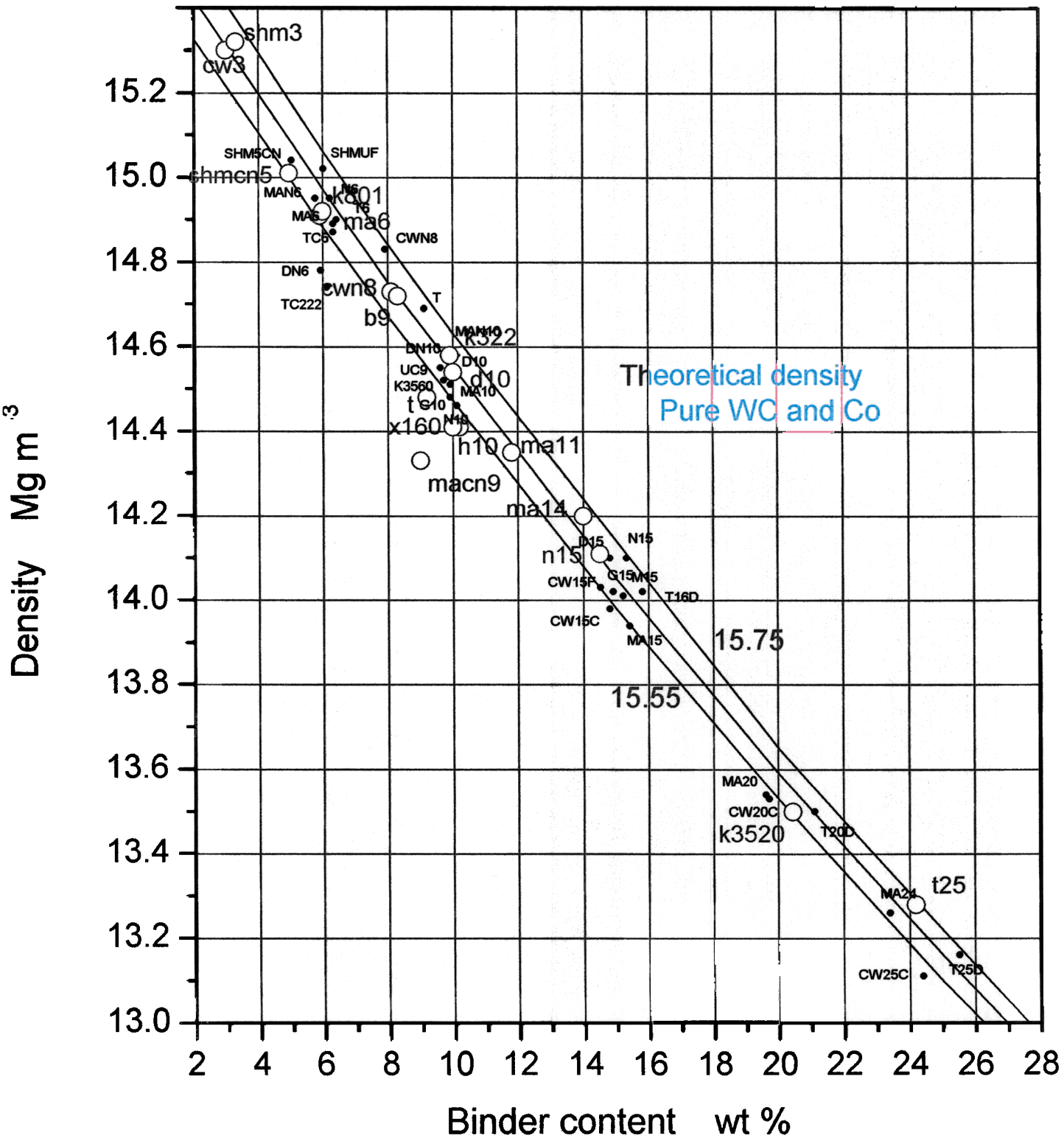
Fig 59 Palmqvist toughness data plotted against WC grain size

Fig 60 Palmqvist property map for non-standard CPM materials

Fig 61 Comparison of NPL and source HV30 values.

Fig 62 Razor blade notched toughness data compared with Palmqvist results

Fig 63 Abrasion/toughness property map for baseline and wide grained hardmetals



Density measurements

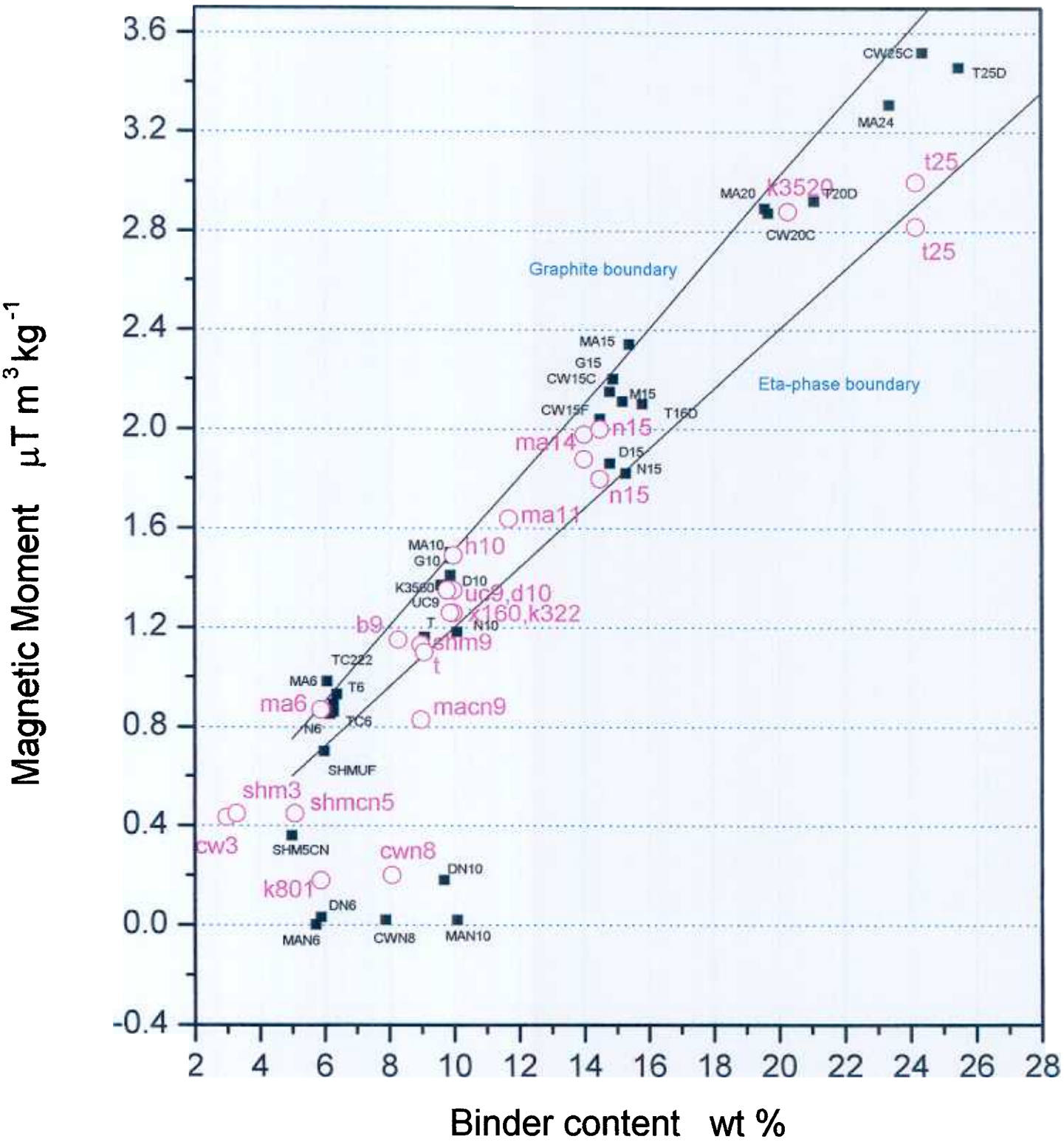
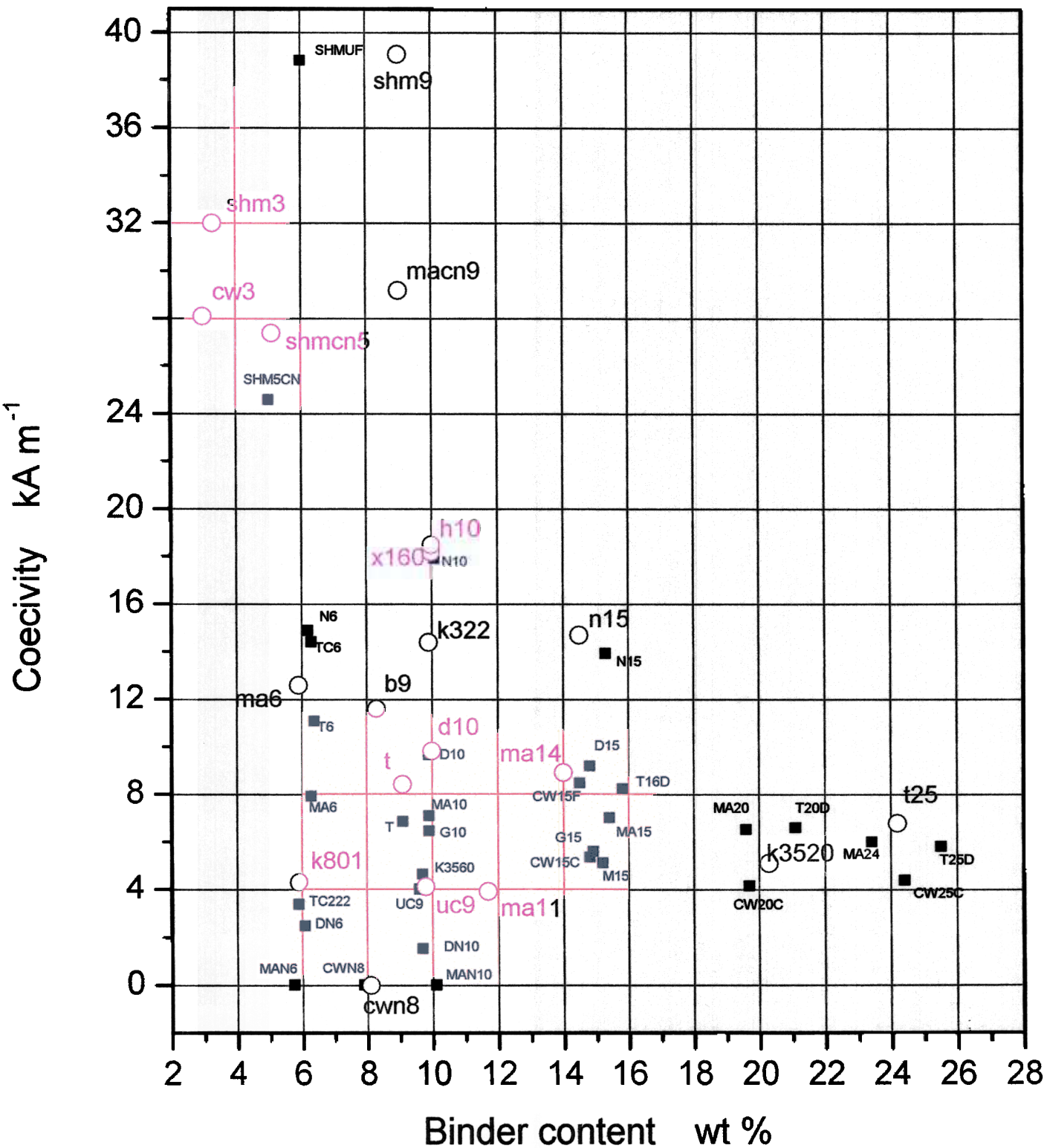


Fig 2 Magnetic moment measurements



Coercivity measurements

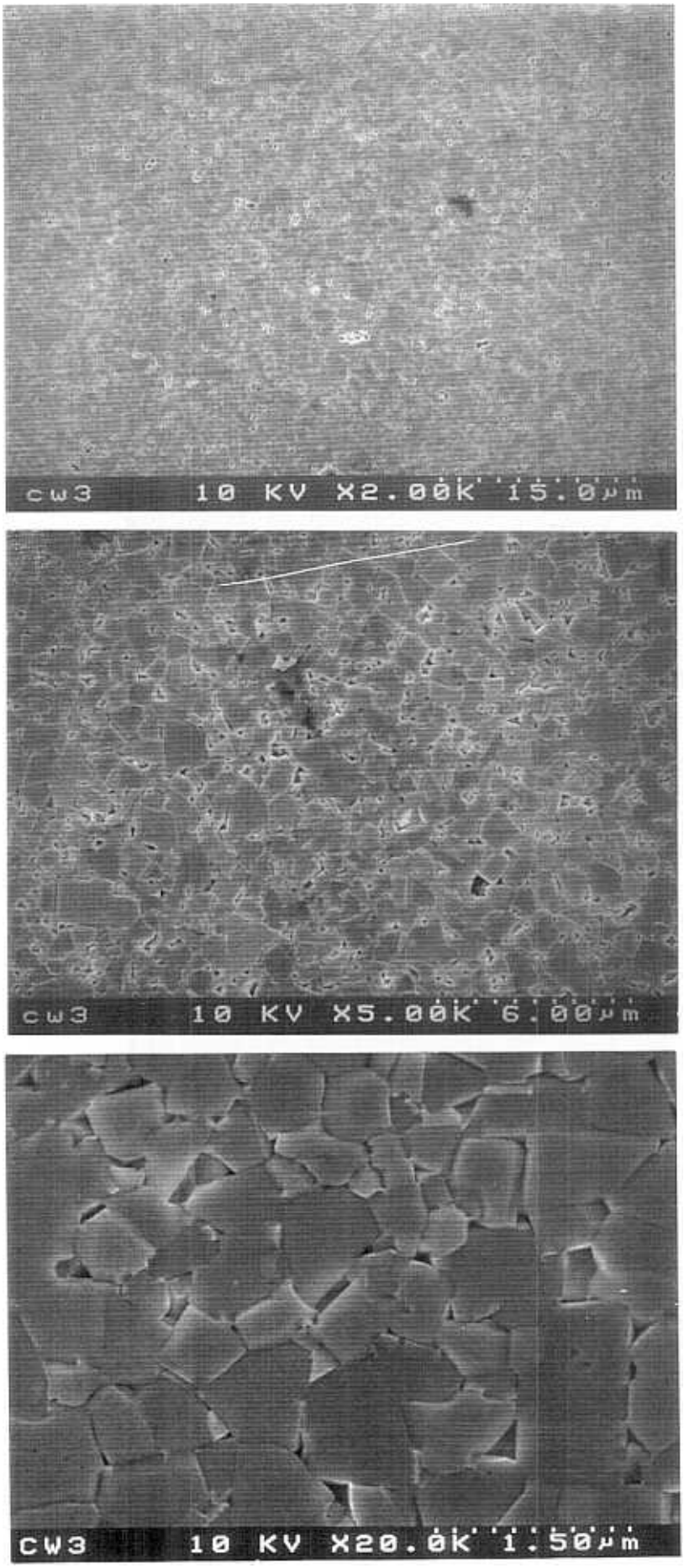
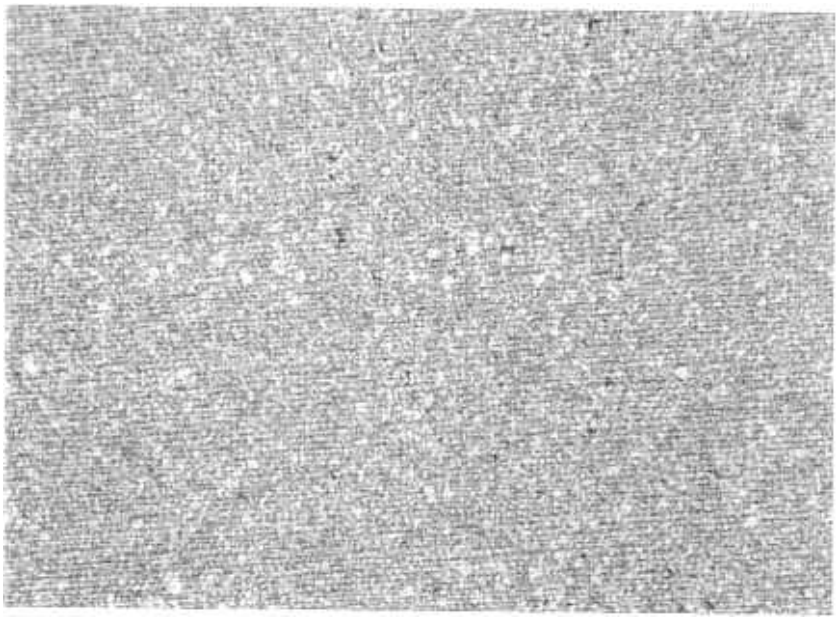


Fig 4 SEM micrographs of cw3



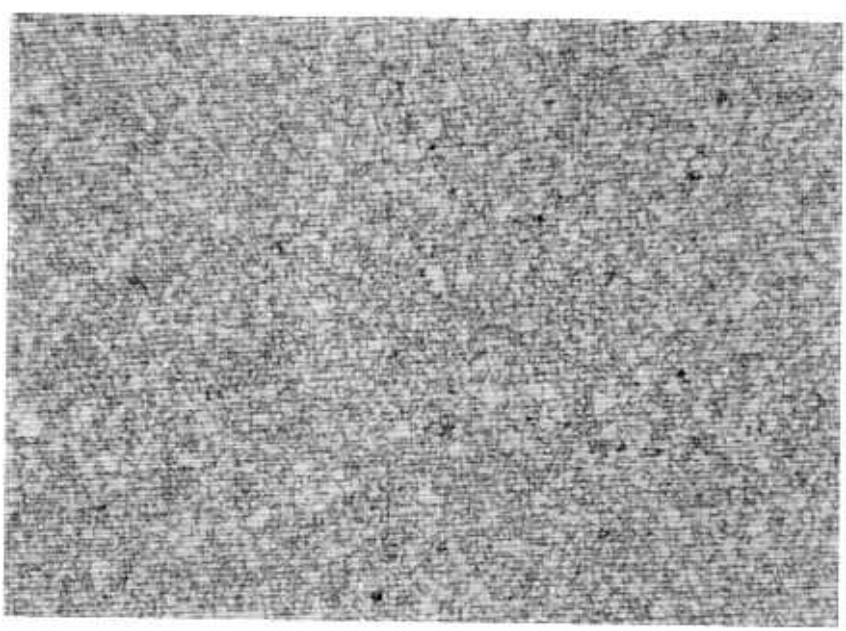


Fig 5 Optical micrographs of cw3

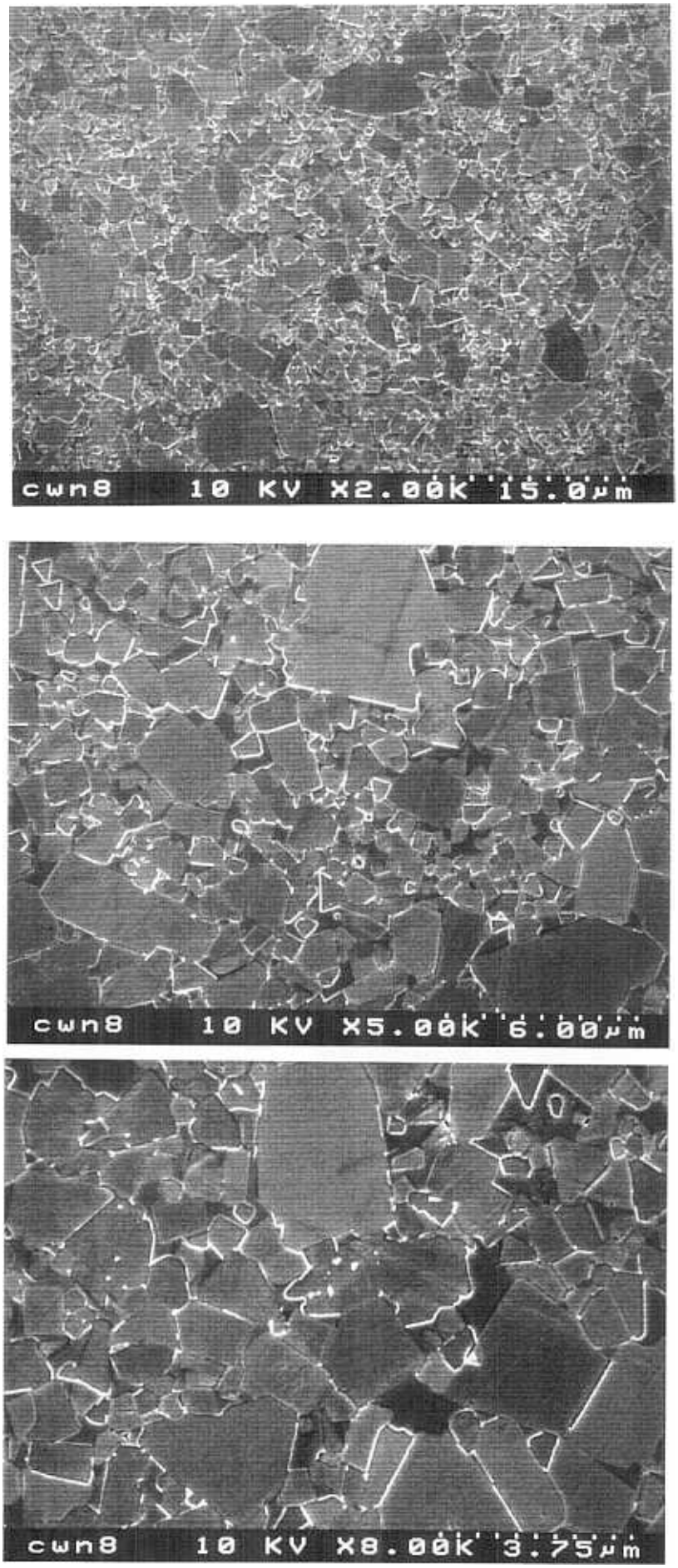
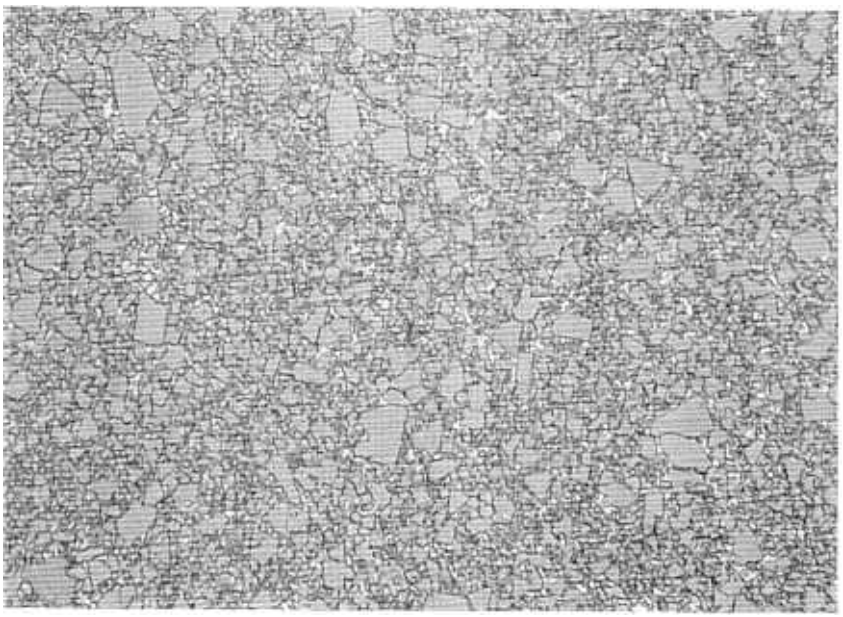
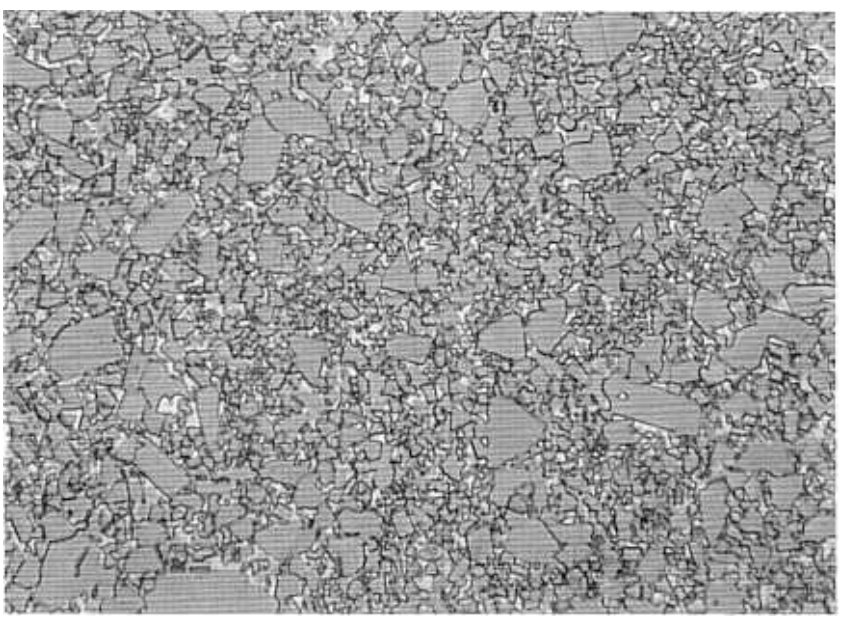


Fig 6 SEM micrographs cwn8



×1000



×1500

3 8

Fig 7 Optical micrographs of cwn8

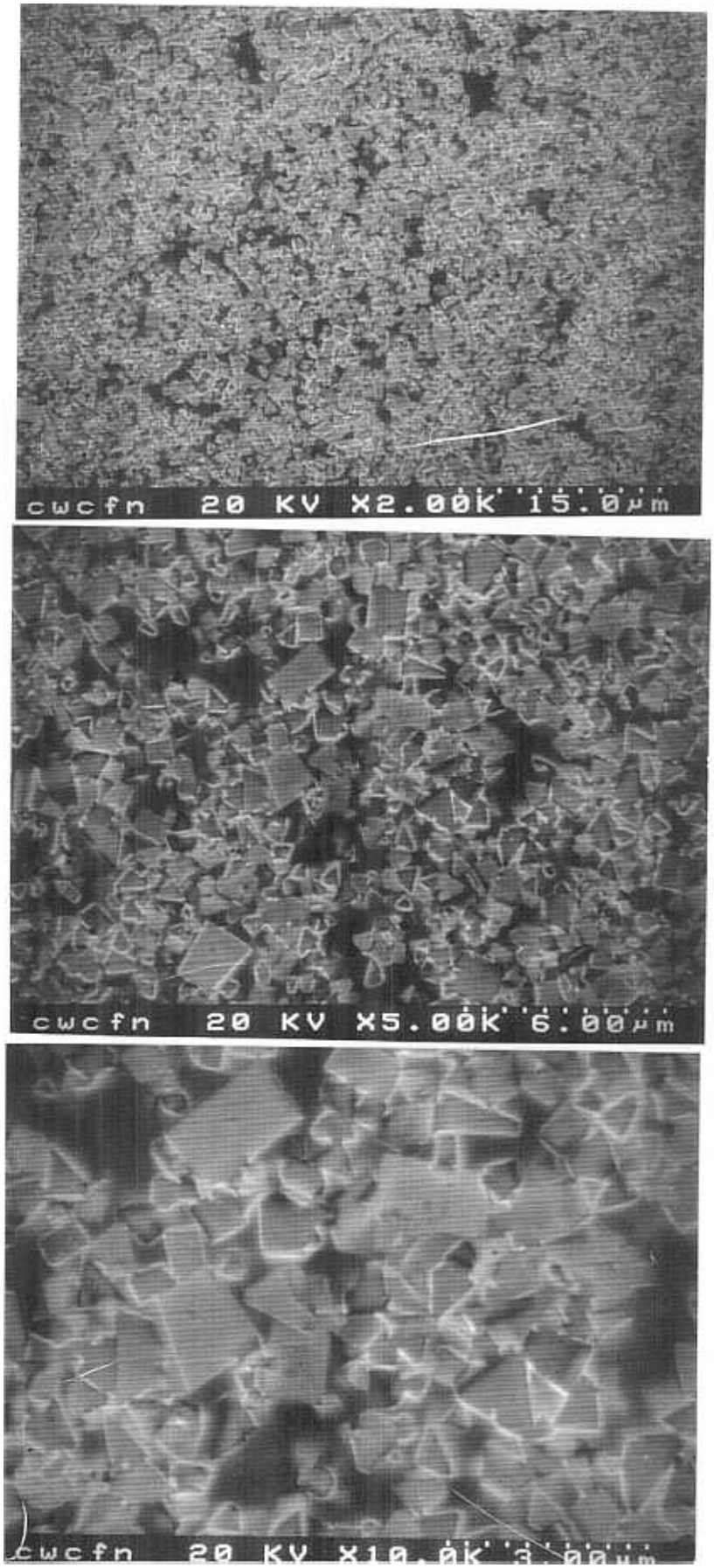


Fig 8 SEM micrographs of cwfnc20

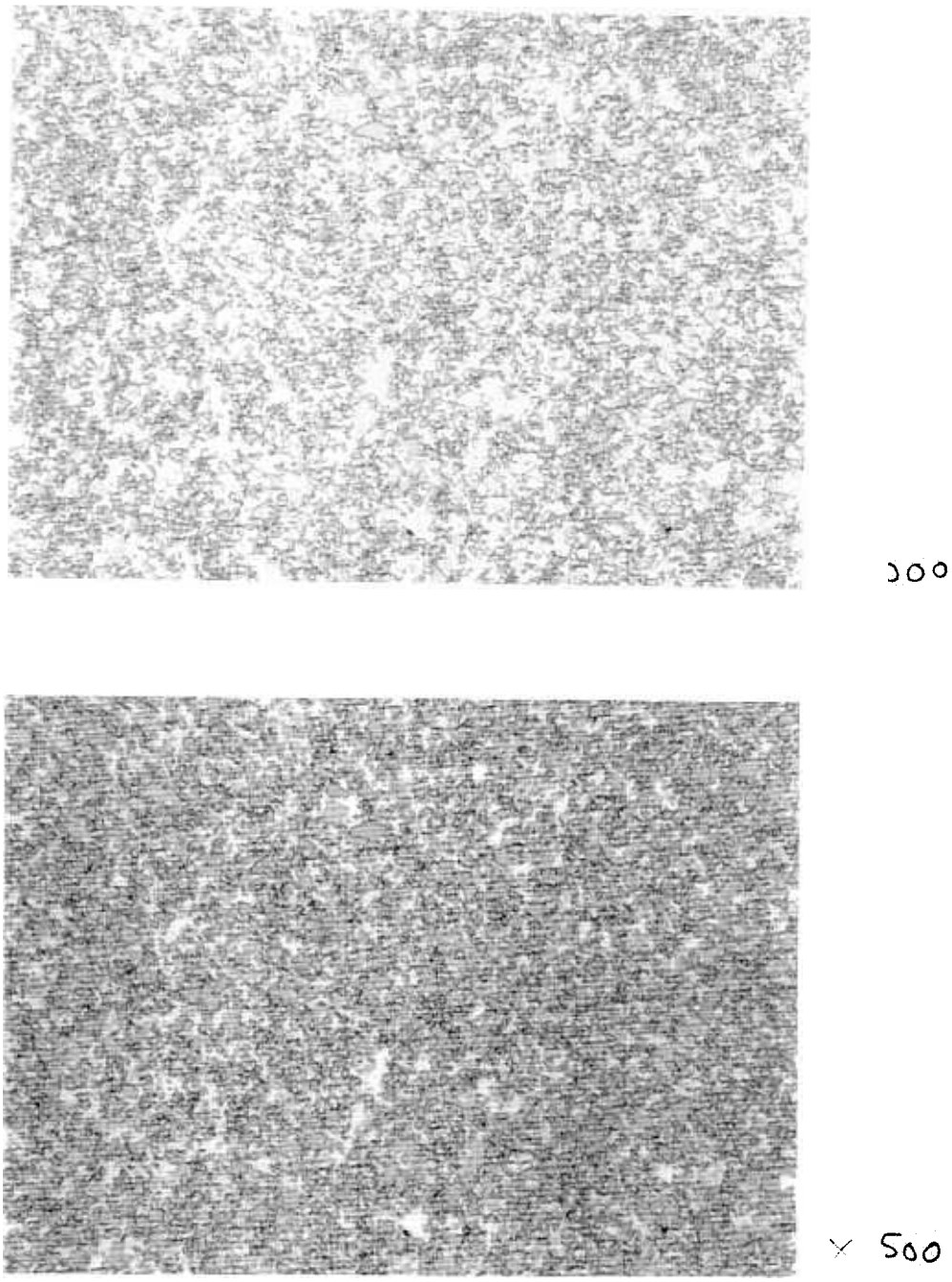


Fig 9 Optical micrographs of cwfnc20

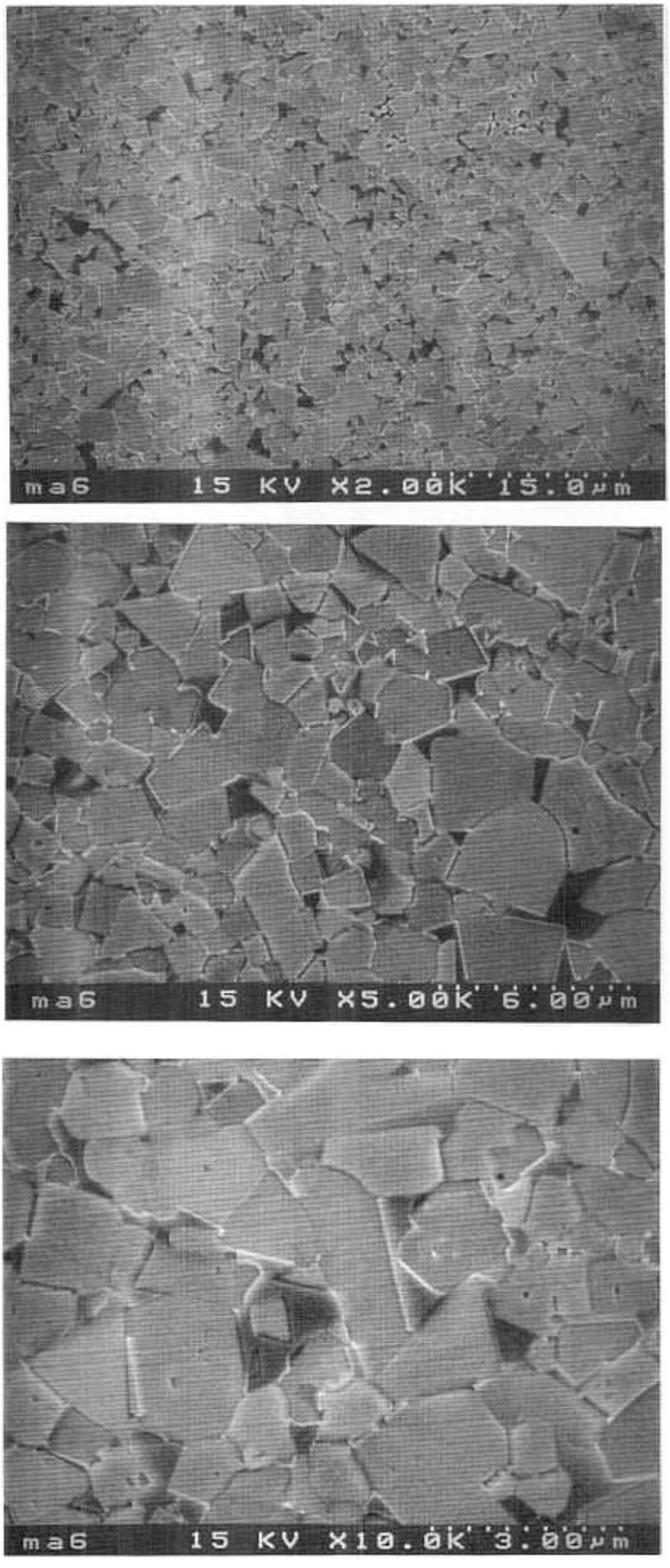
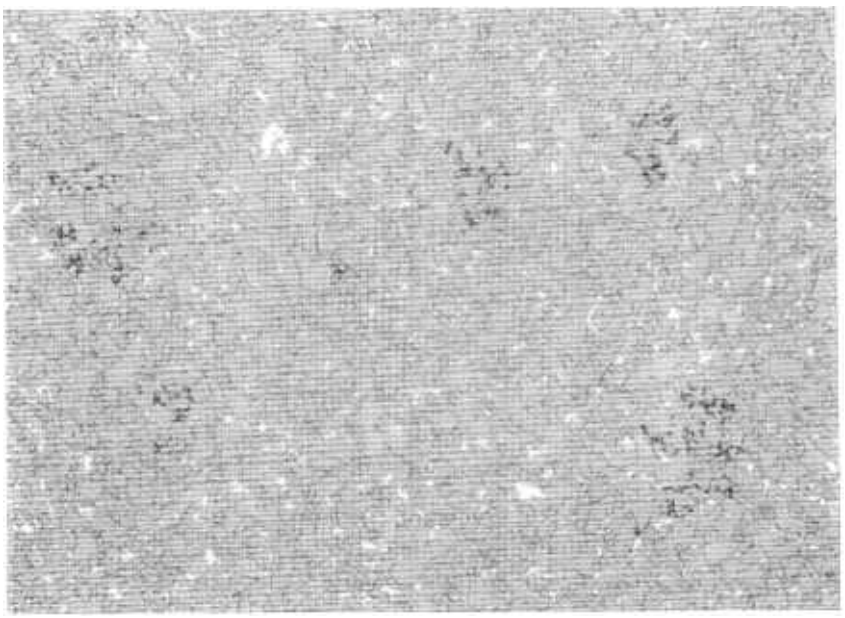
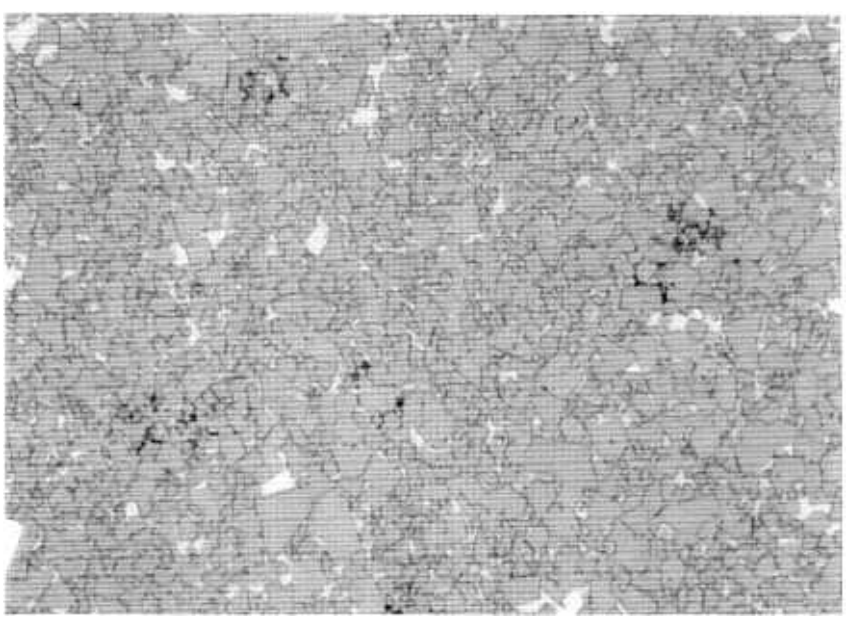


Fig 10 SEM micrographs of ma6





ma 6

Fig 11 Optical micrographs of ma6

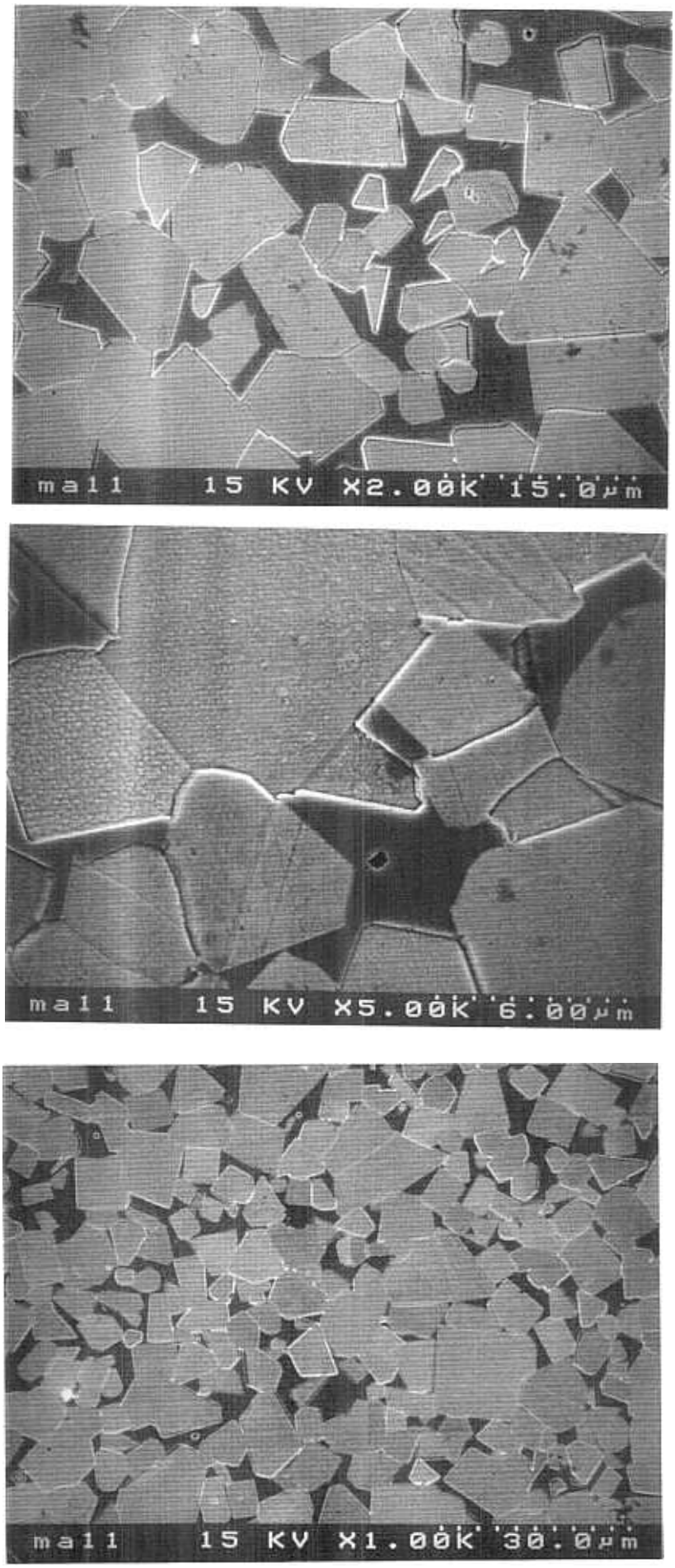
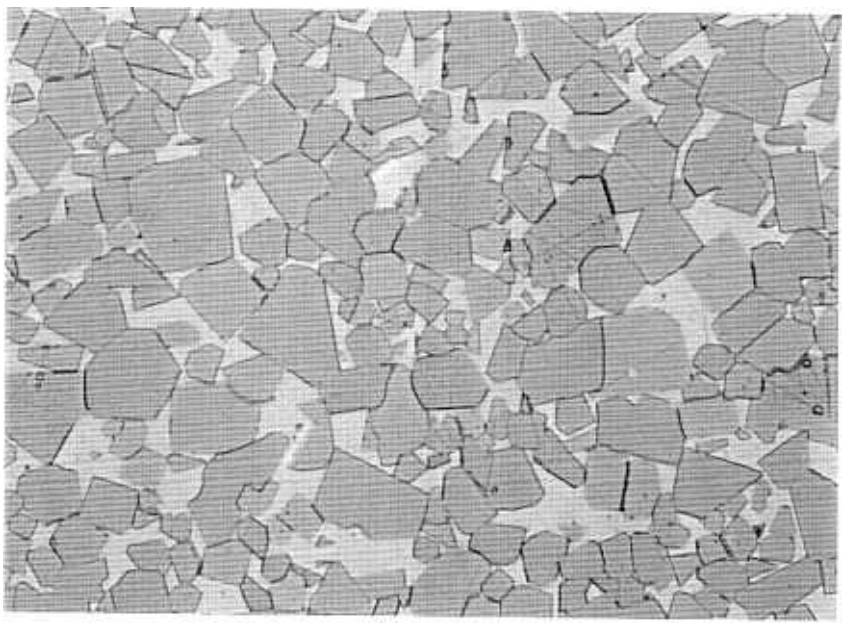
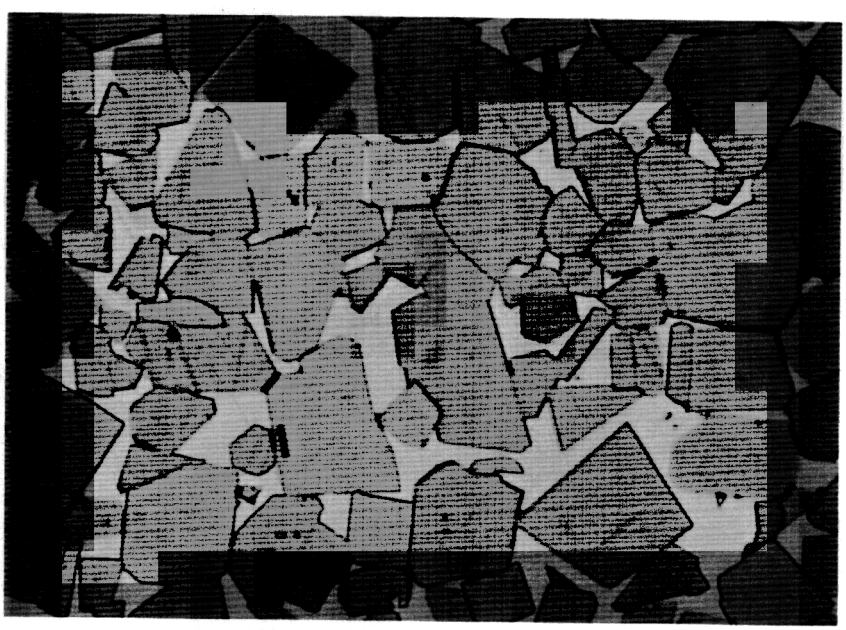


Fig 12 SEM micrographs of ma11





Ma

Fig 13 Optical micrographs of ma11

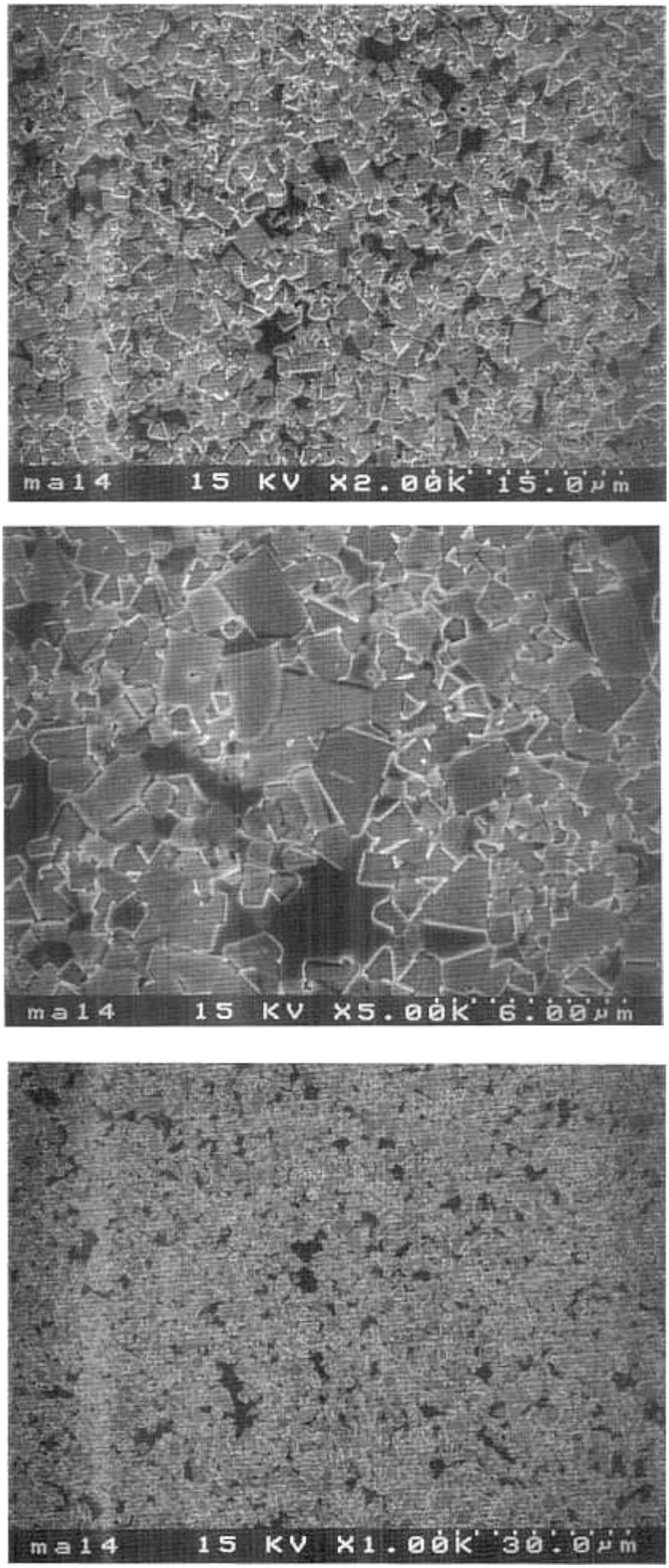
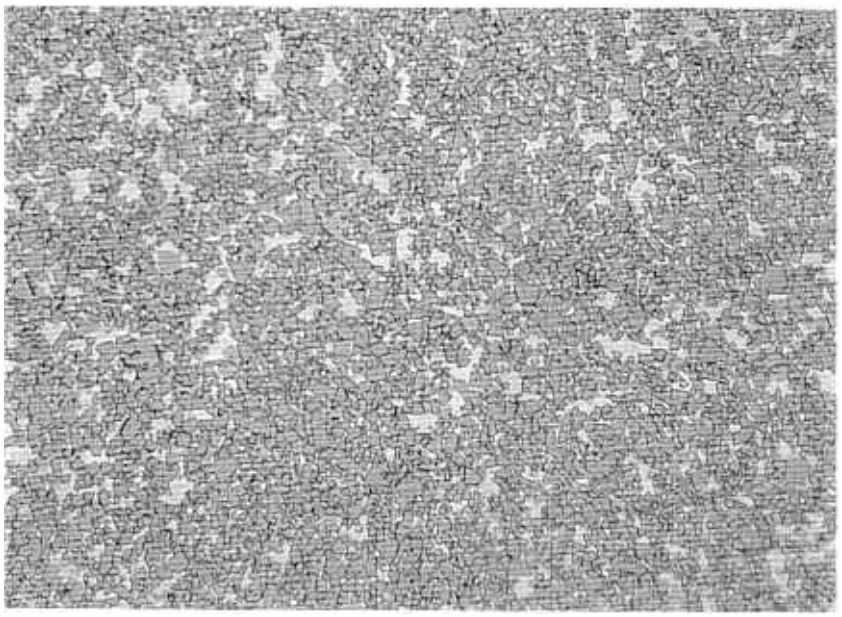


Fig 14 SEM micrographs of ma14



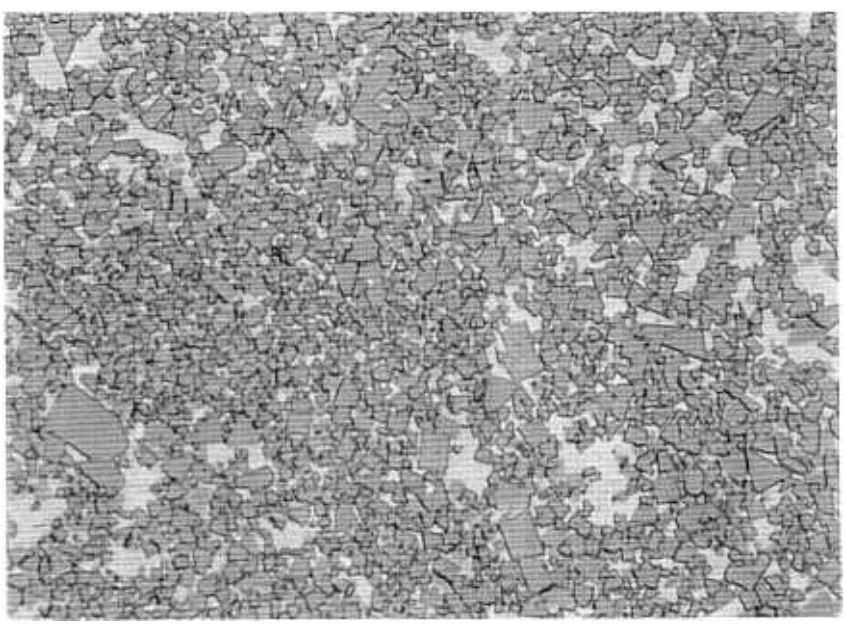


Fig Optical micrographs ma14

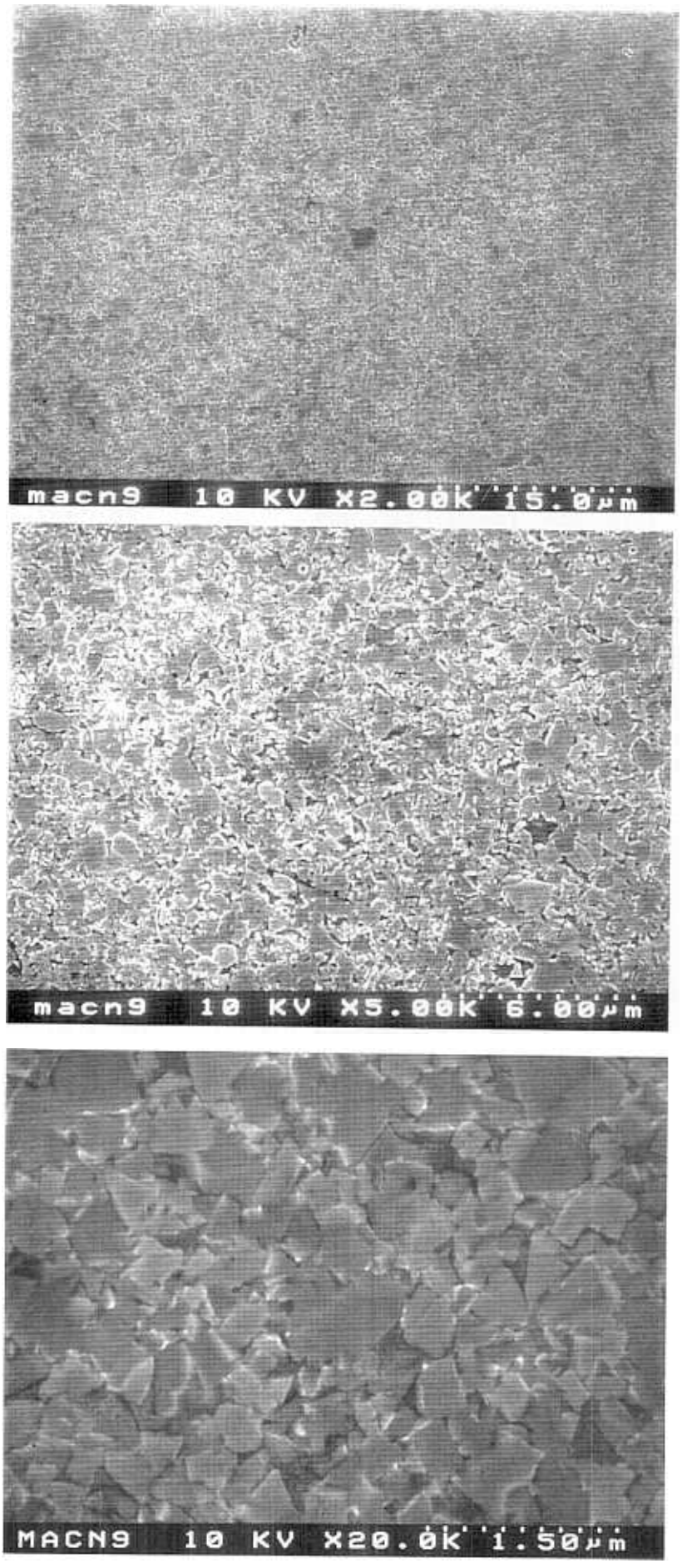
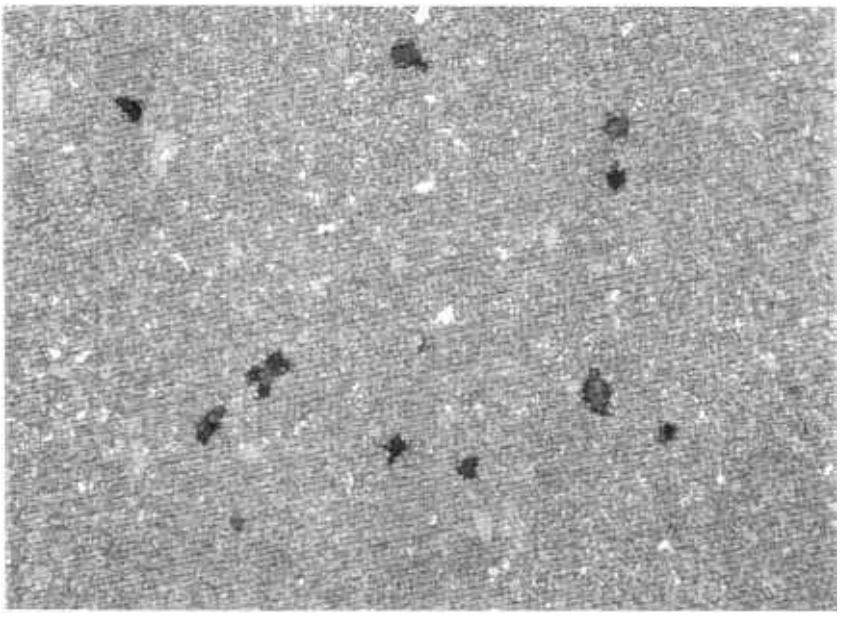
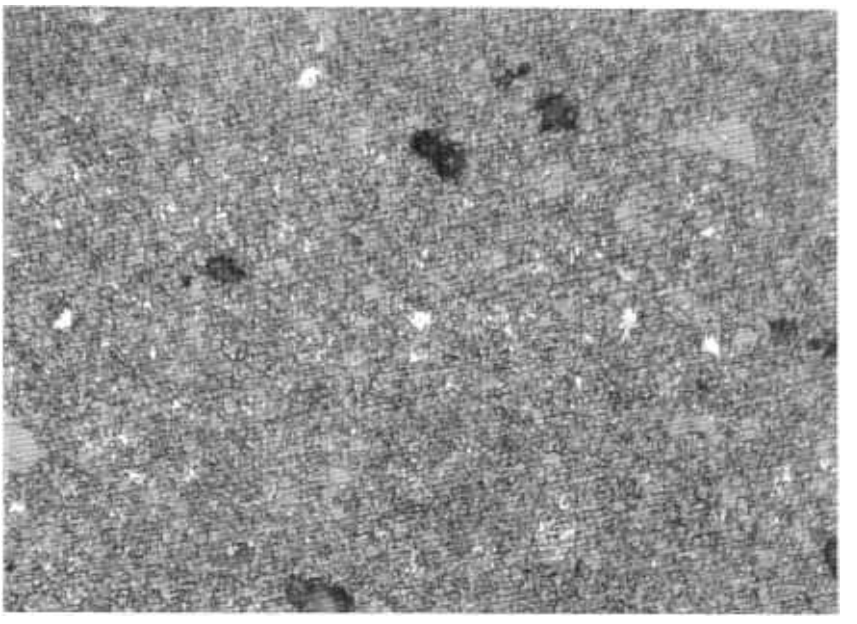


Fig 16 SEM micrographs of macn9



X1000



X1500

na

Fig 17 Optical micrographs of macn9

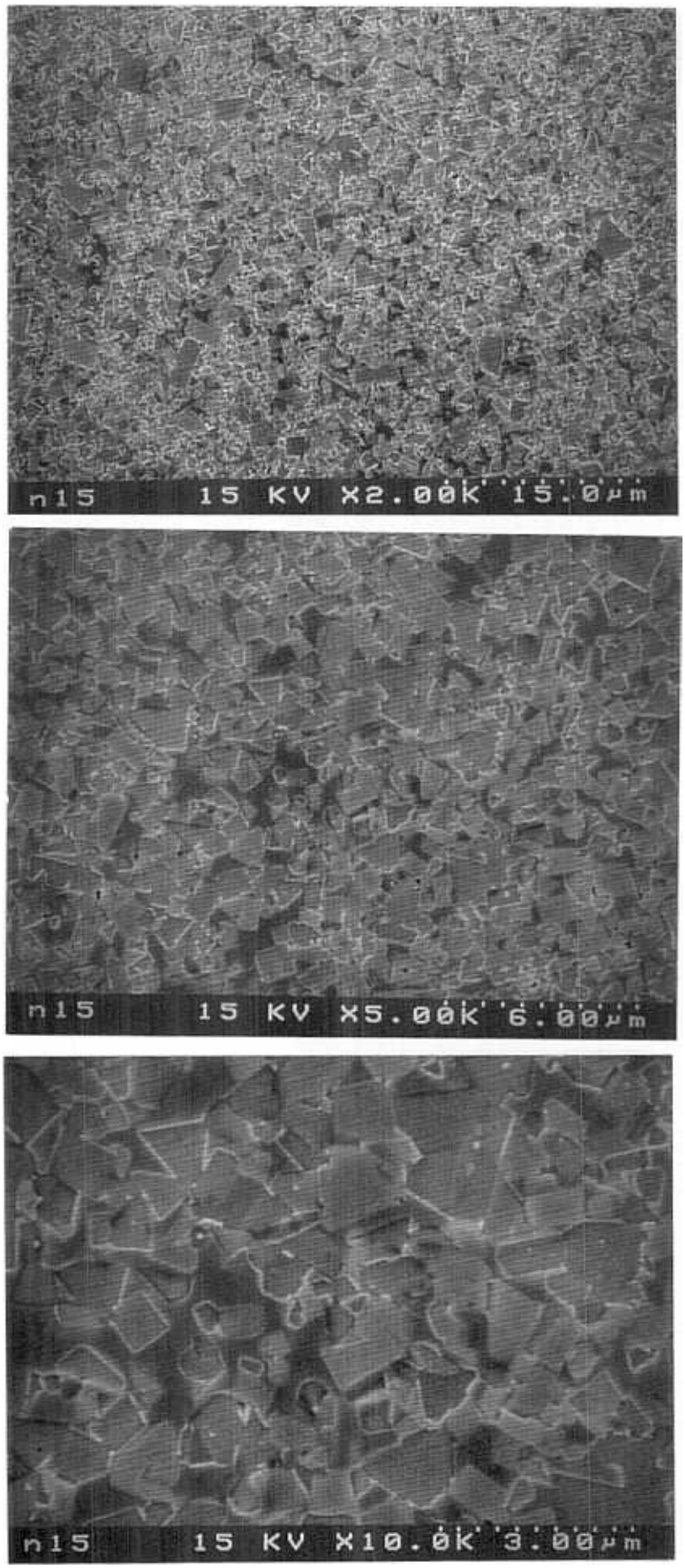
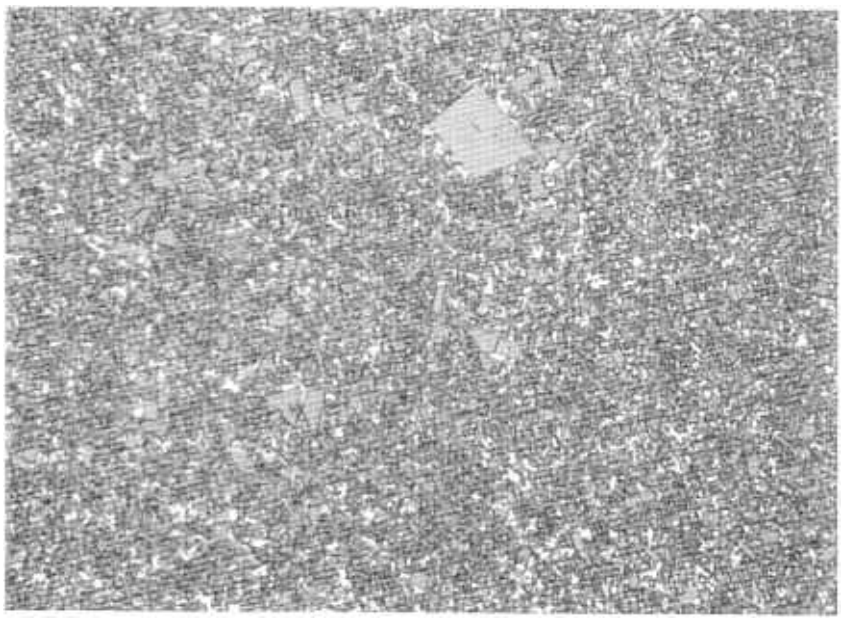
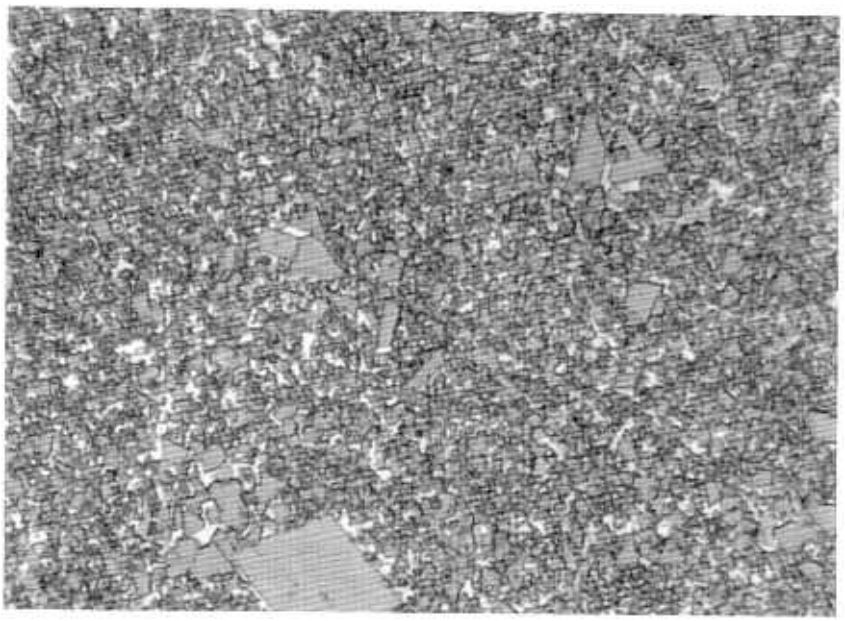


Fig 18 SEM micrographs of n15



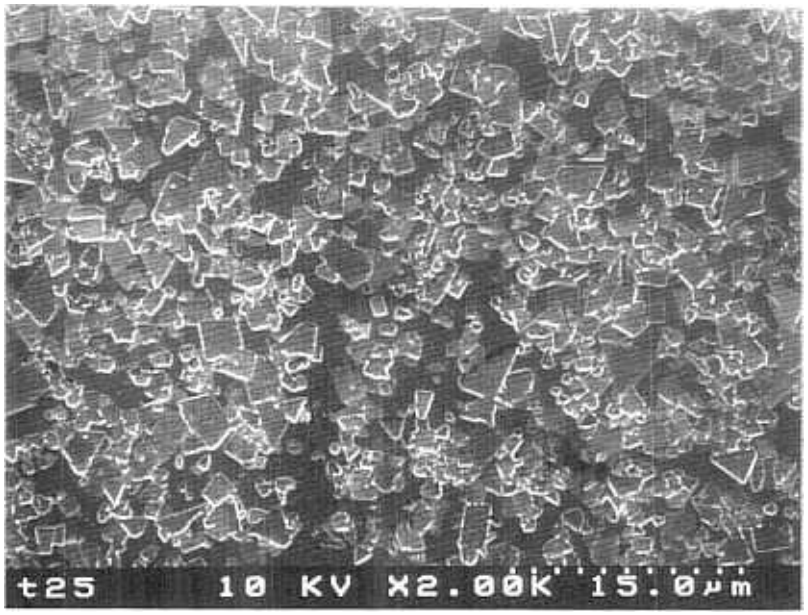
X 000

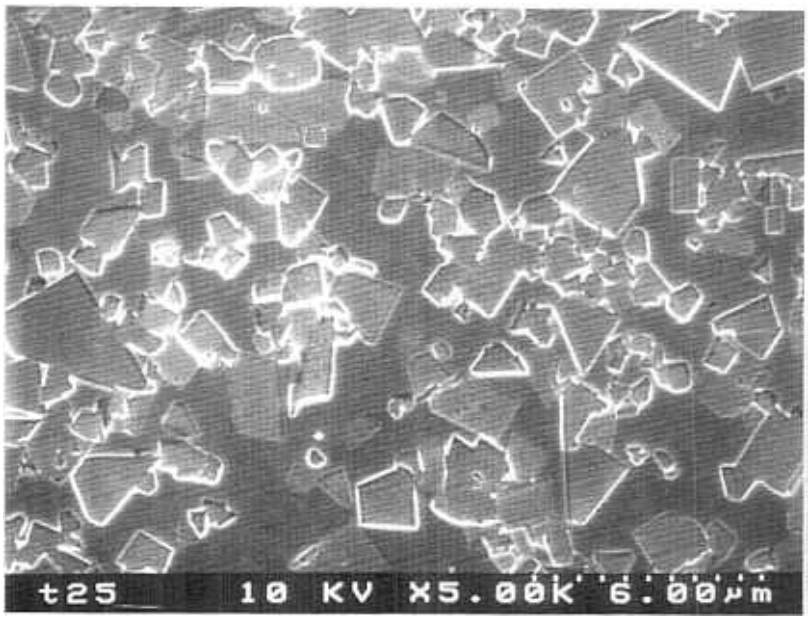


X1500

n15

Fig 19 Optical micrographs of n15





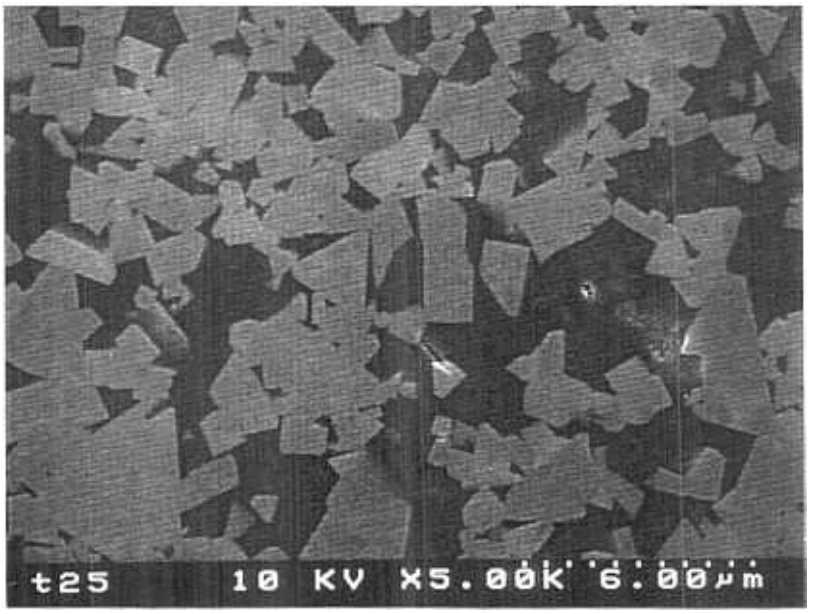
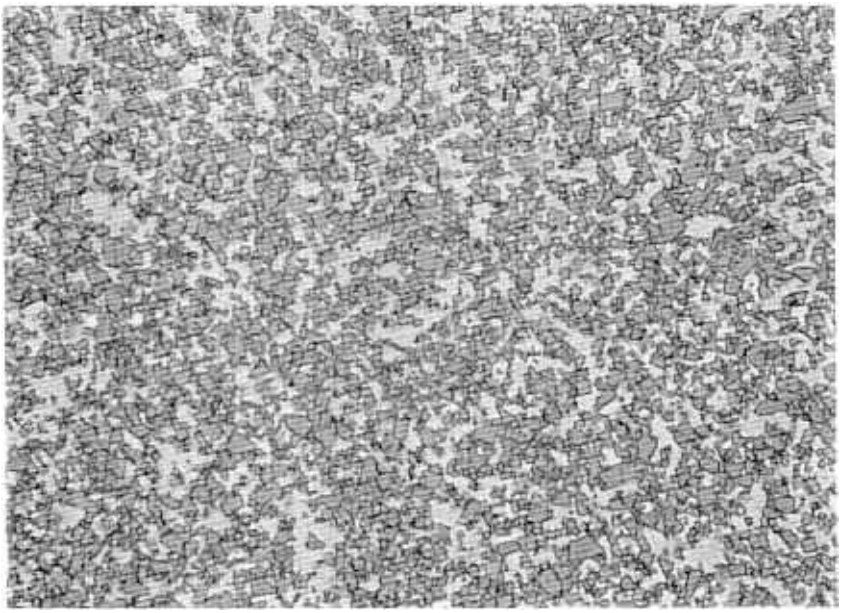
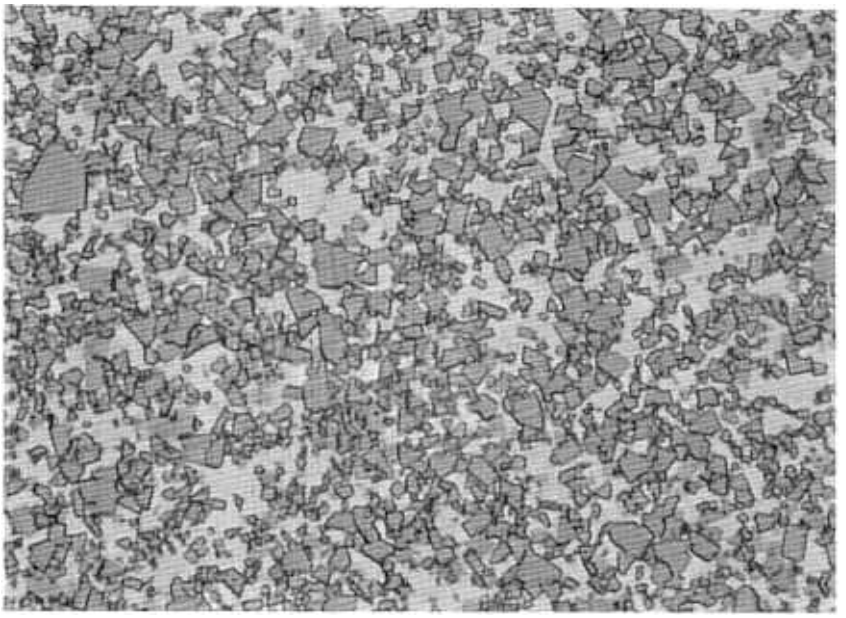


Fig 20 SEM micrographs of t25





X1500

2

Fig 21 Optical micrographs of t25

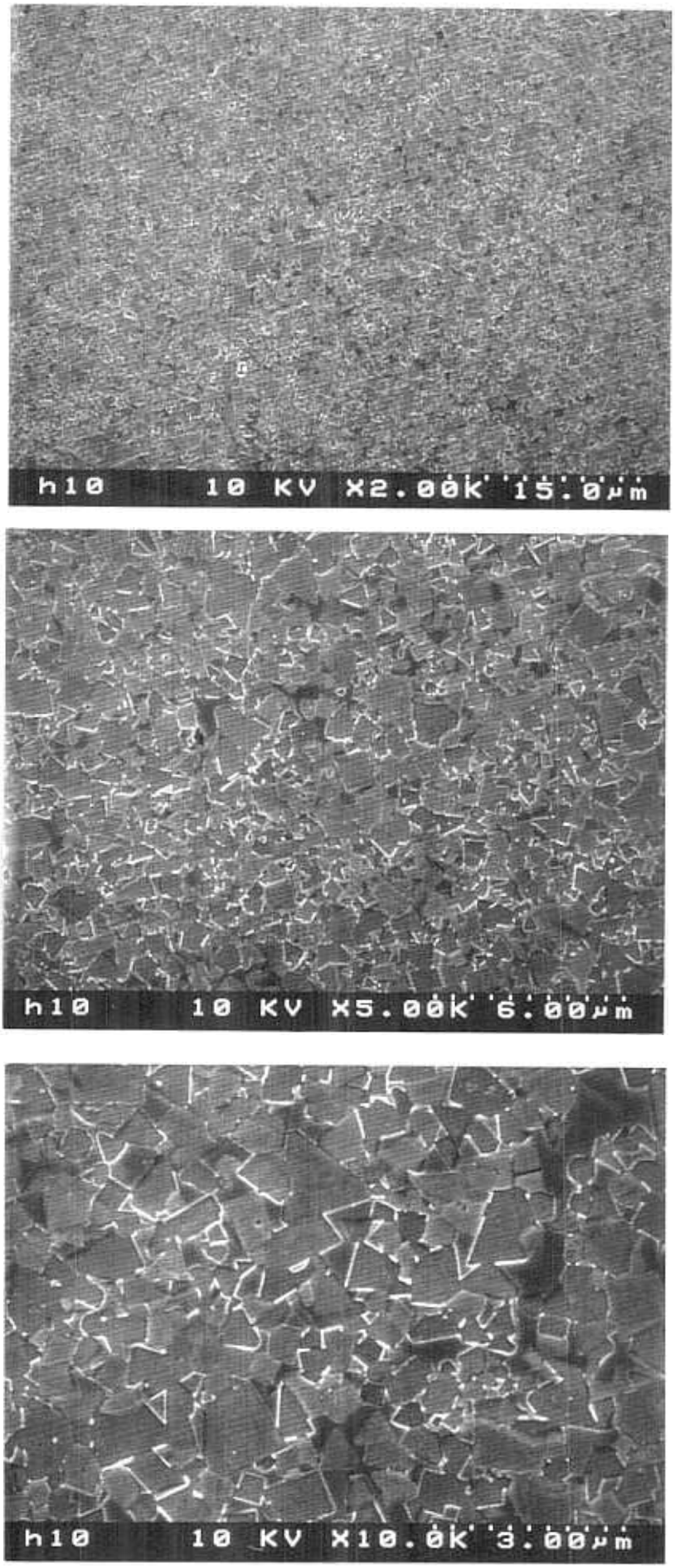
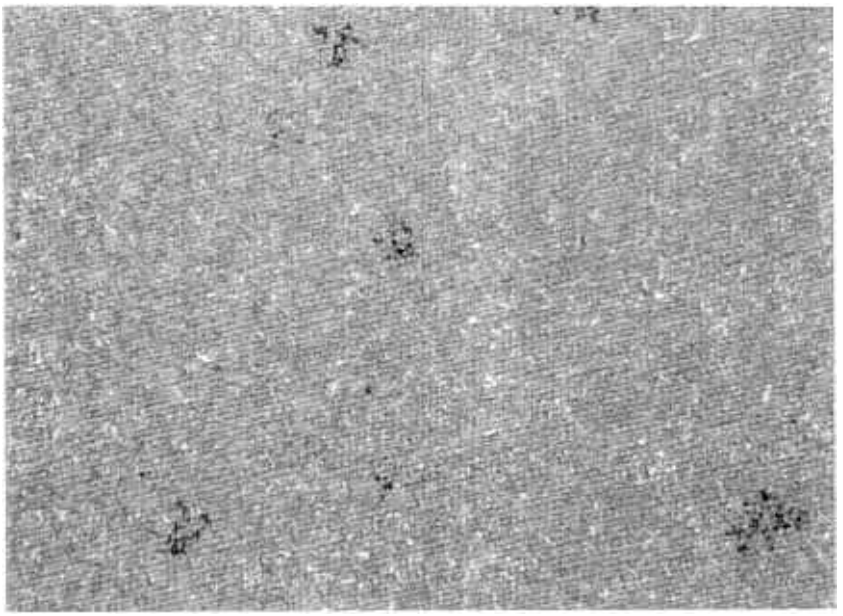


Fig 22 SEM micrographs of h10



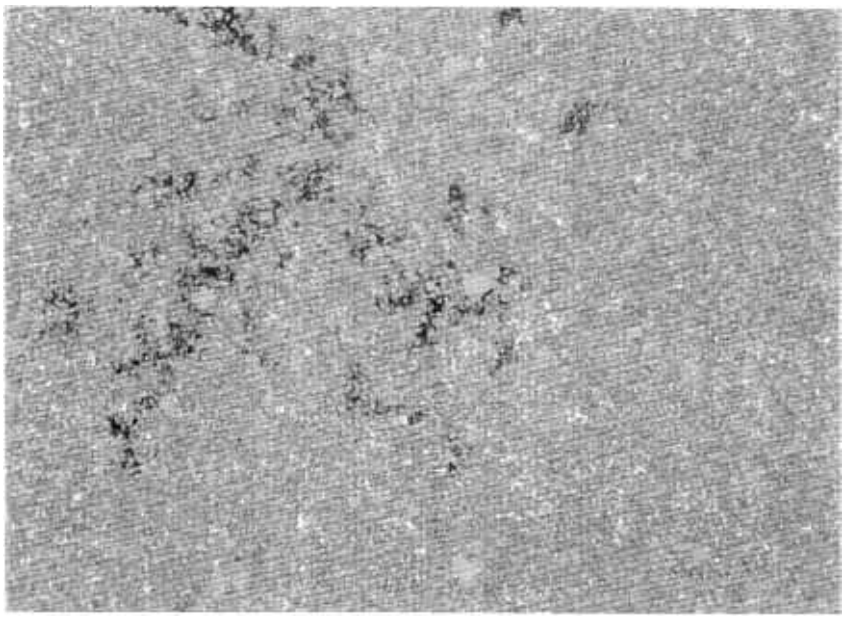


Fig Optical micrographs h10

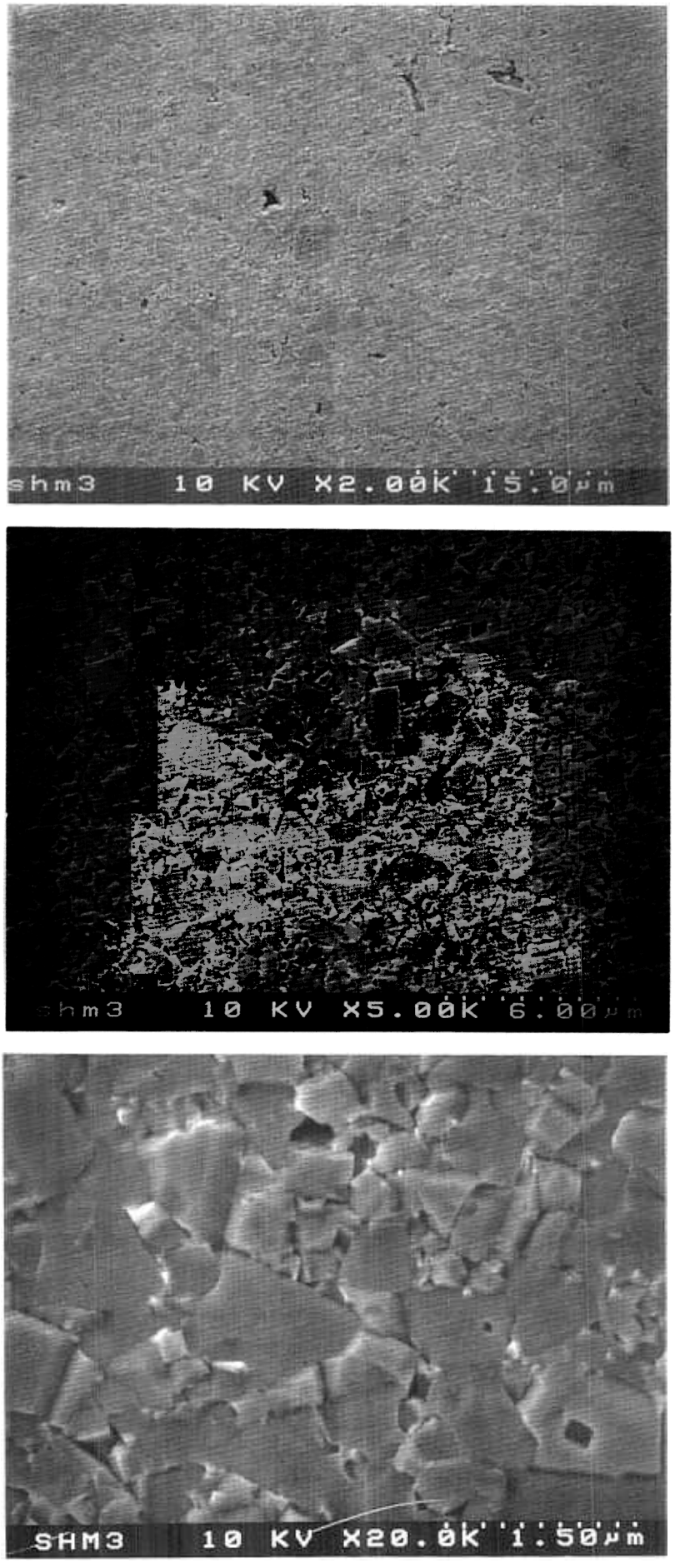
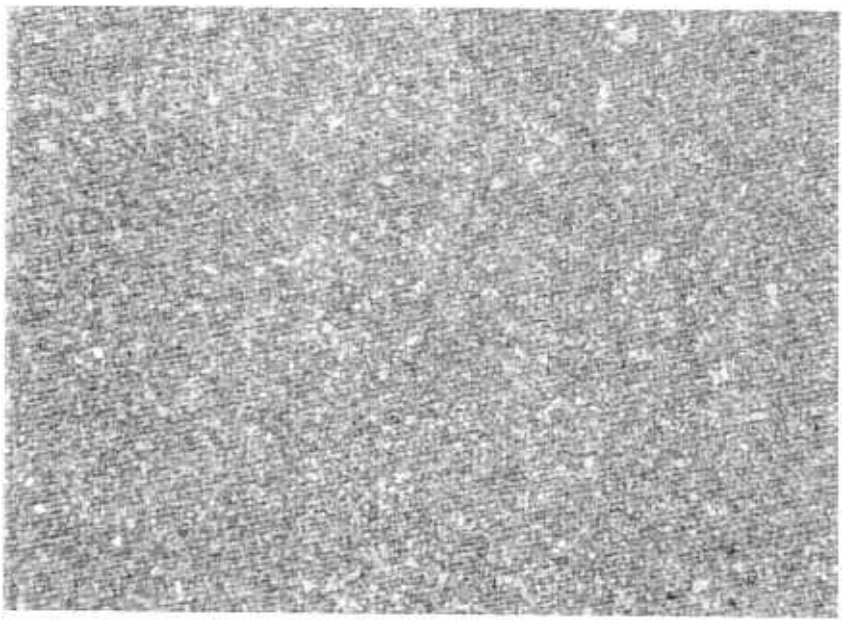
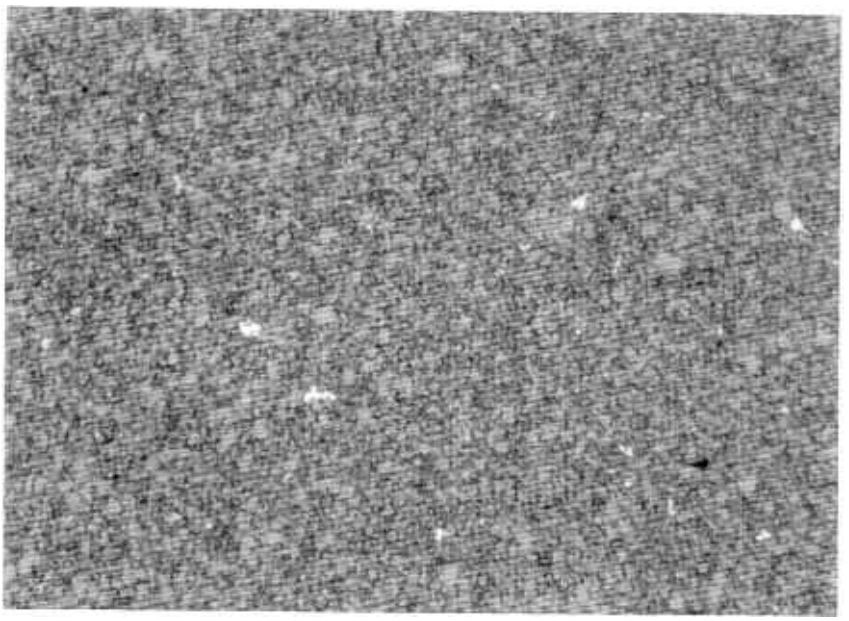


Fig 24 SEM micrographs of shm3





Shm3

Fig 25 Optical micrographs of shm3

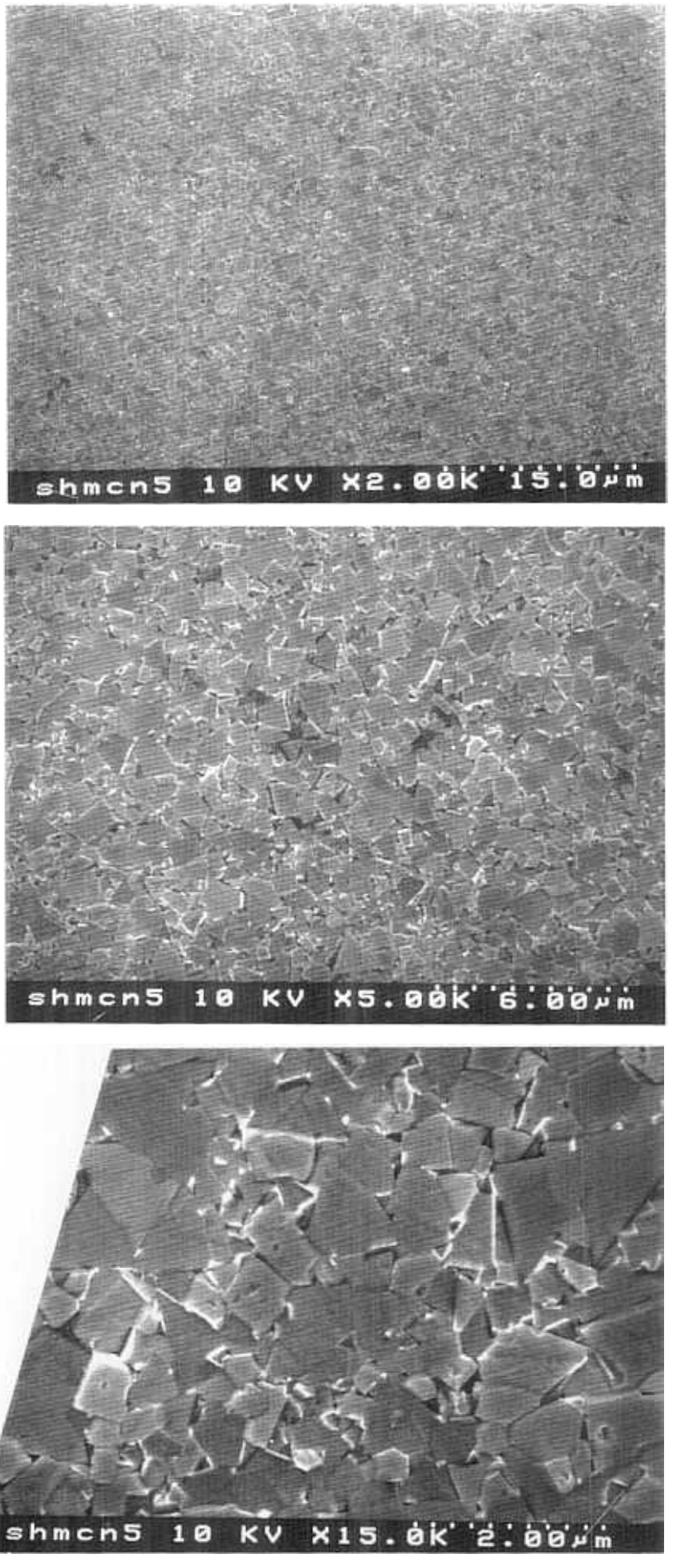
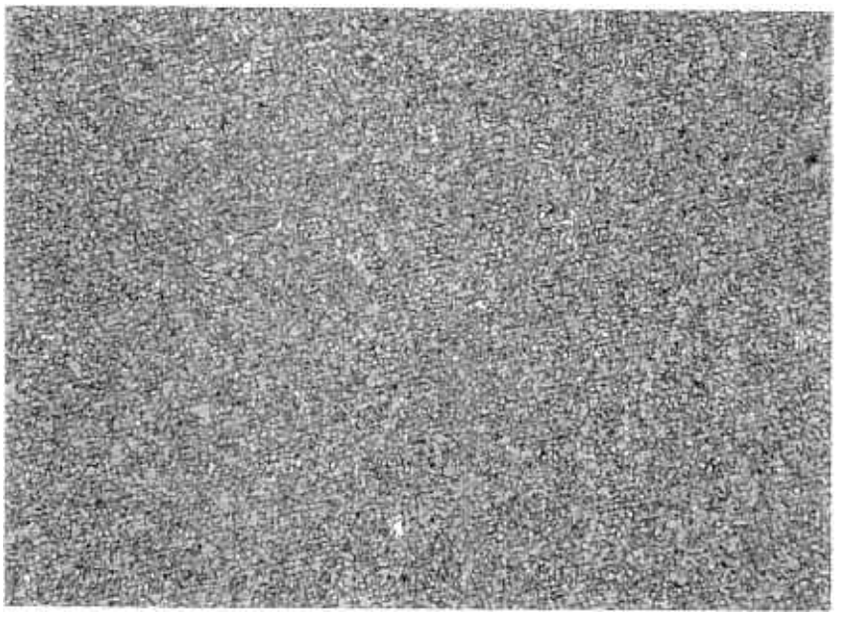
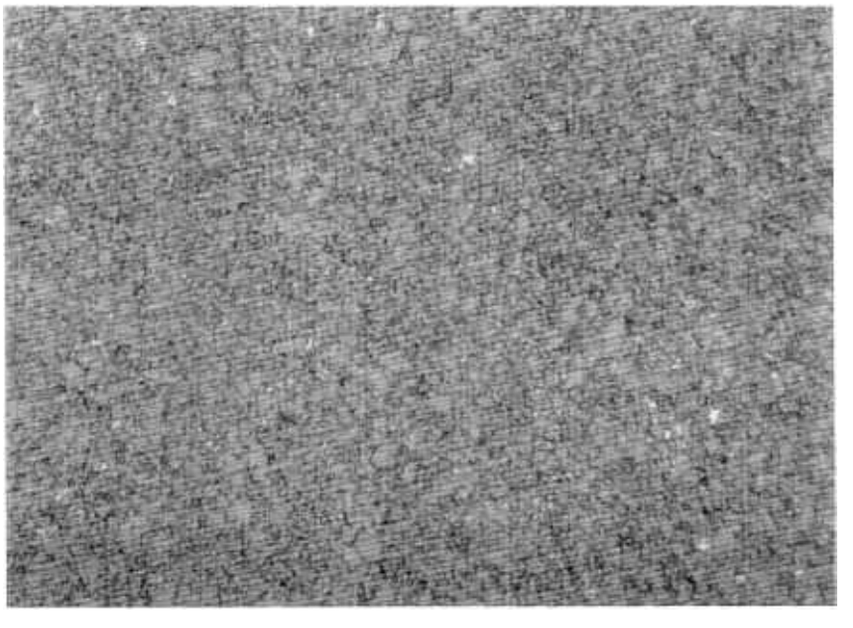


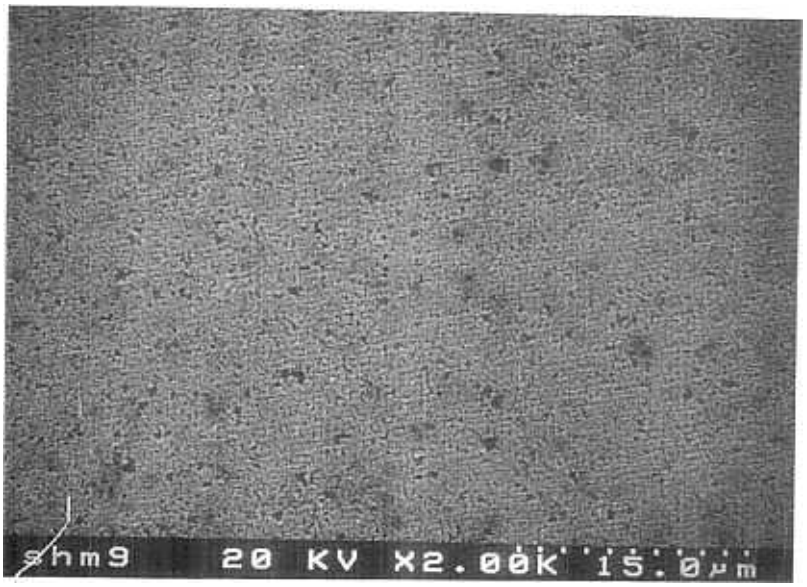
Fig SEM micrographs shmcn5





Shmcn

Fig 27 Optical micrographs of shmcn5



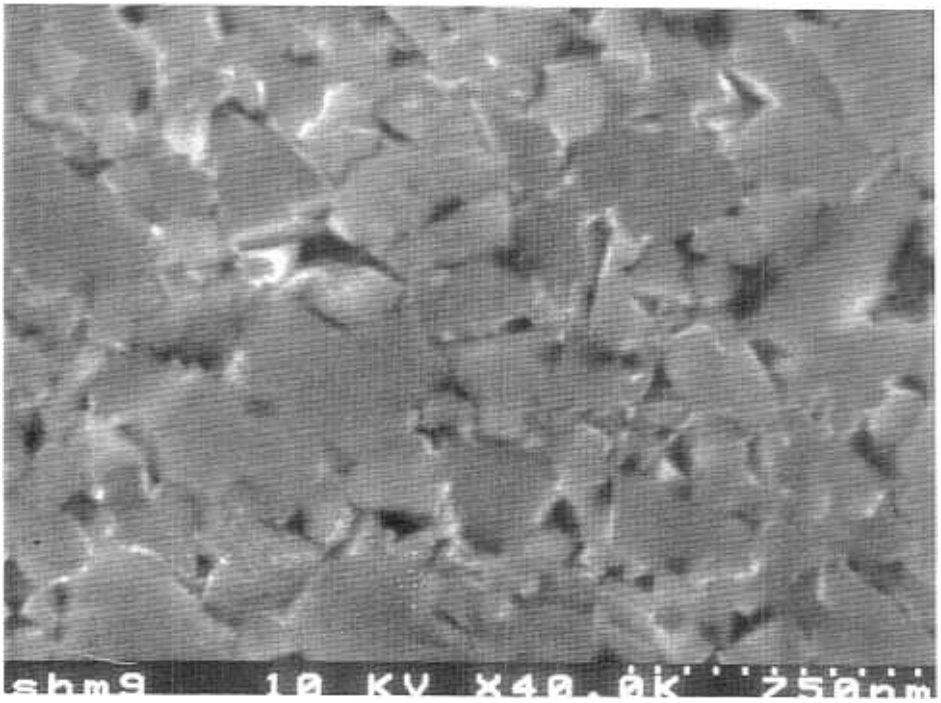


Fig 28 SEM micrographs of shm9

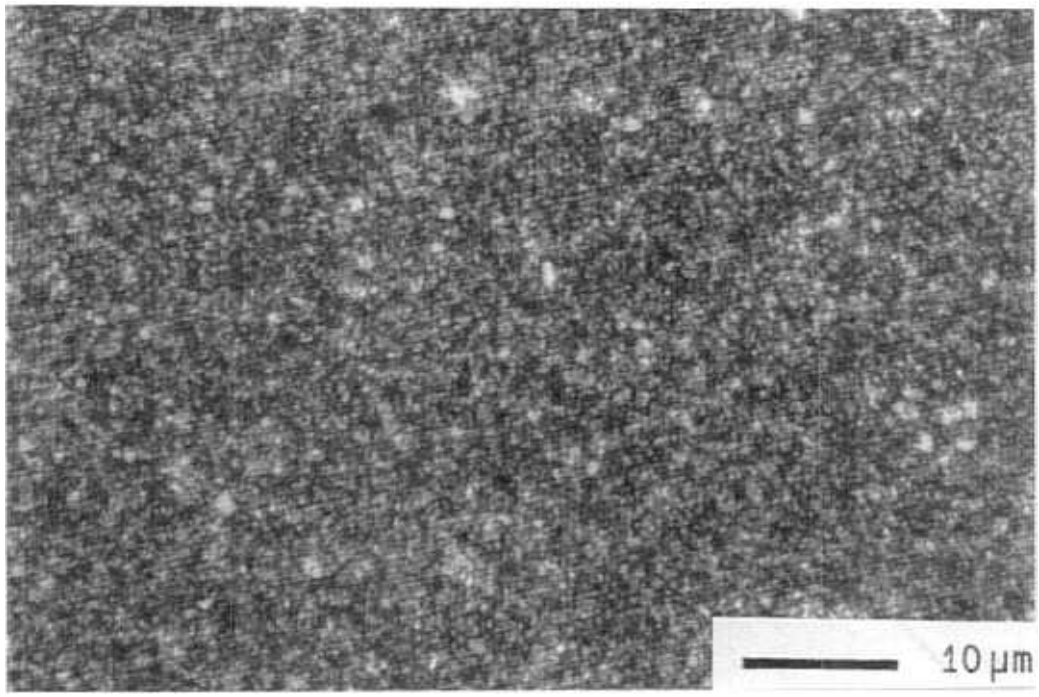


Fig 29 Optical micrographs of shm9

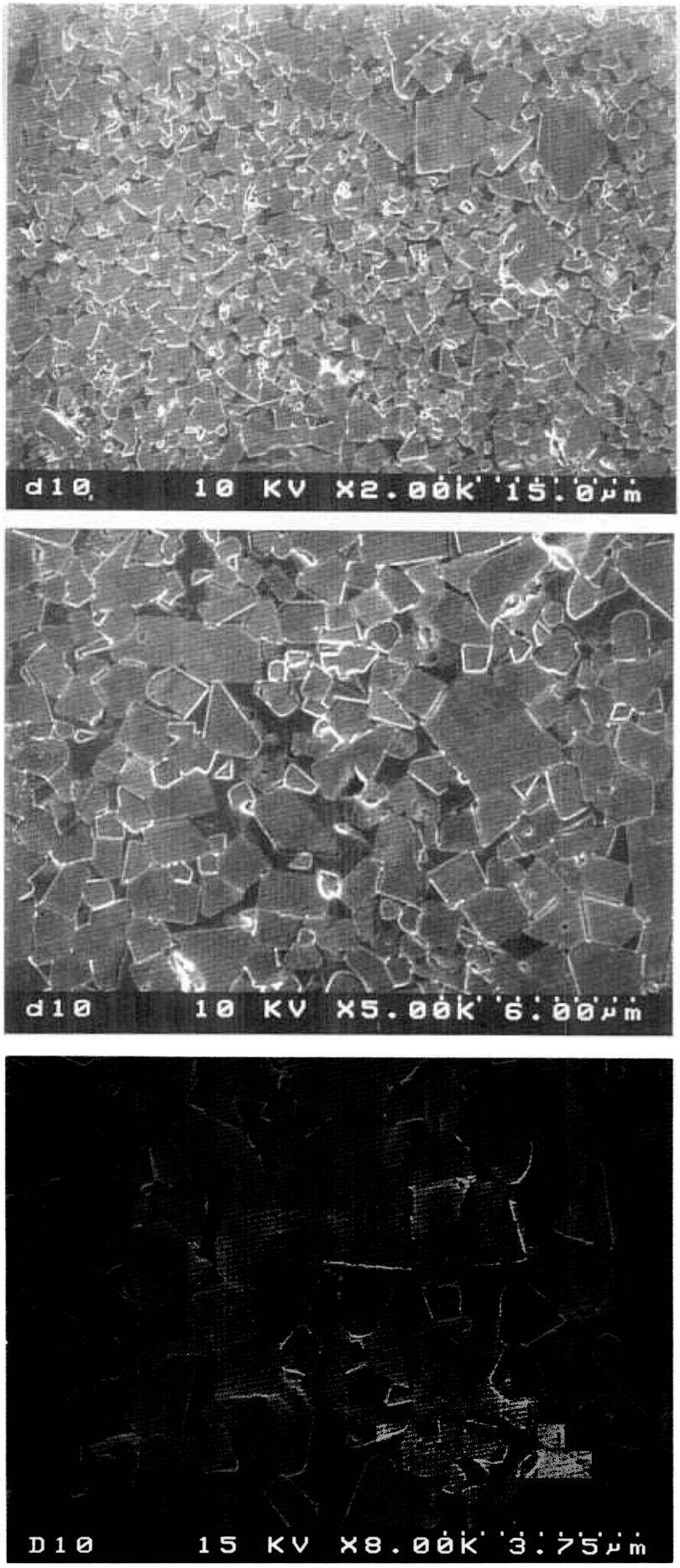
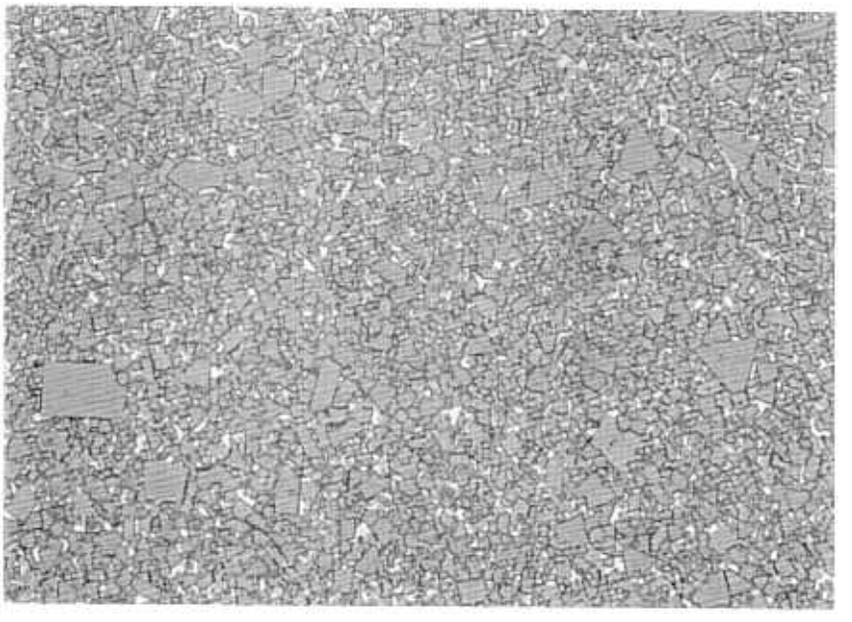
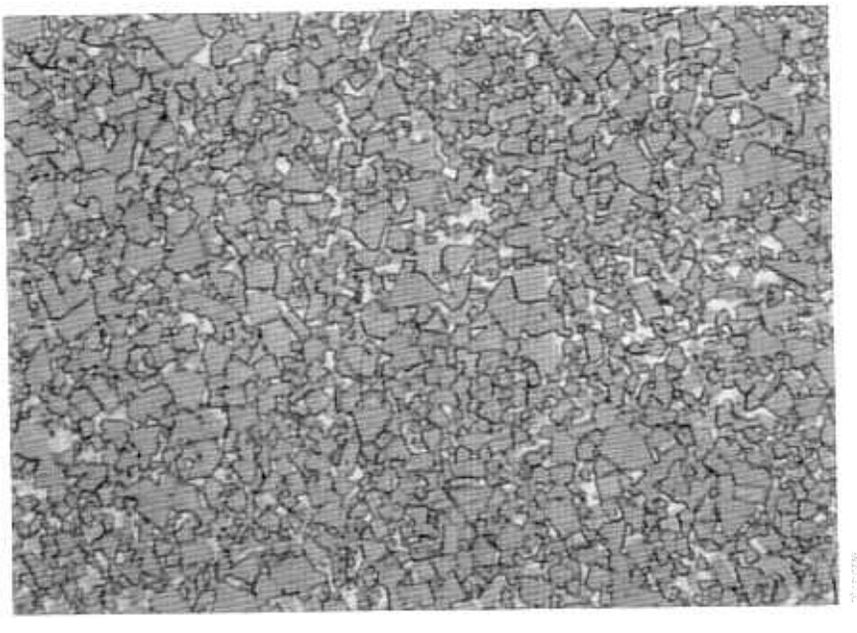


Fig 30 SEM micrographs of d10





d10

Fig 31 Optical micrographs of d10

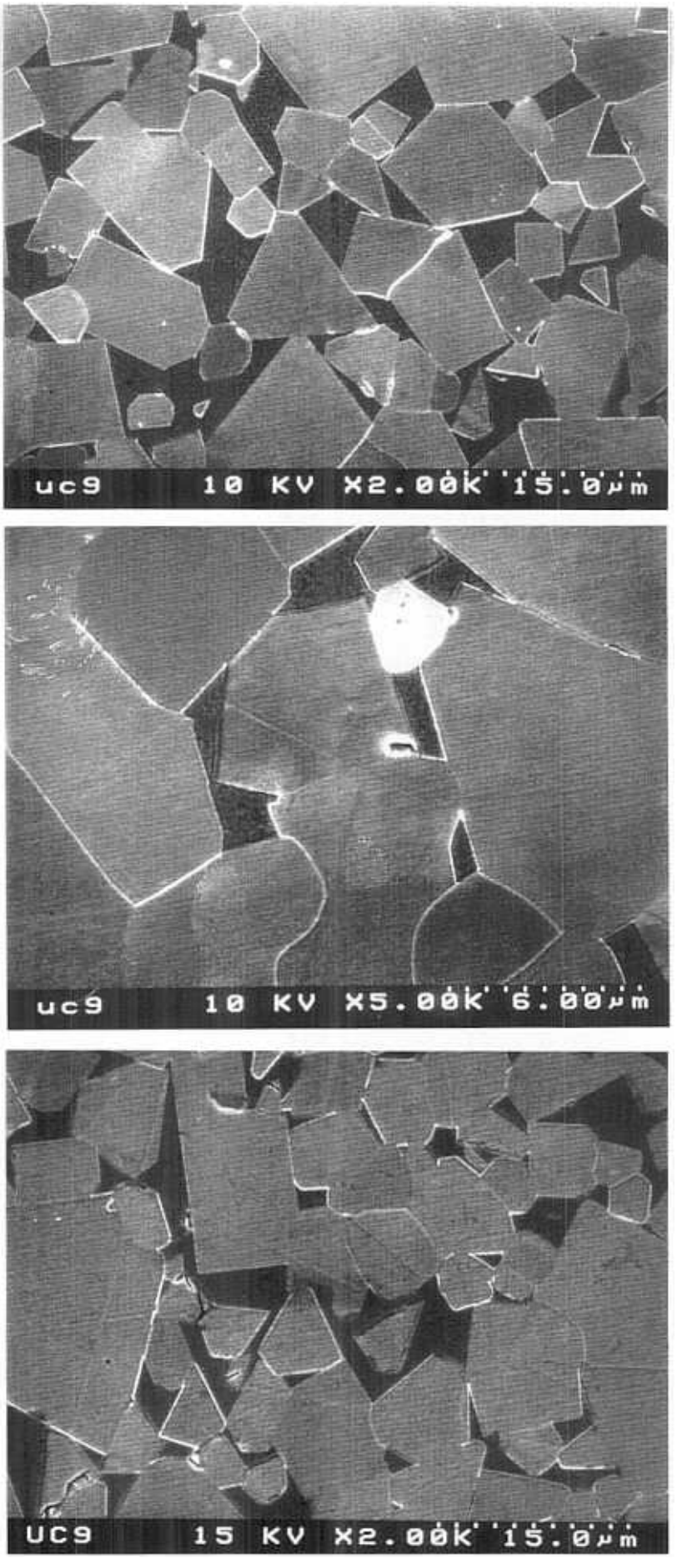
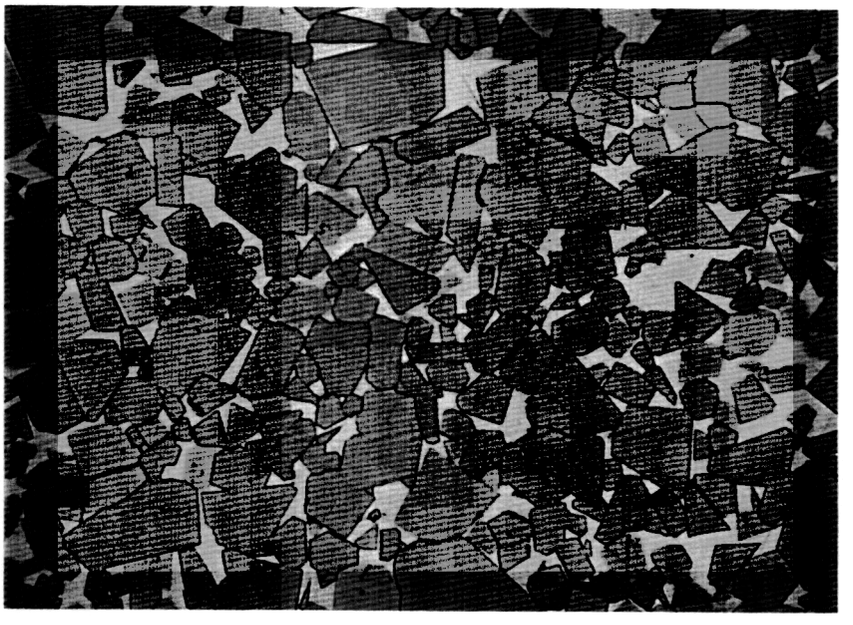
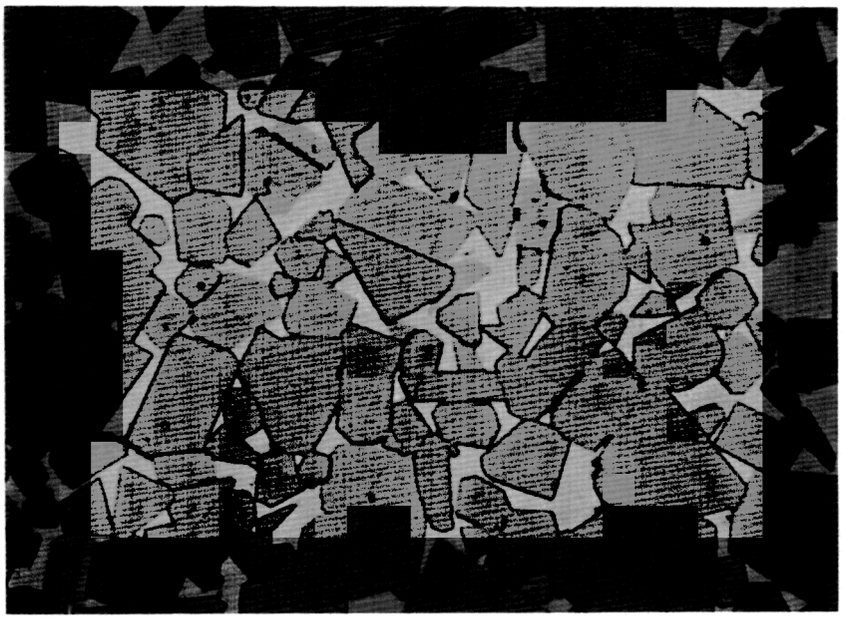


Fig 32 SEM micrographs of uc9





uc9

Fig 33 Optical micrographs of uc9

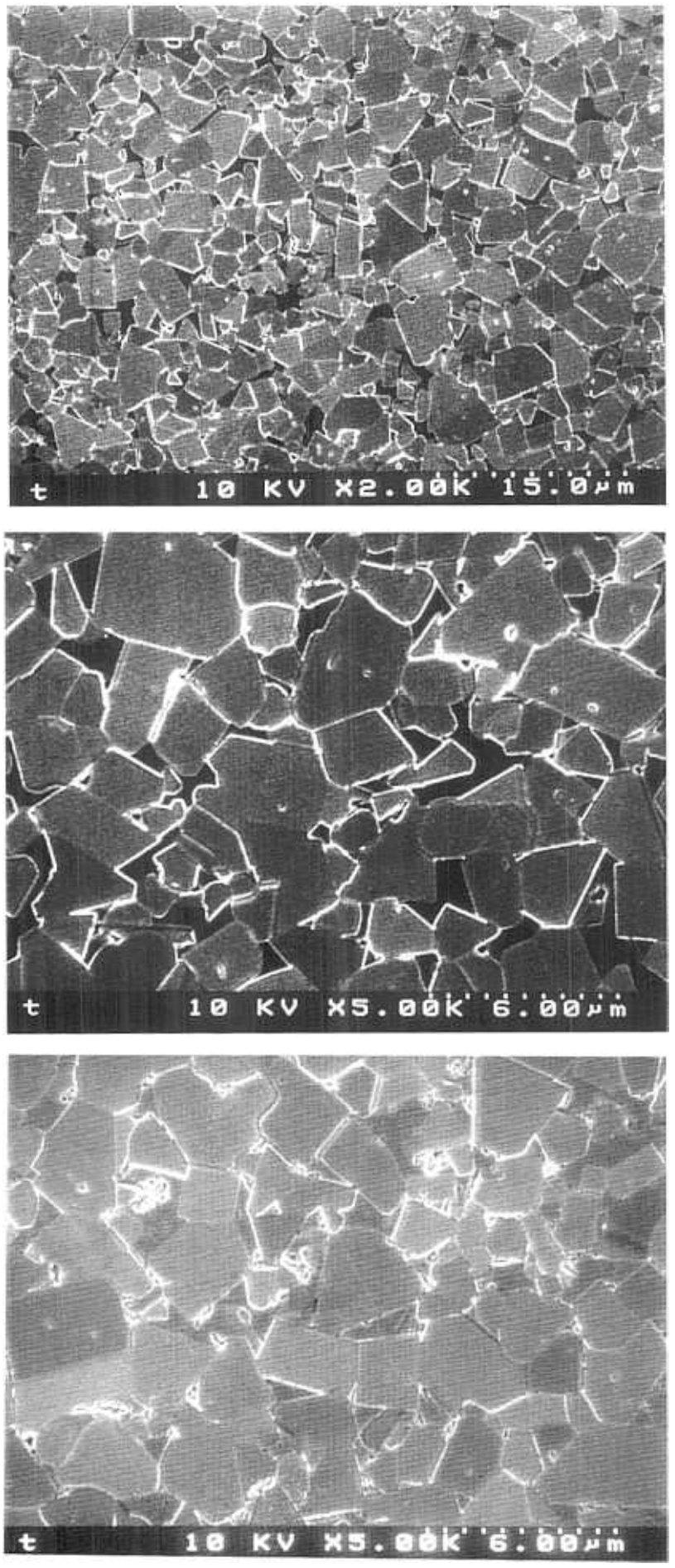
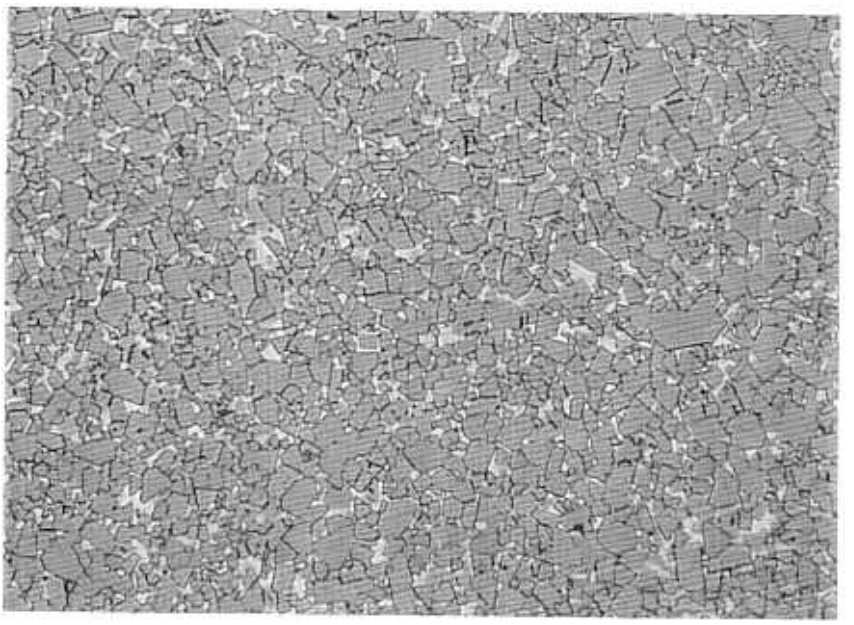
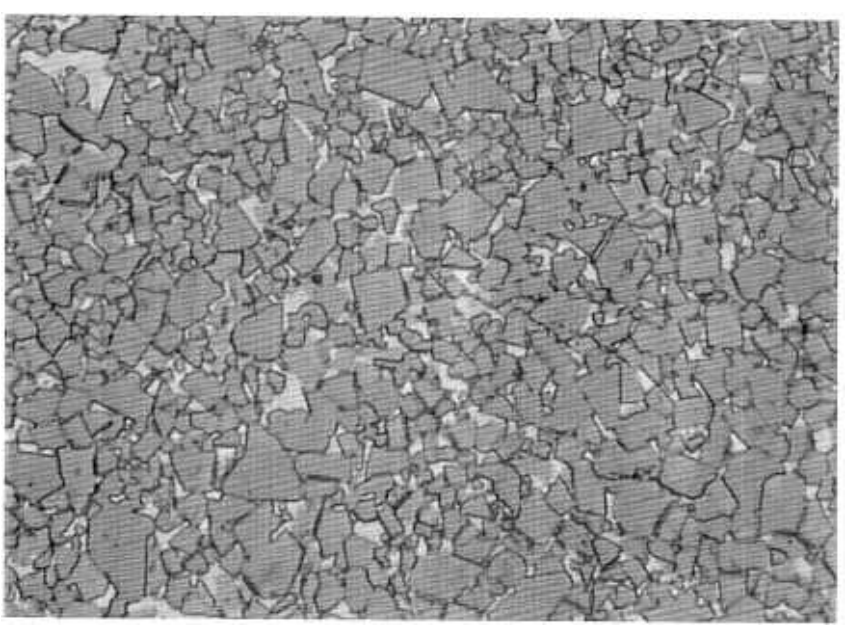


Fig 34 SEM micrographs of t





t

Fig 35 Optical micrographs of t

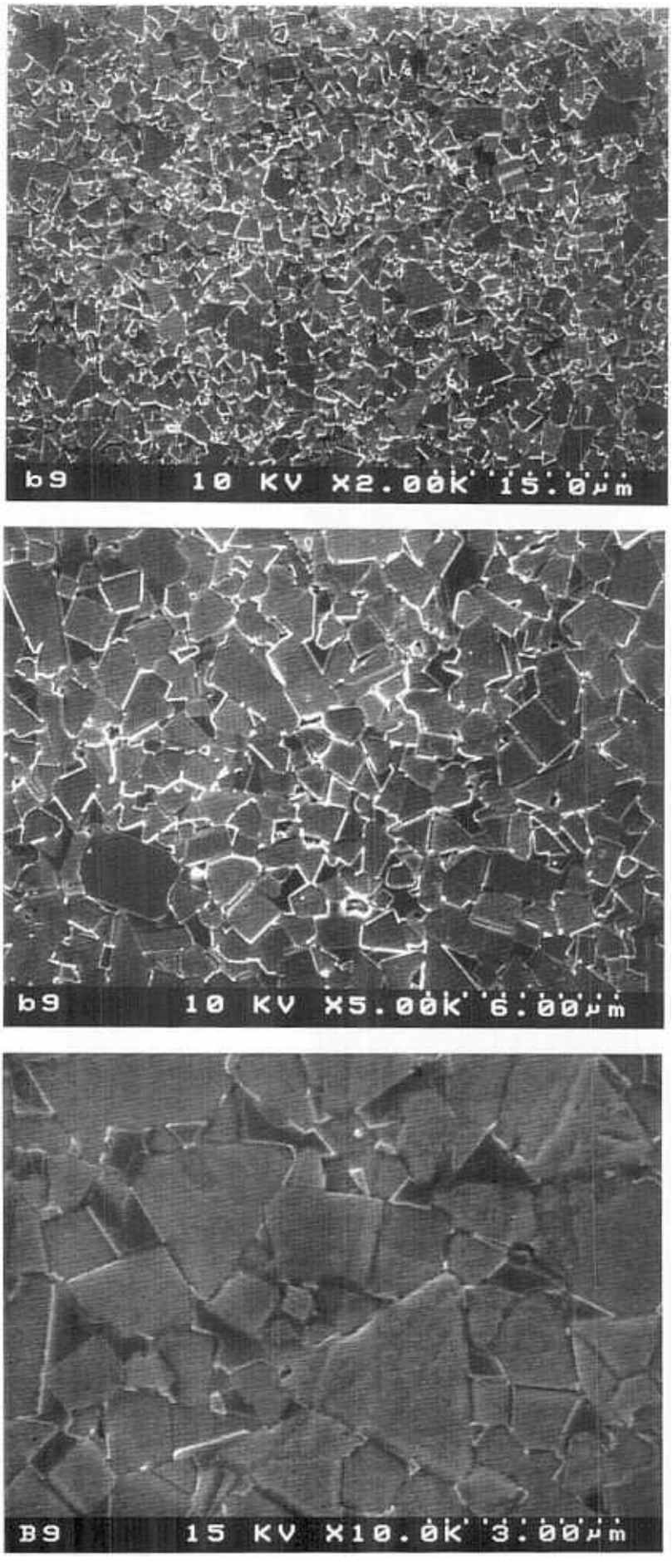
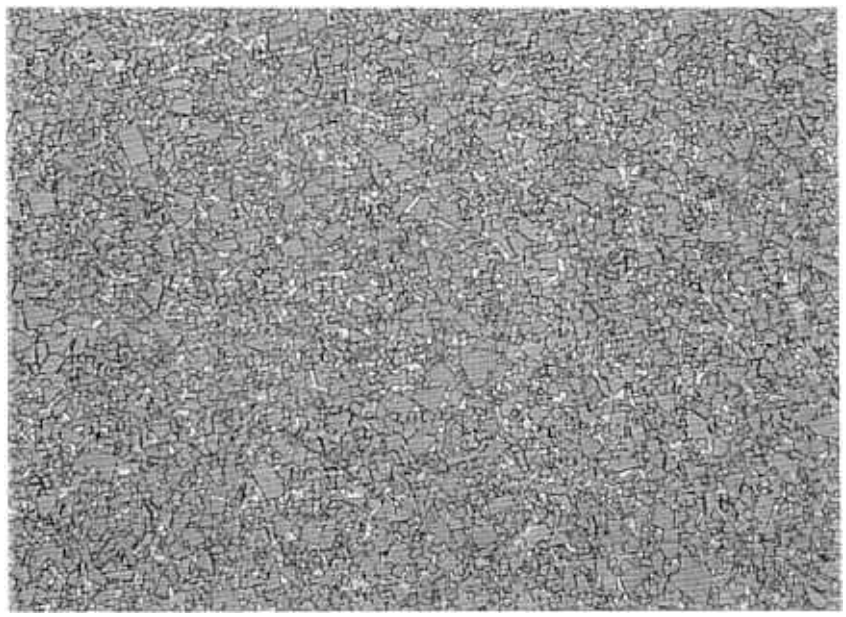
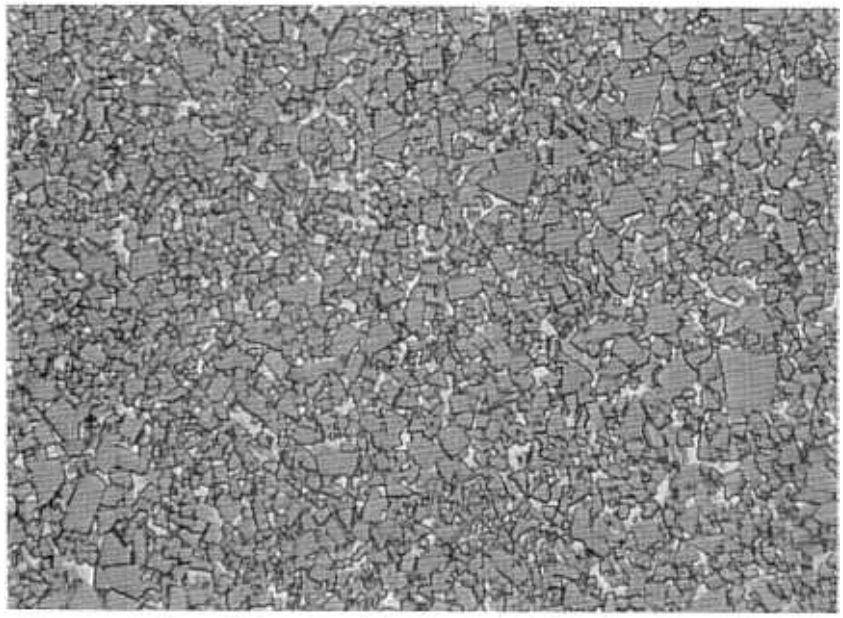


Fig 36 SEM micrographs of b9





b

Fig Optical micrographs of

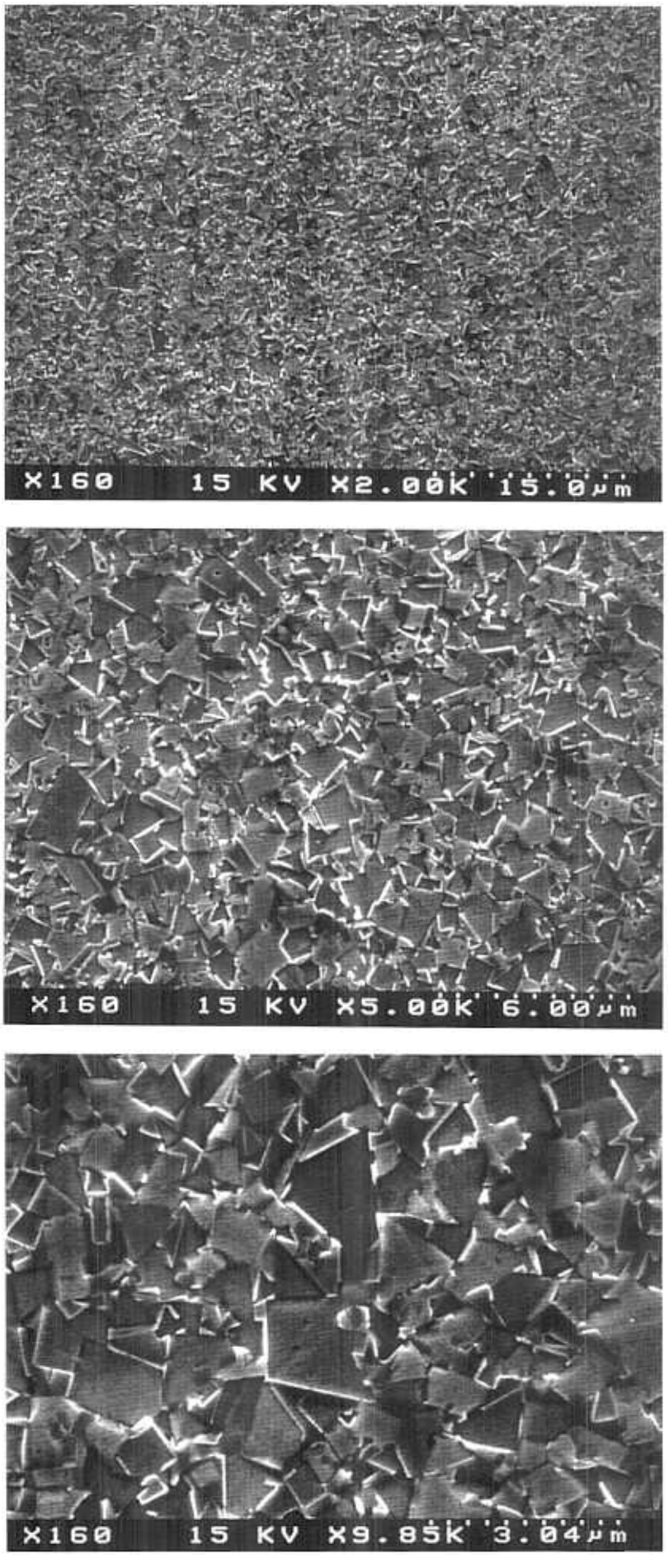
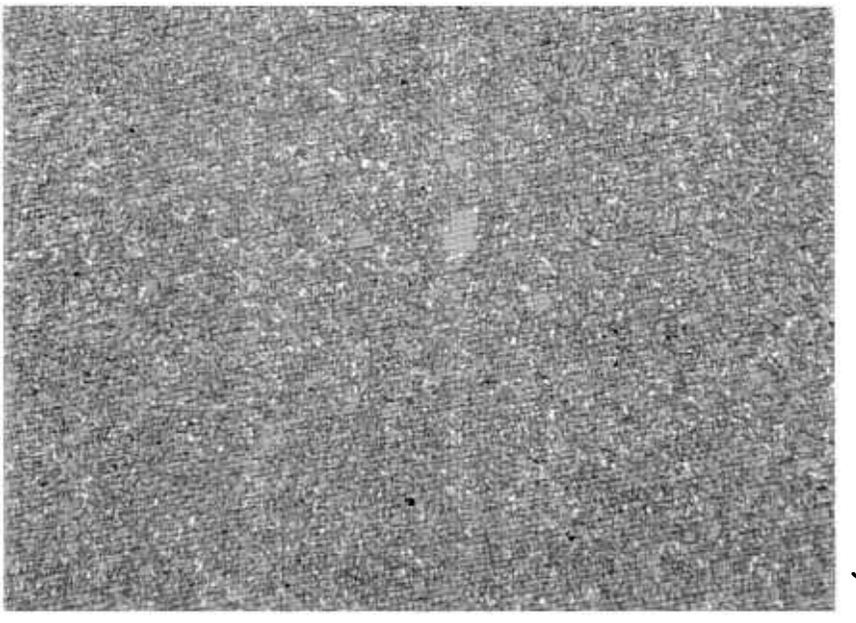
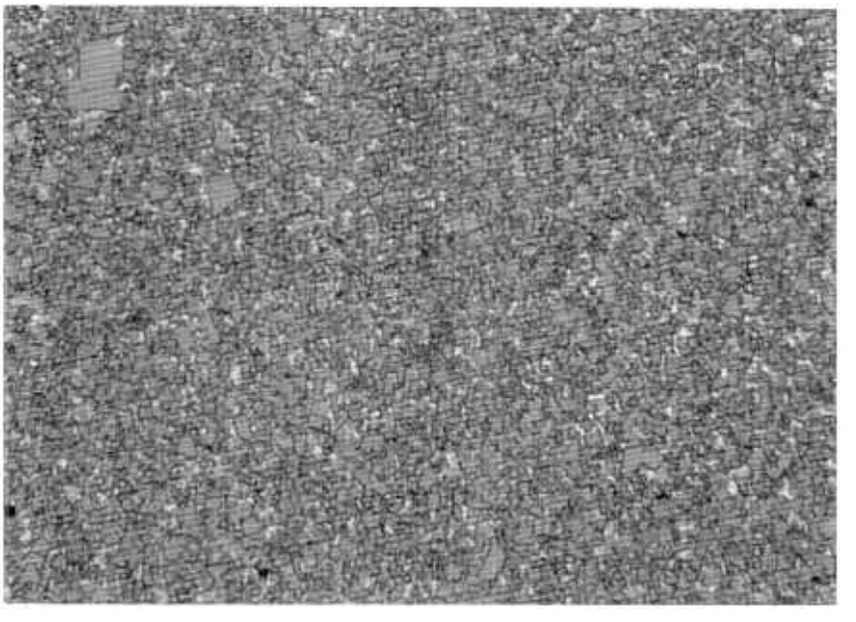


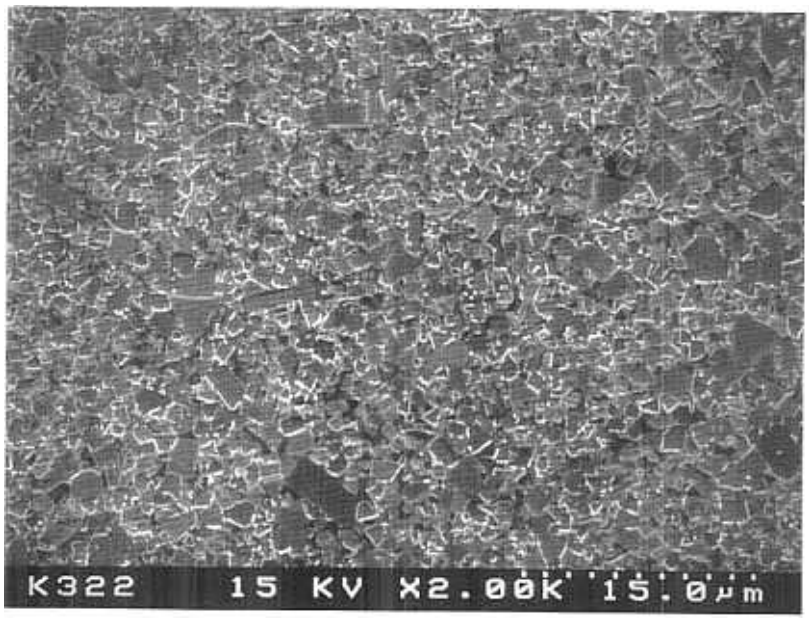
Fig 38 SEM micrographs of x160

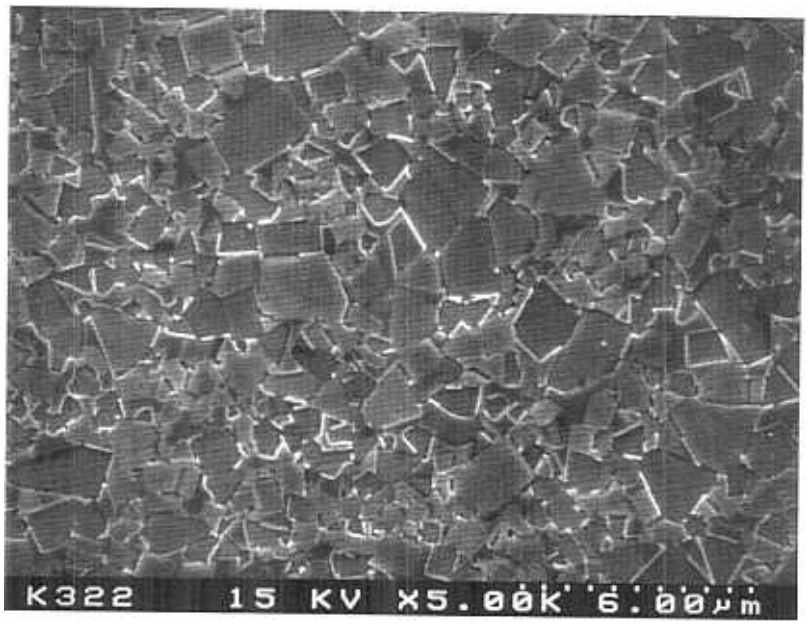




X160

Fig 39 Optical micrographs of x160





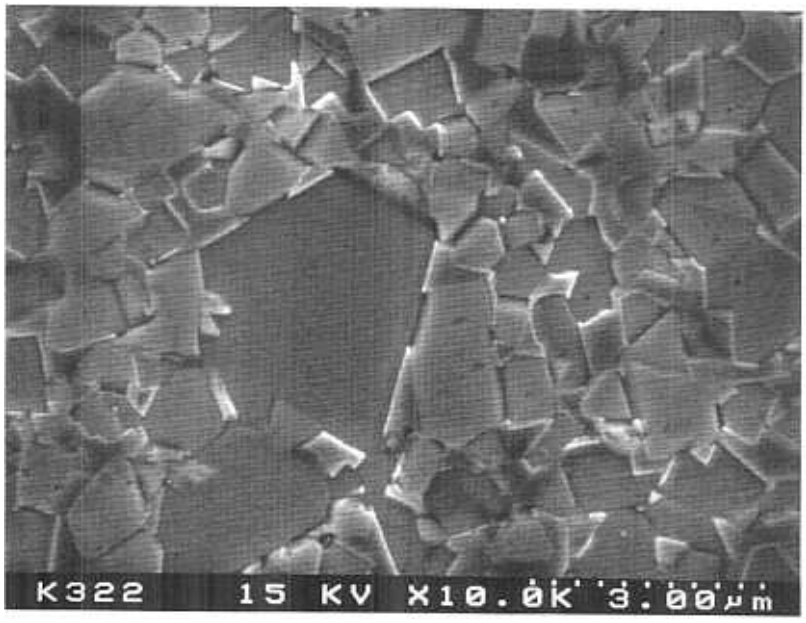
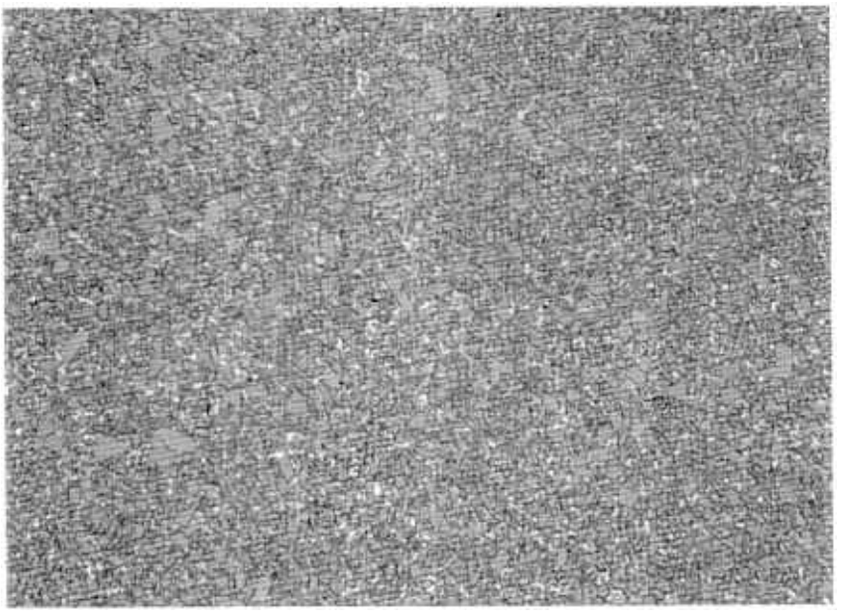
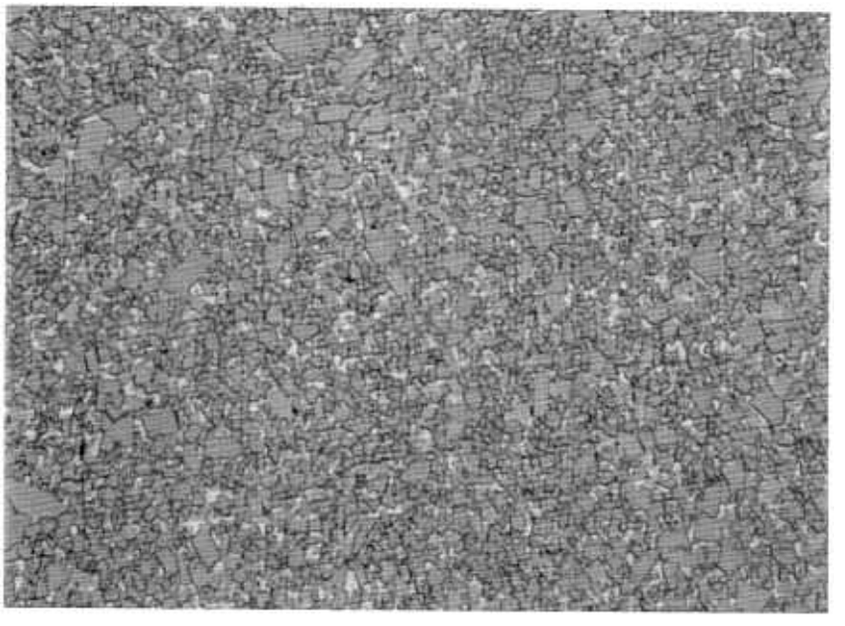


Fig 40 SEM micrographs of k322



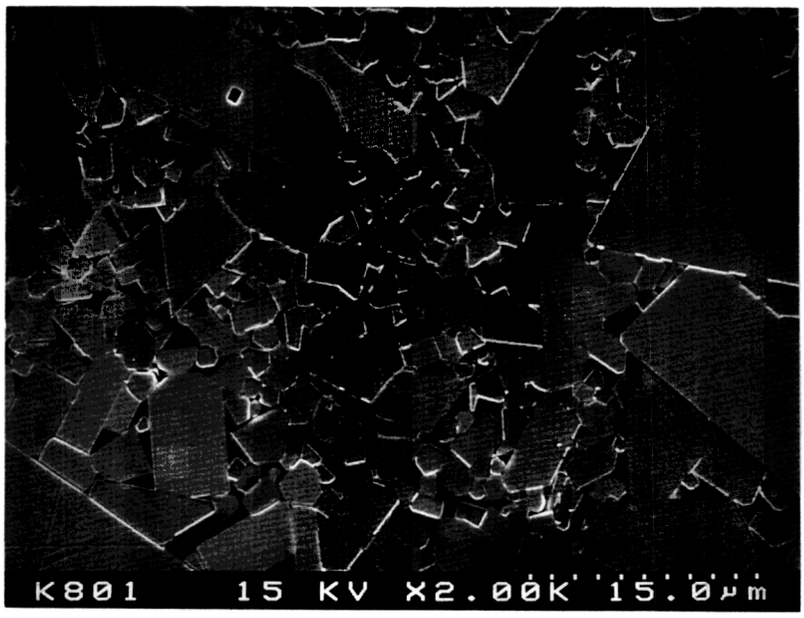
X1000

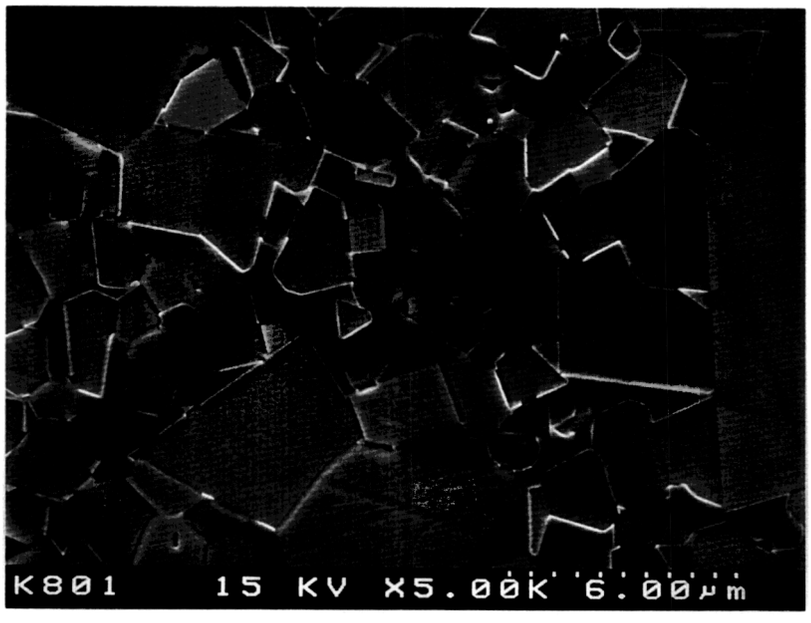


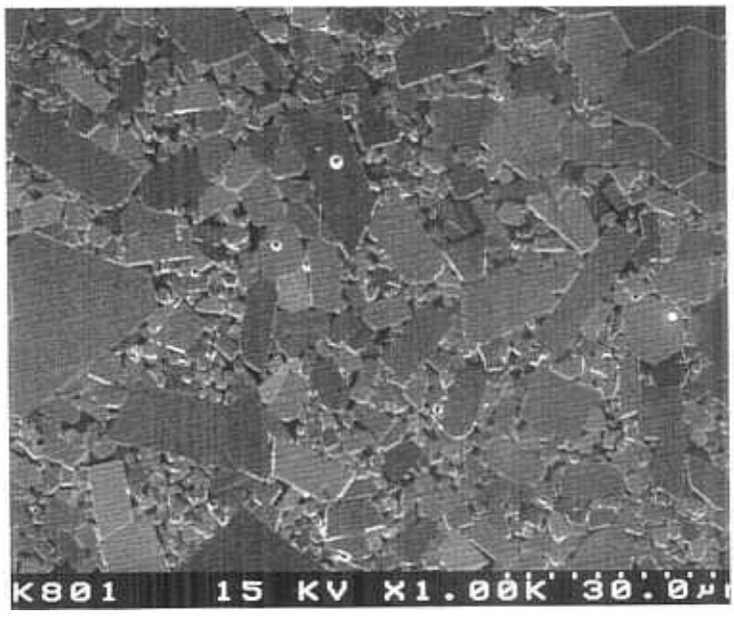
X1500

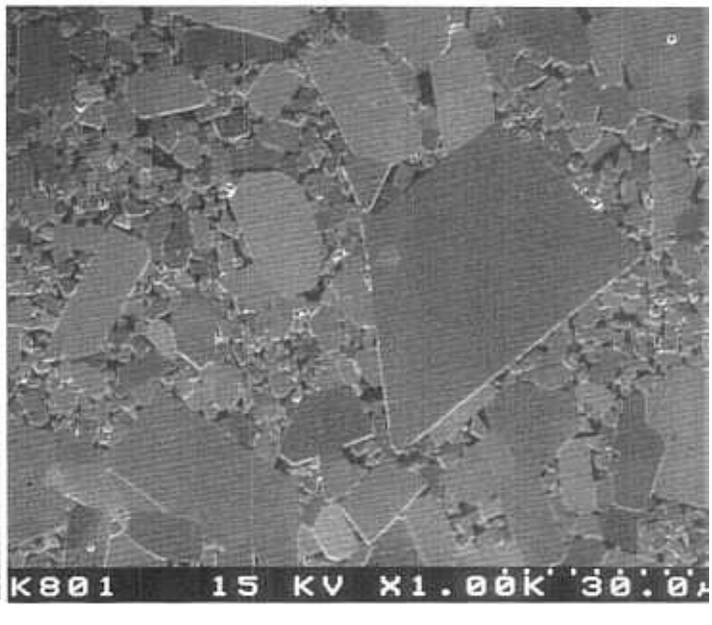
k322

Fig 41 Optical micrographs of k322









SEM tographs k801

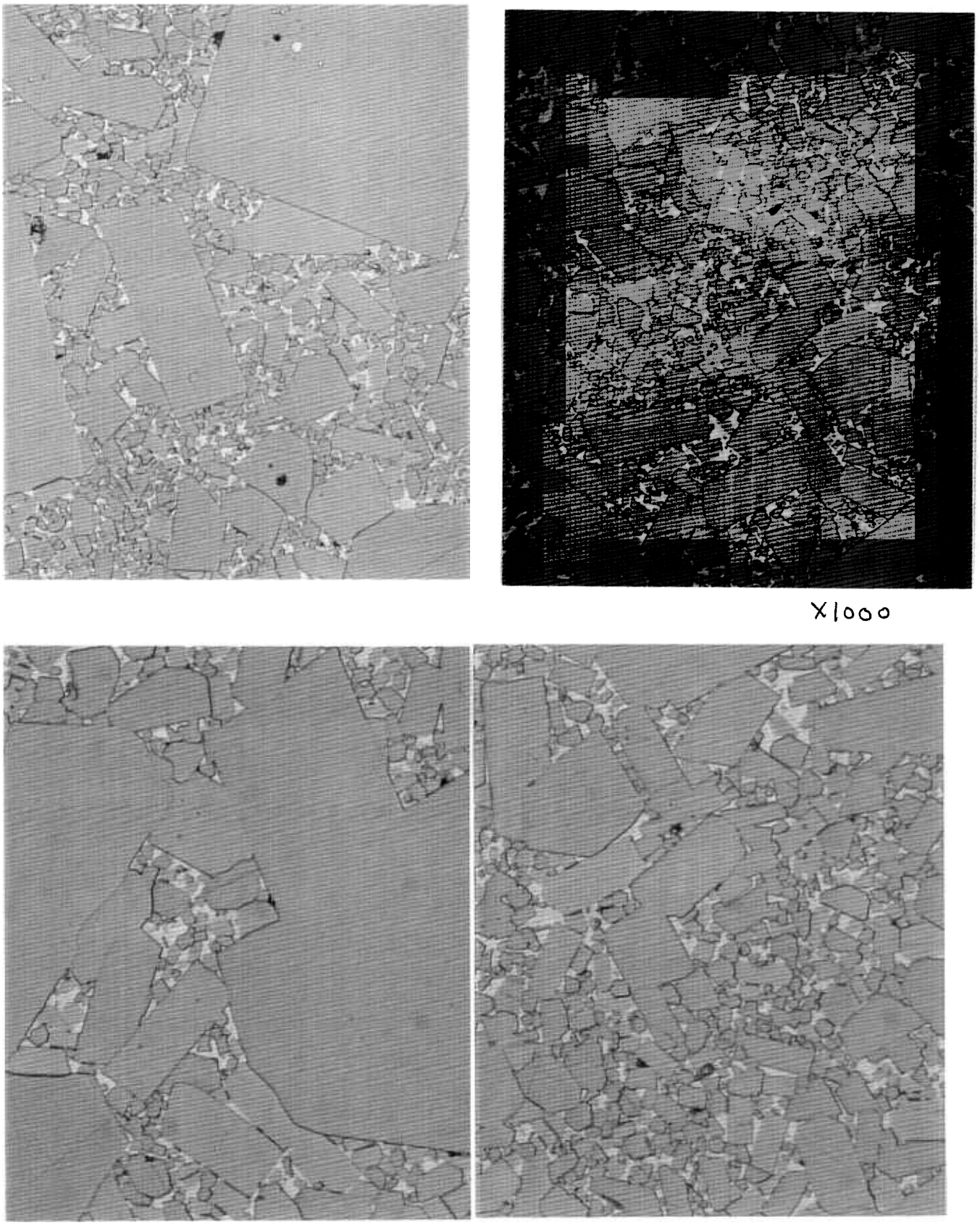


Fig 43 Optical micrographs of k801

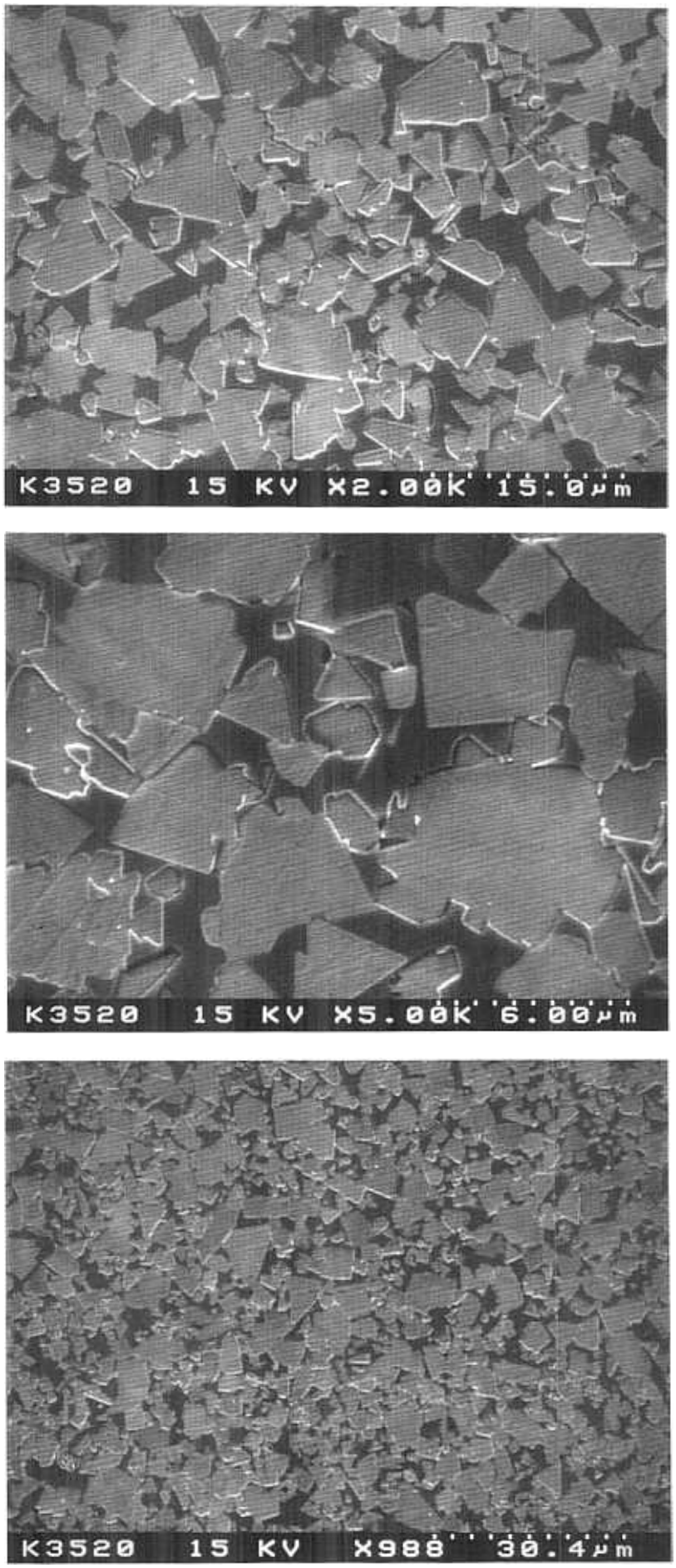
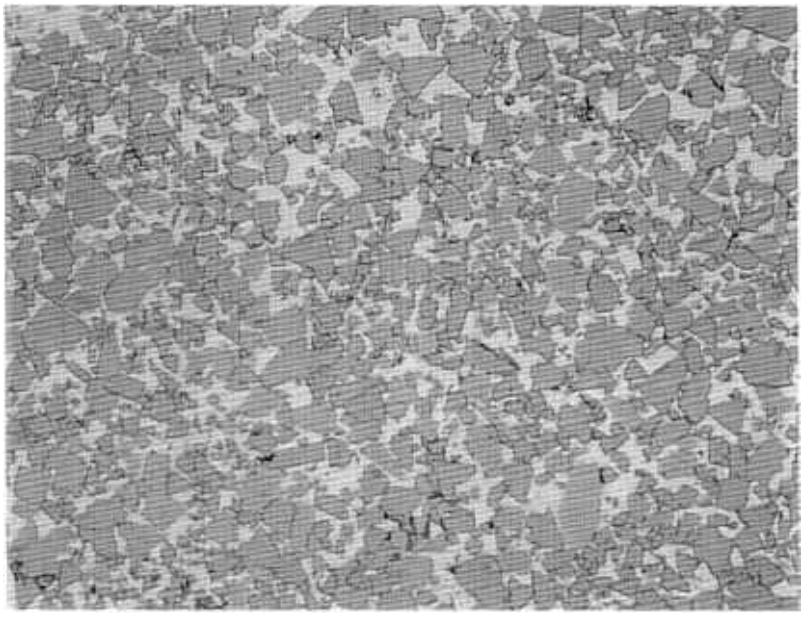
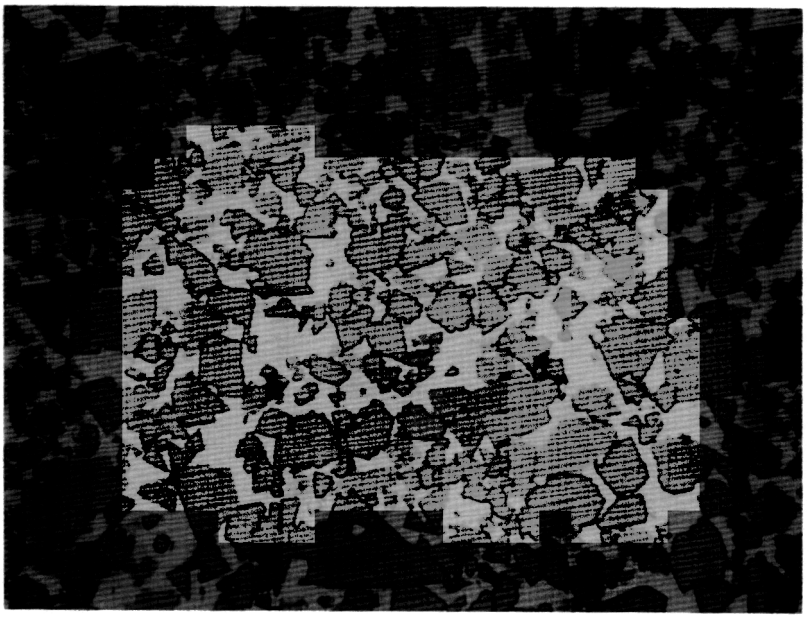


Fig SEM micrographs k3520



X1000



X1500

k3520

Fig 45 Optical micrographs of k3520

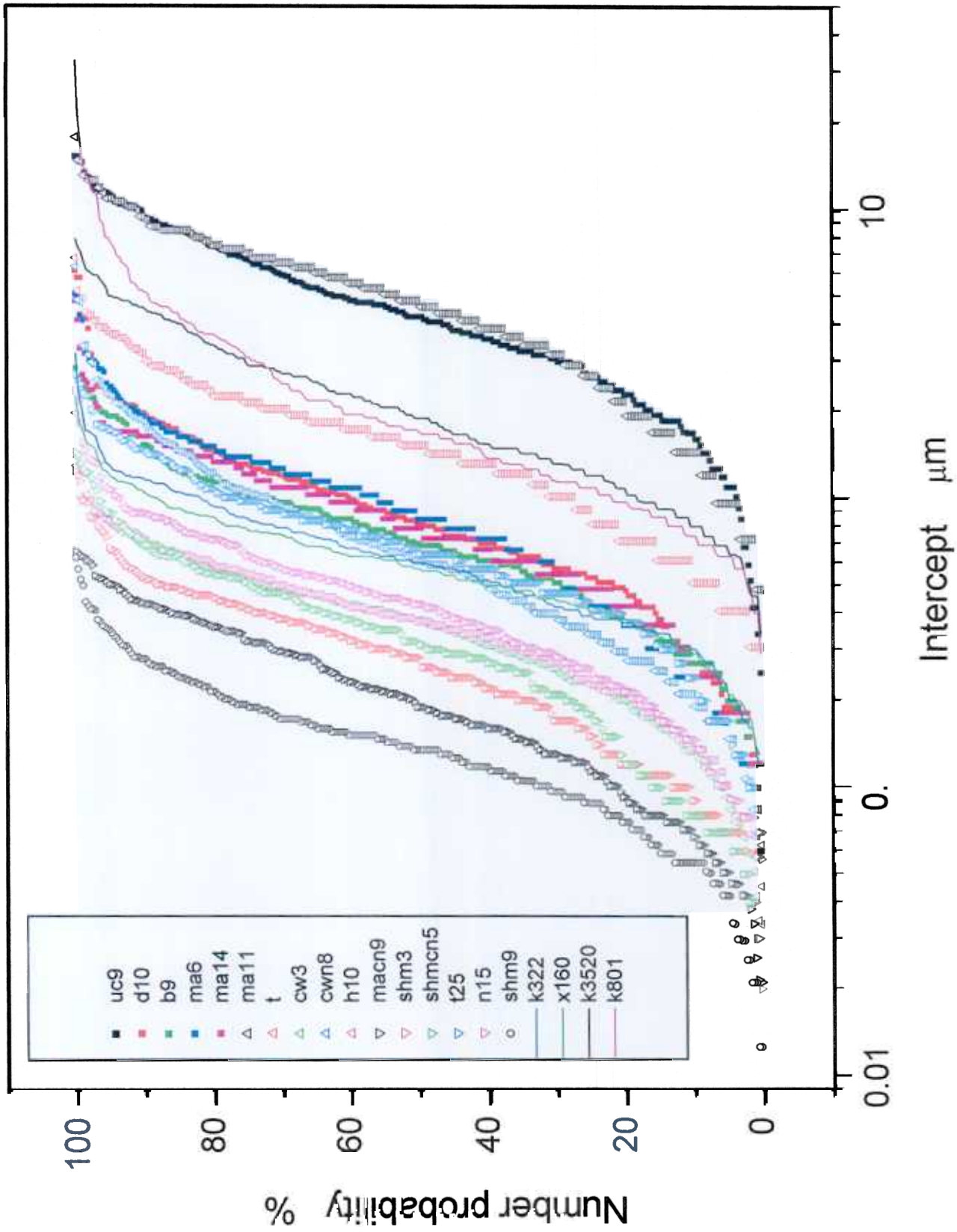


Fig 46 Cumulati number distributi of intercept data for all the materials

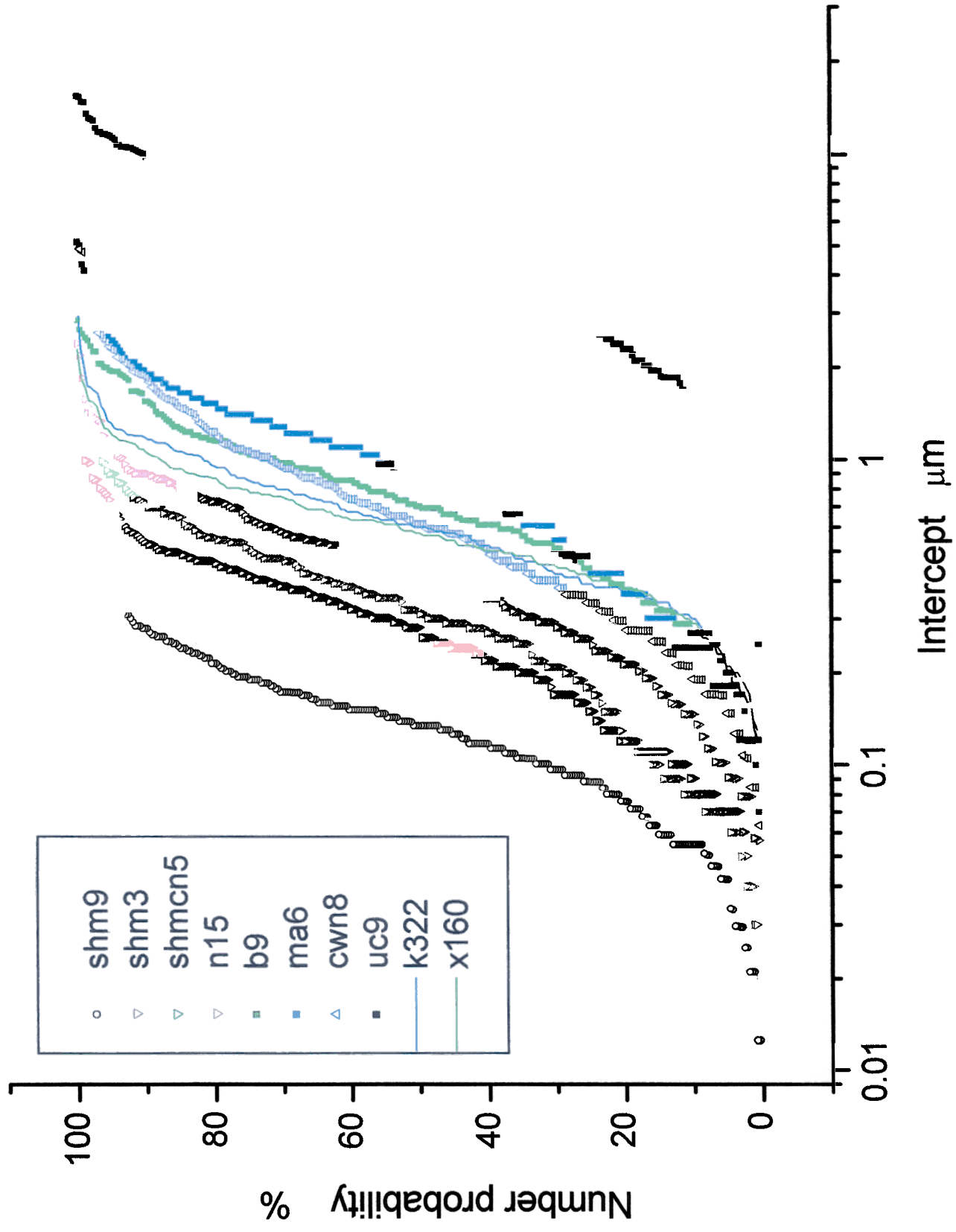


Fig 47 Cumulative number distributions for shm9, shm3, shmcn5, n15, b9, ma6, cwn8, uc9, k322 and x160

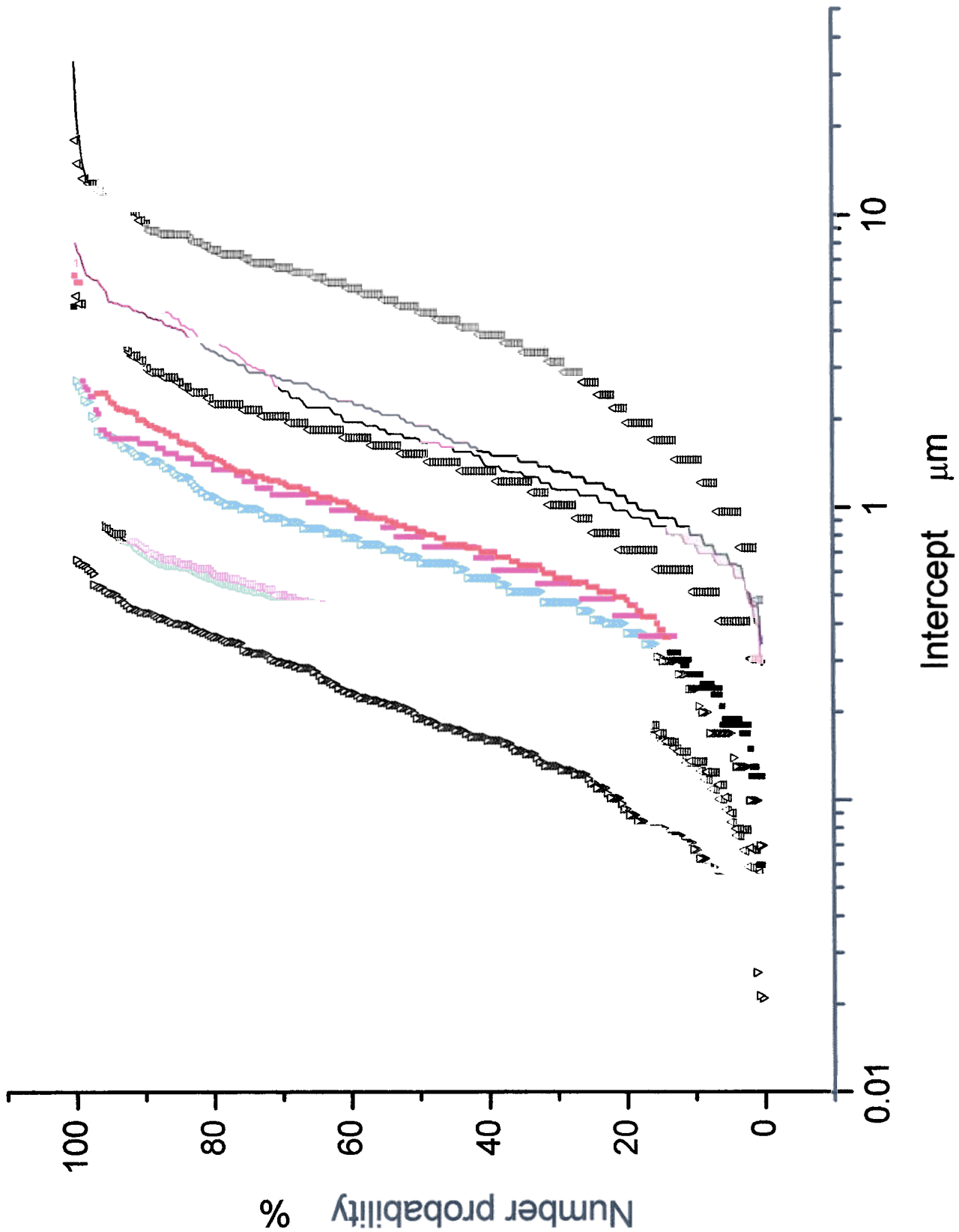


Fig 48 Cumulative number distributions for macn9, cw3, h10, t25, ma14, d10, t, ma11, k3520 and k801

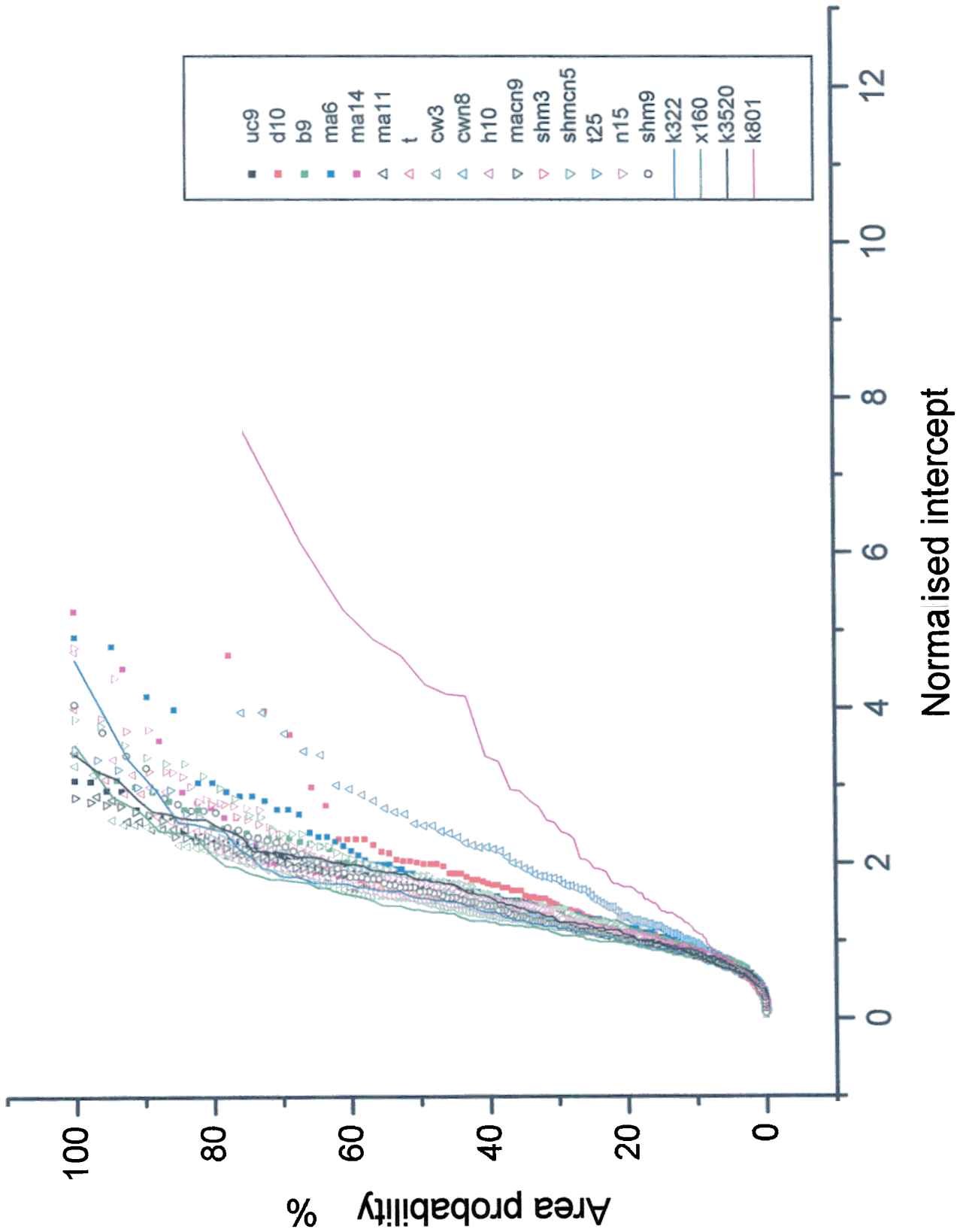


Fig 49 Size distribution of intercept squared data plotted against normalised intercepts for all the materials

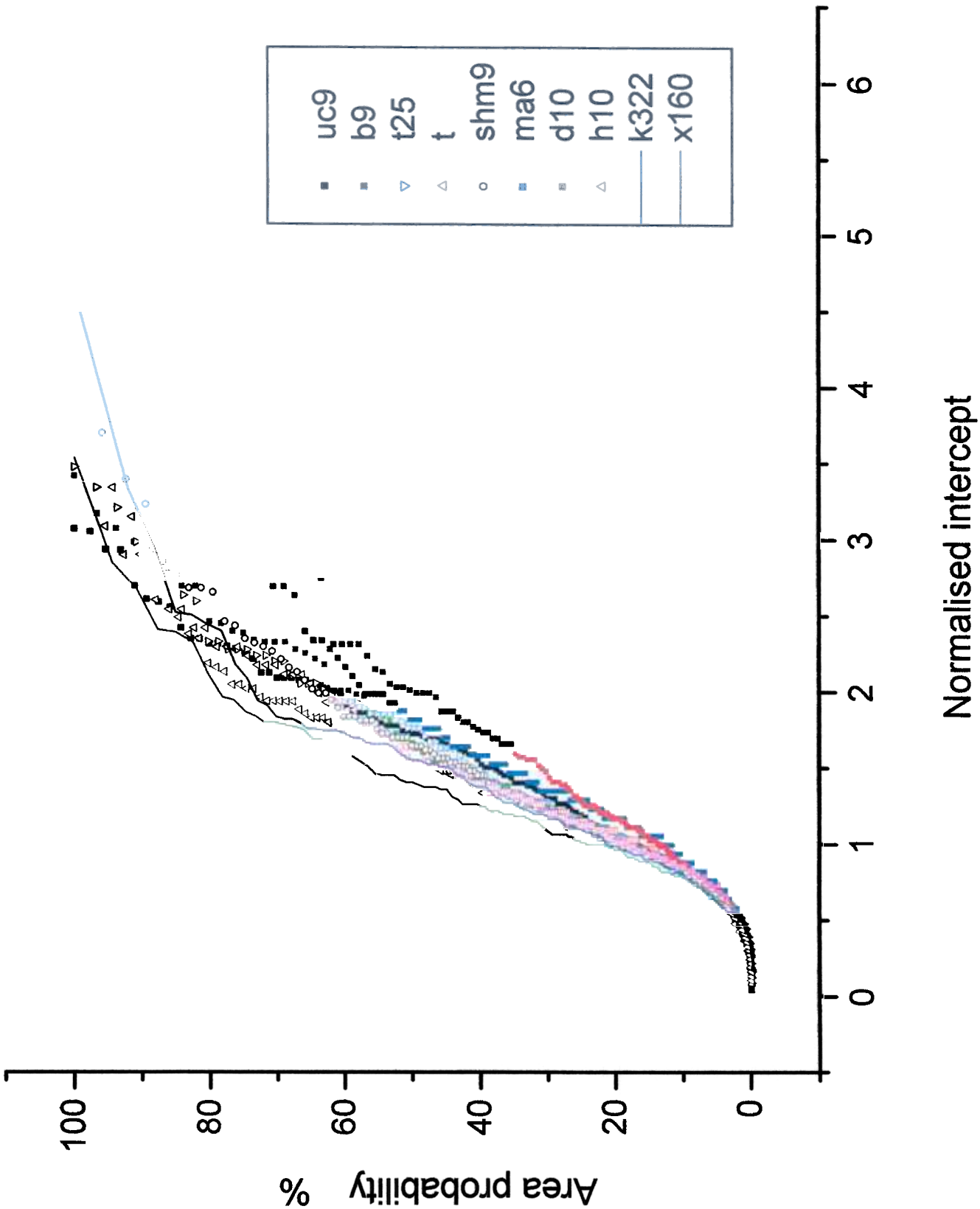


Fig 50 Cumulative size distributions for shm9, shm3, shmcn5, n15, b9, ma6, cwn8, uc9, k322 and x160

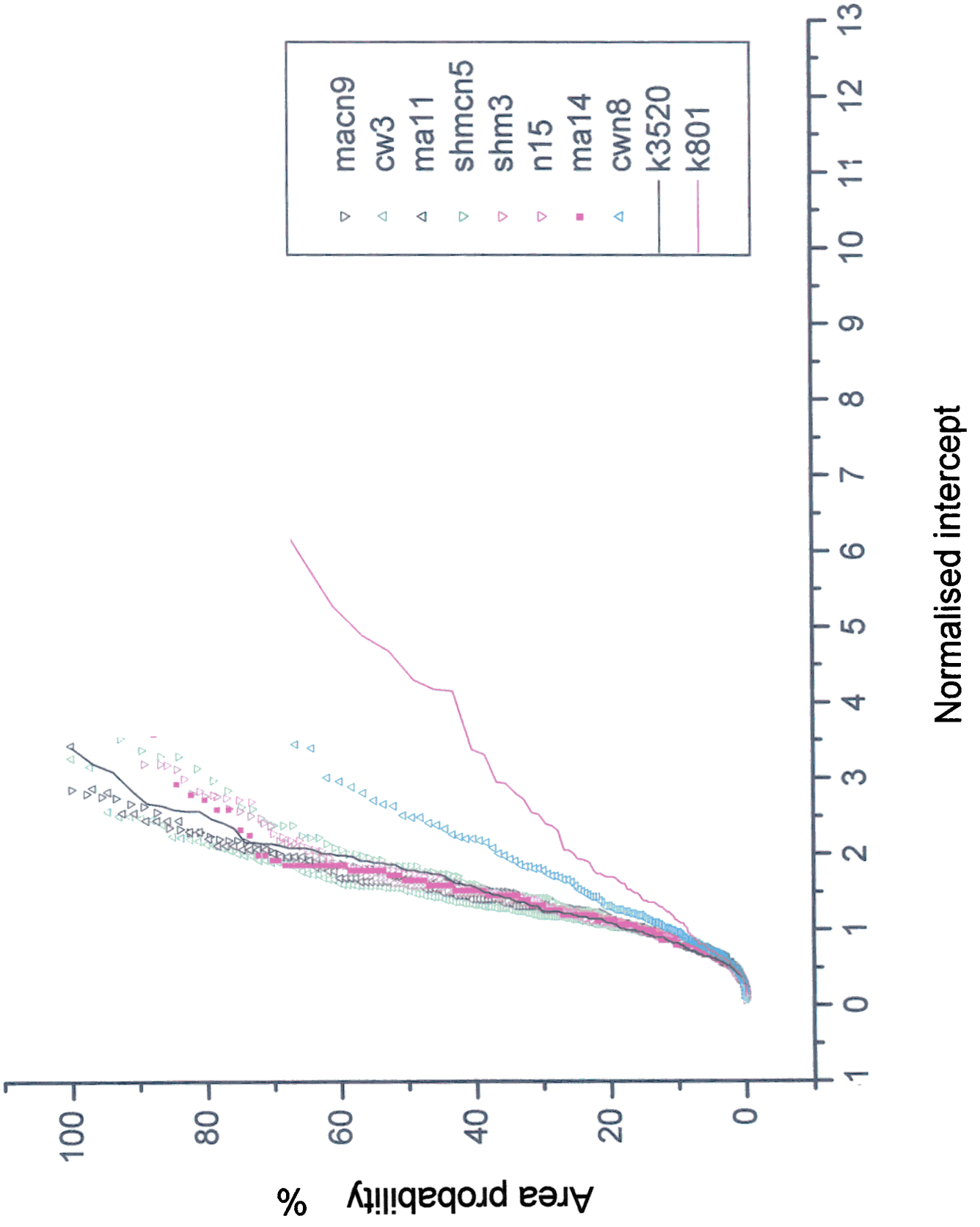


Fig 51 Cumulative size distributions for macn9, cw3, h10, t25, ma14, d10, t, ma11, k3520 and k801

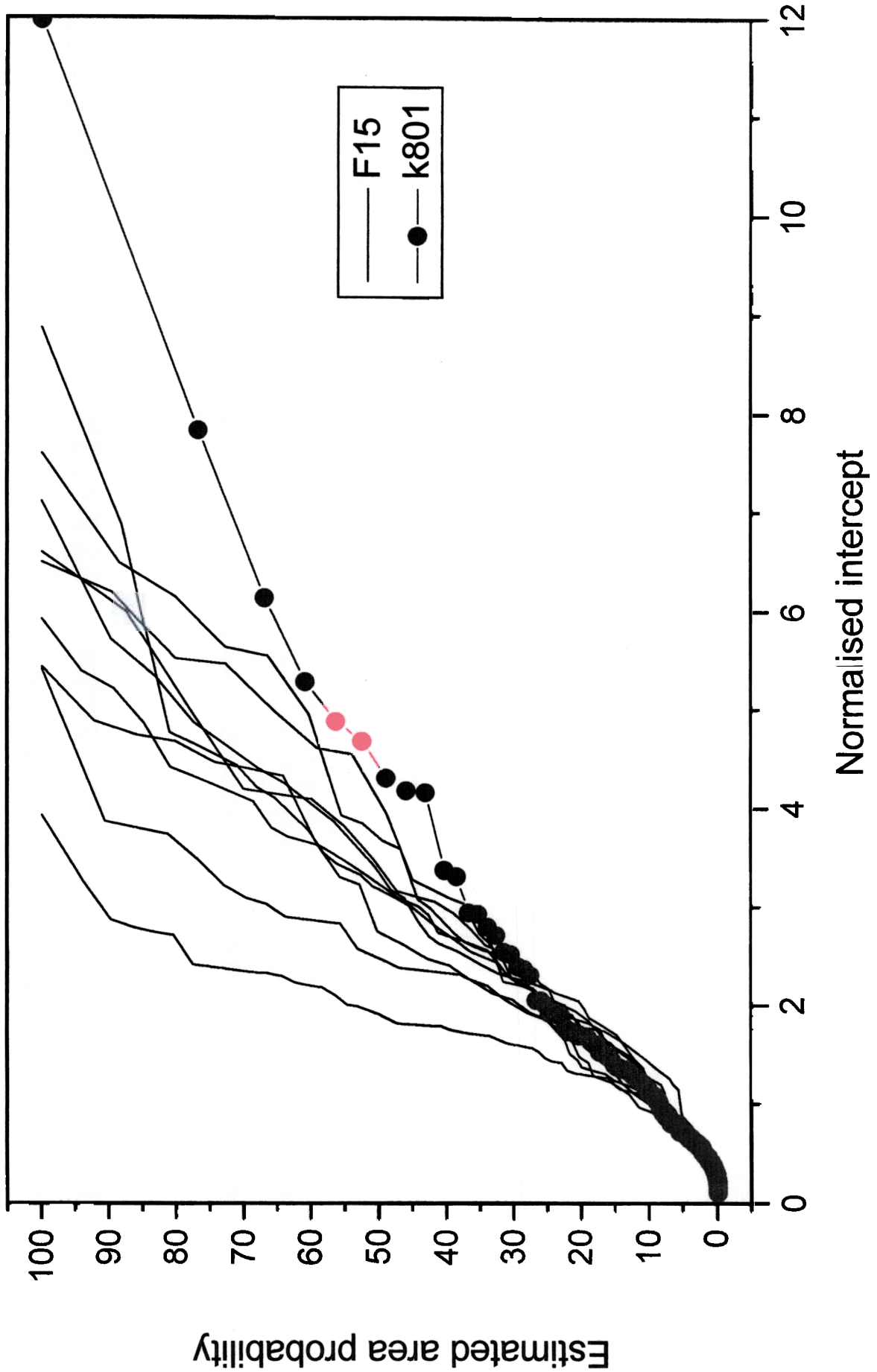


Fig 52 Comparison of WC size distribution data for k801 and material F15

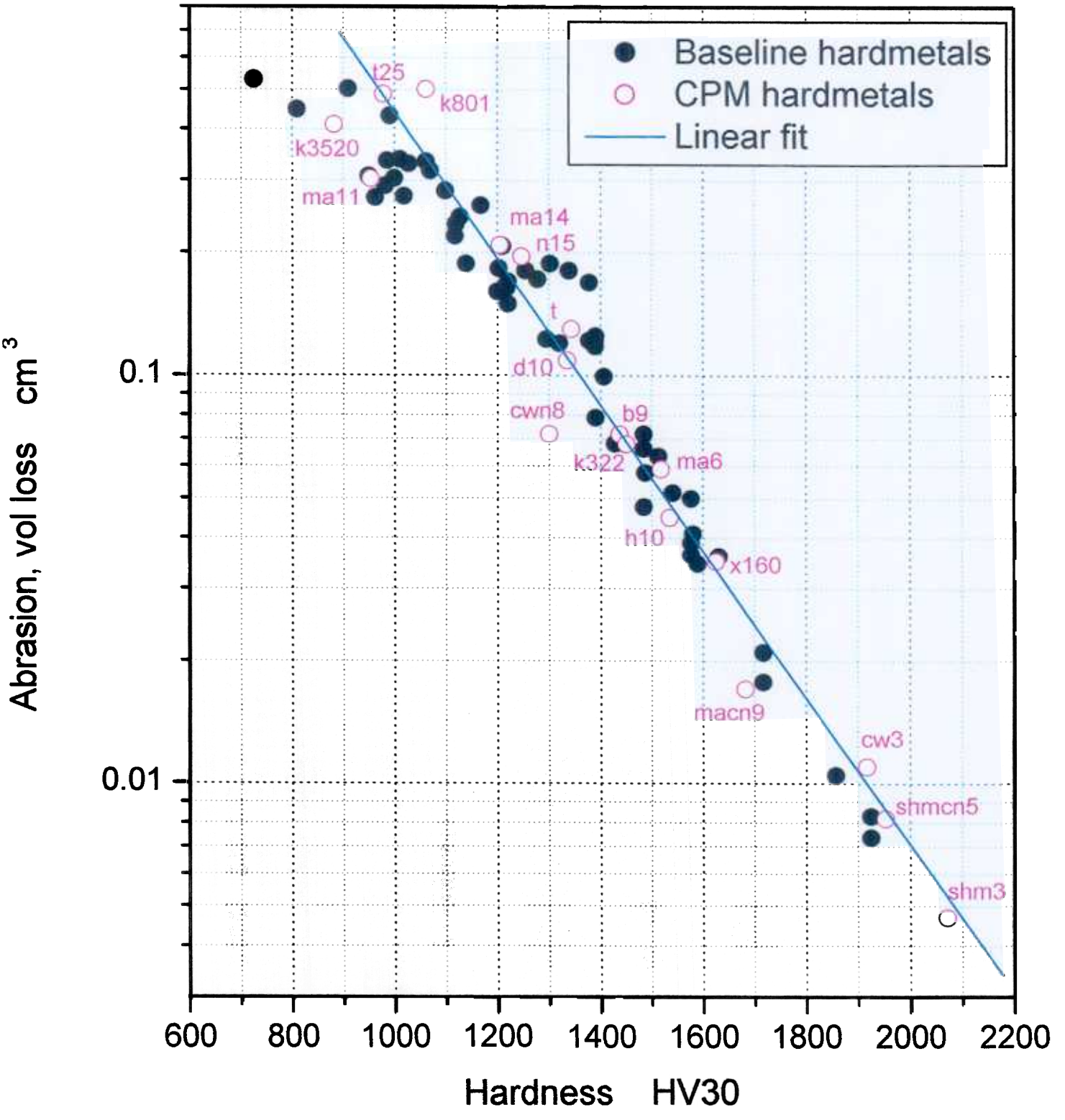
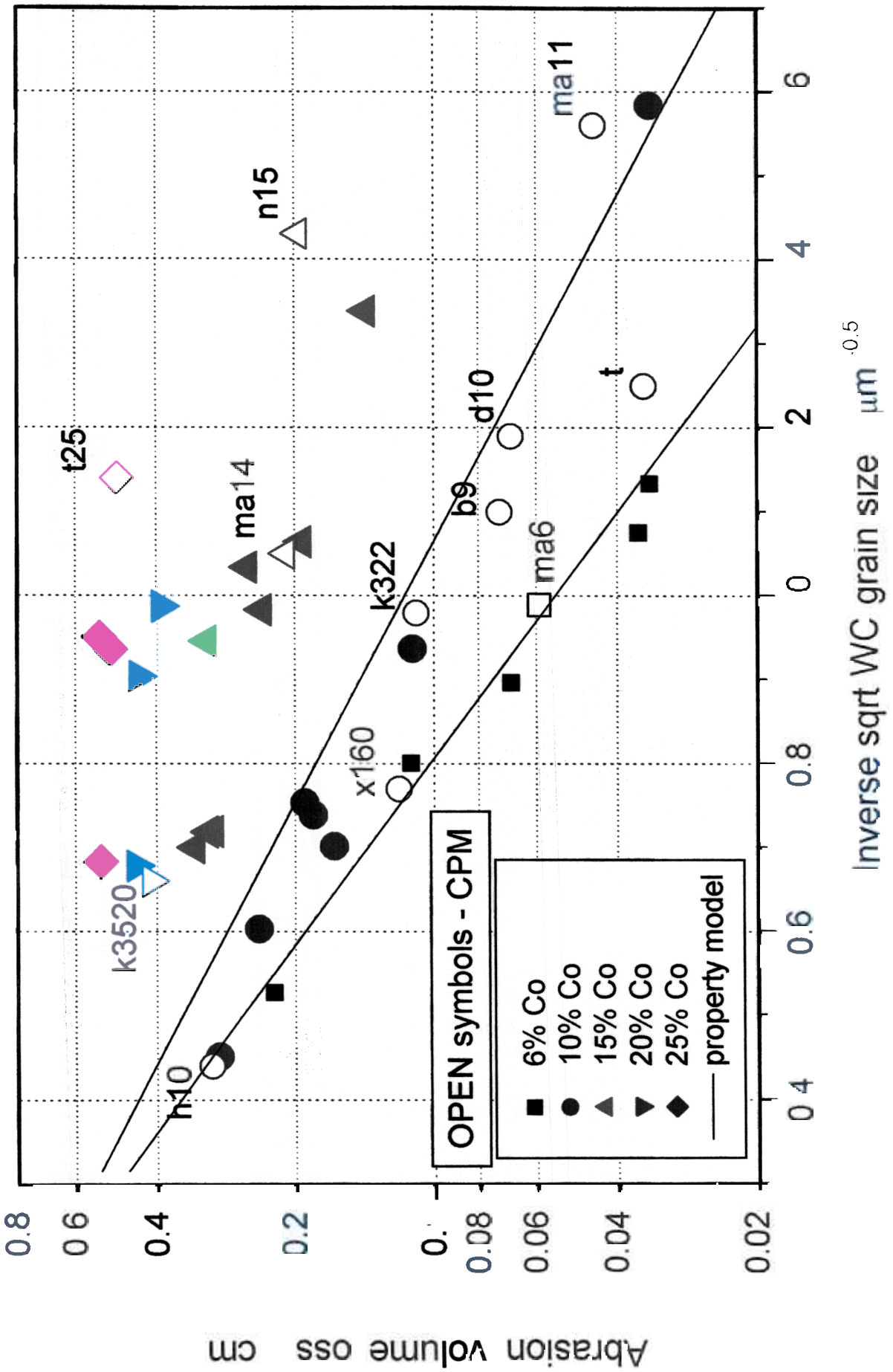


Fig 53 Abrasion test results



Fi 54 Abras ume loss)/in square root grain size for CPM materials

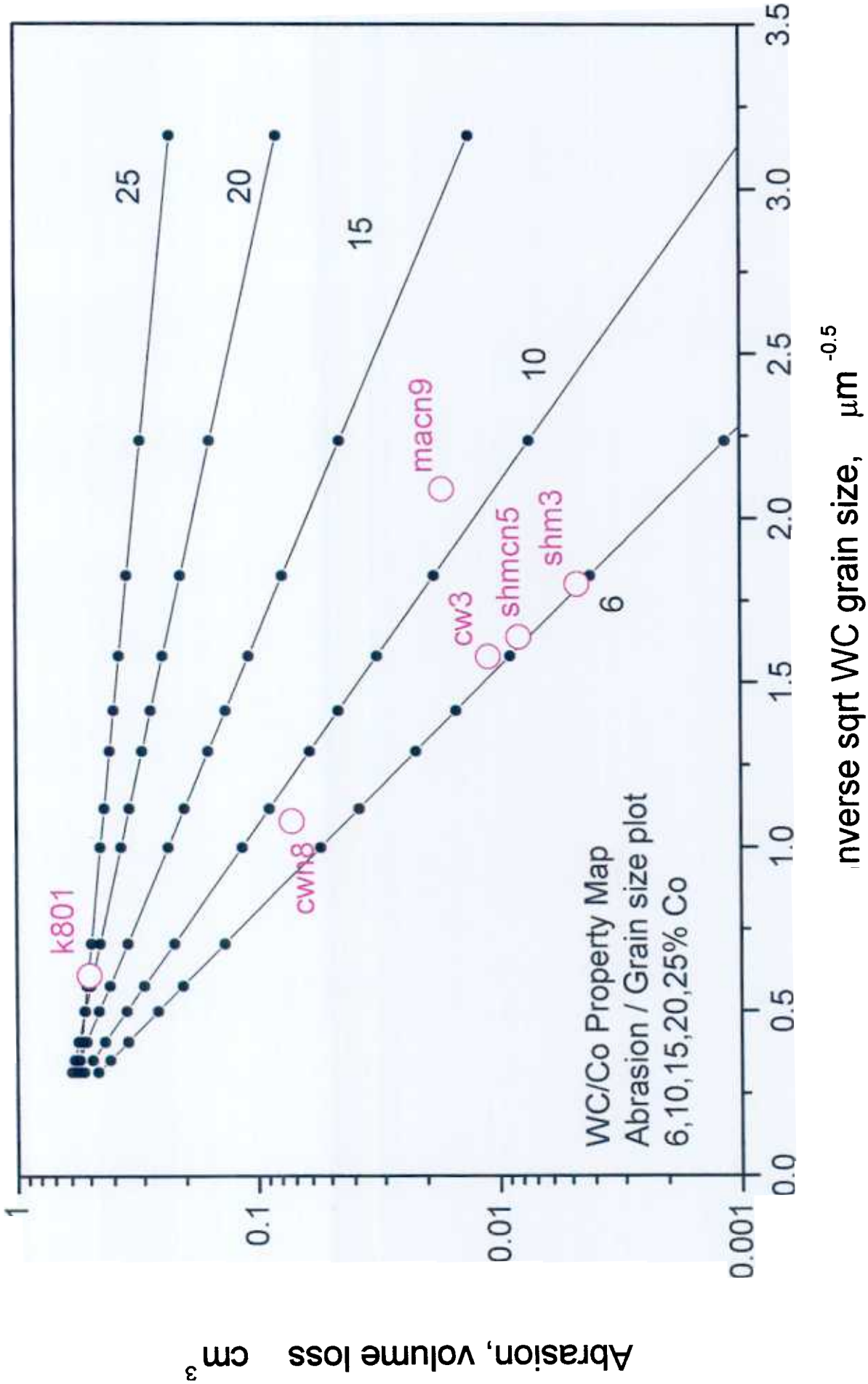


Fig 55 Abrasion property map for non-standard CPM materials

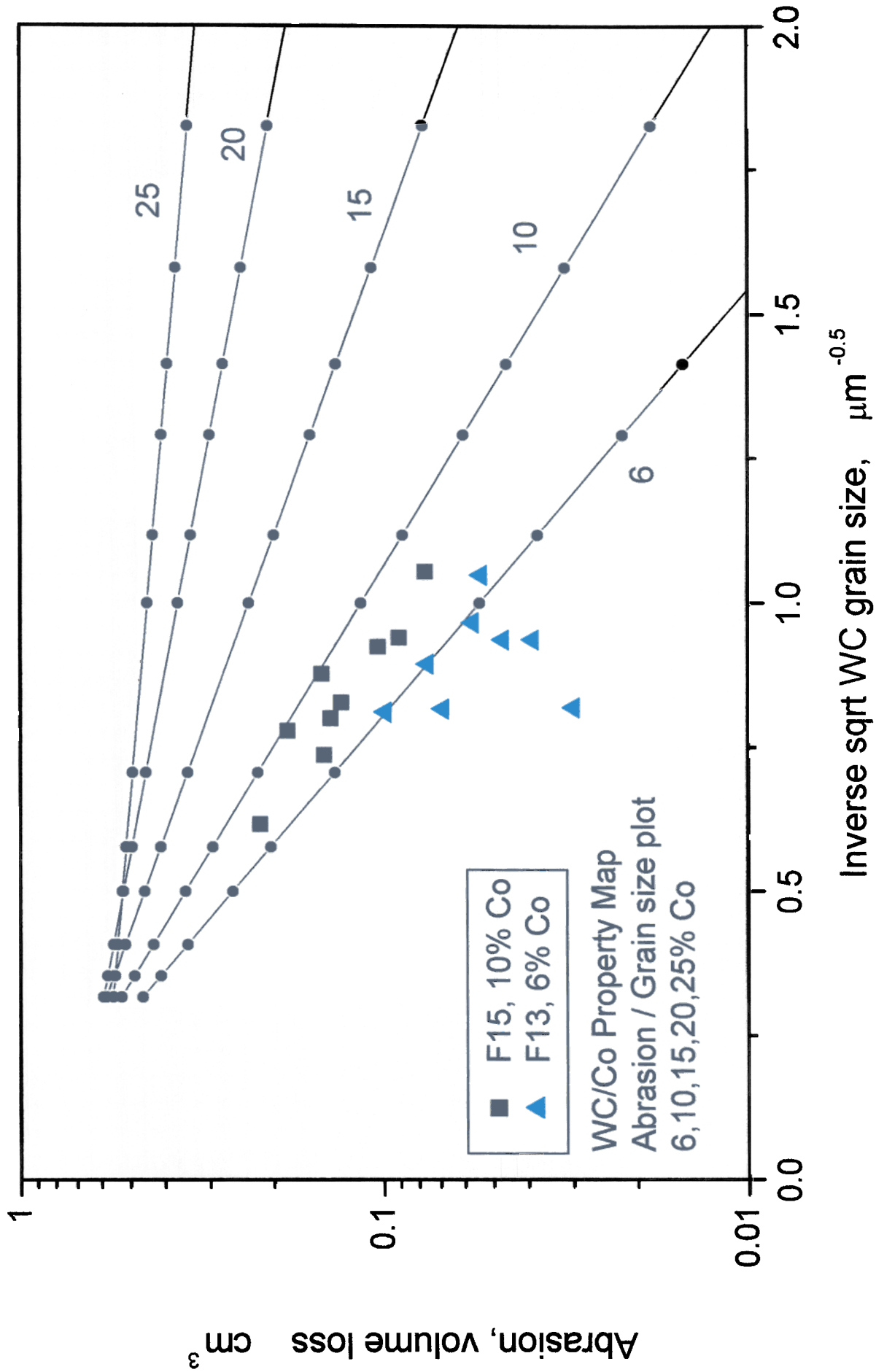


Fig 56 Abrasion property map for the wide grained hardmetals

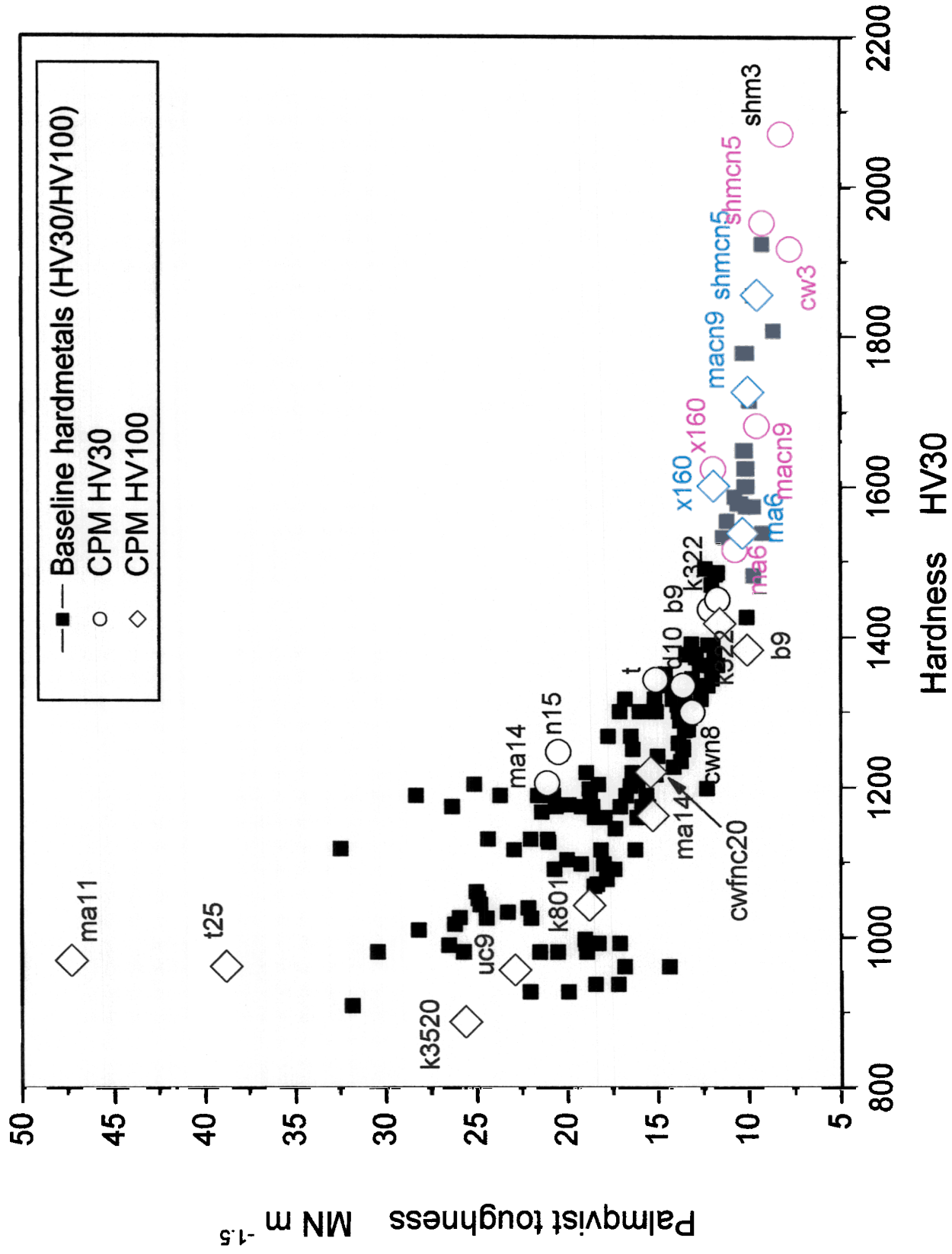


Fig 57 Palmqvist test results compared with previous data

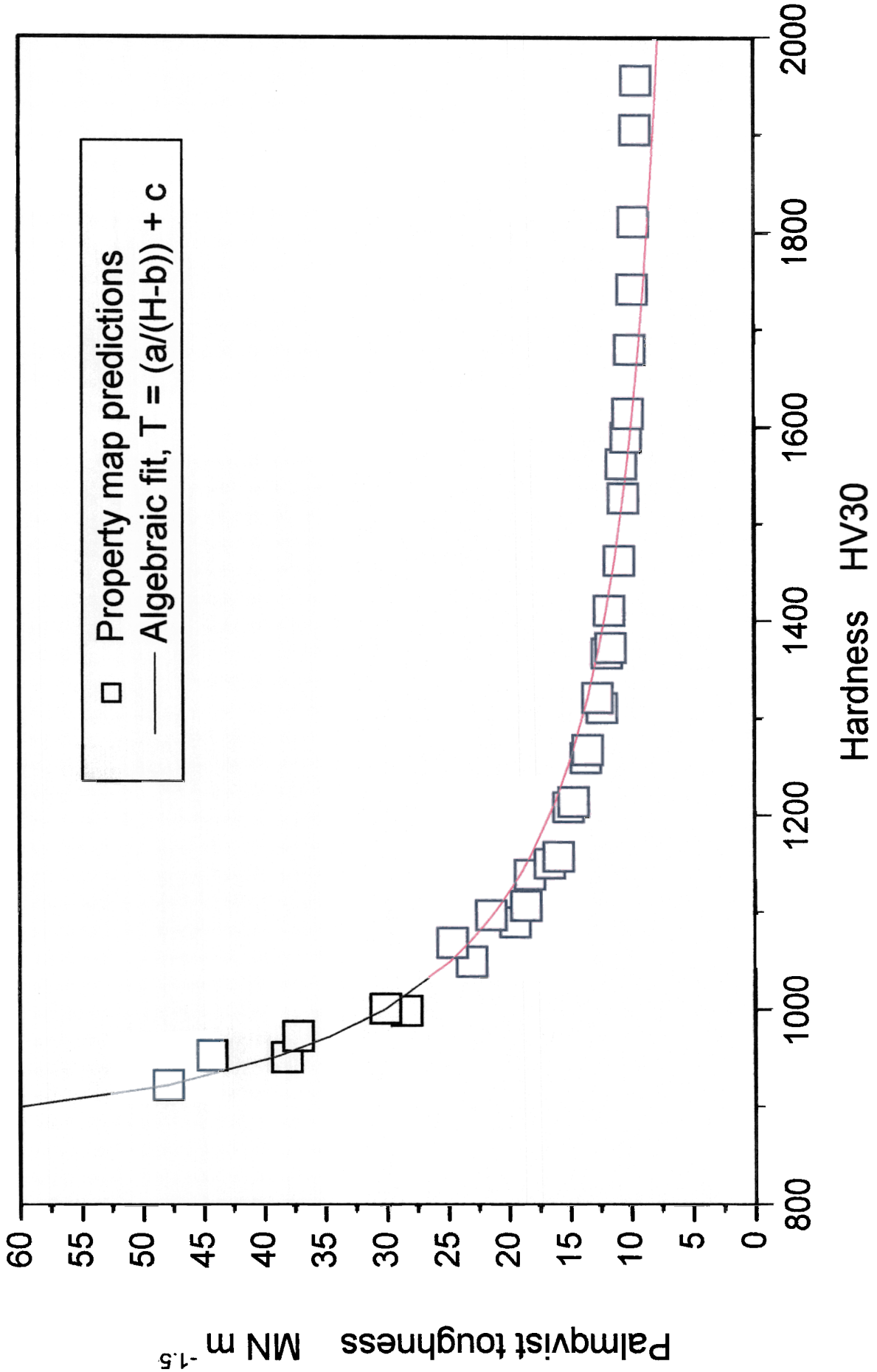


Fig 58 Empirical fit to Palmqvist toughness/Hardness results

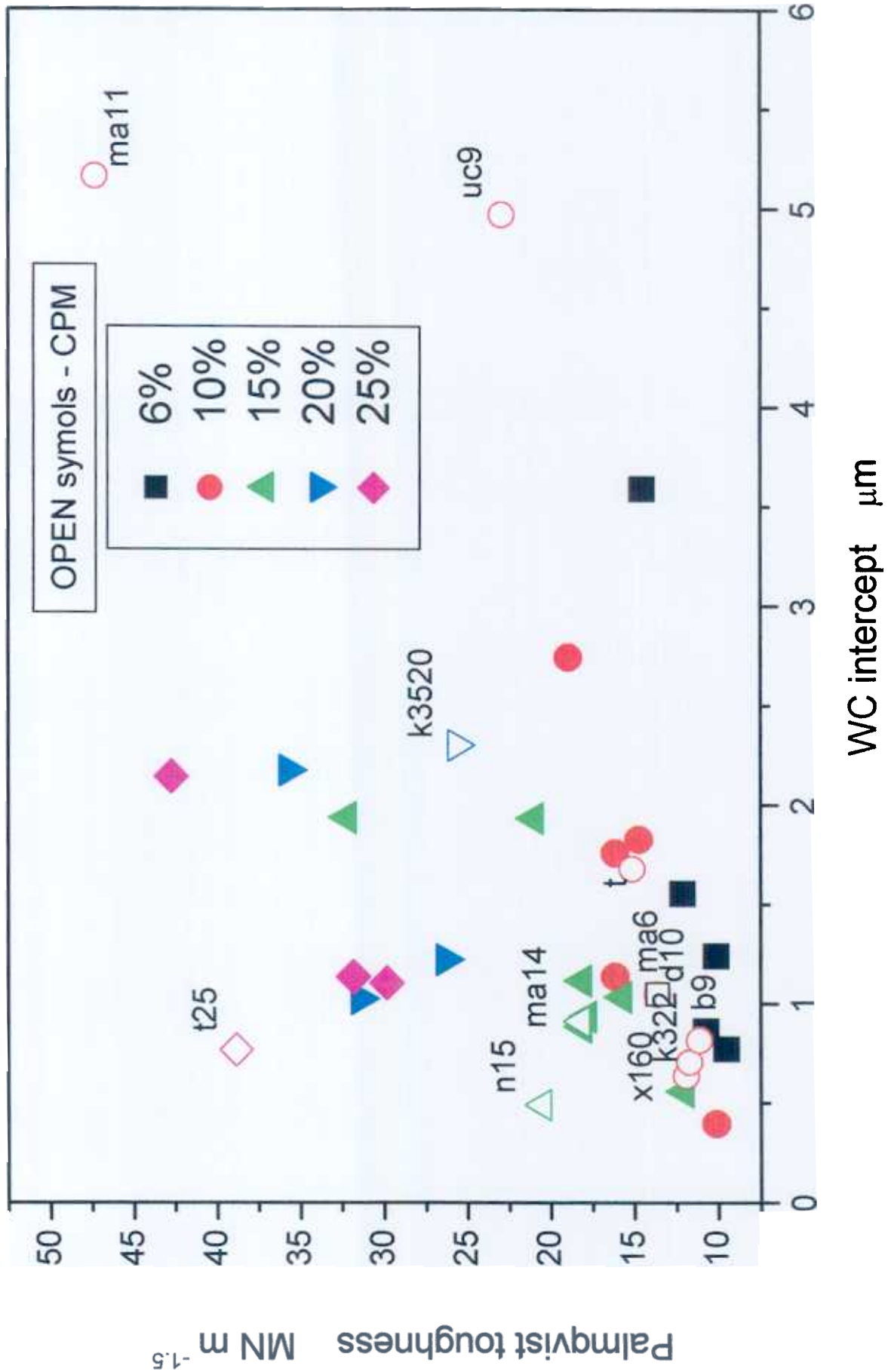


Fig 59 Palmqvist toughness data plotted against WC grain size

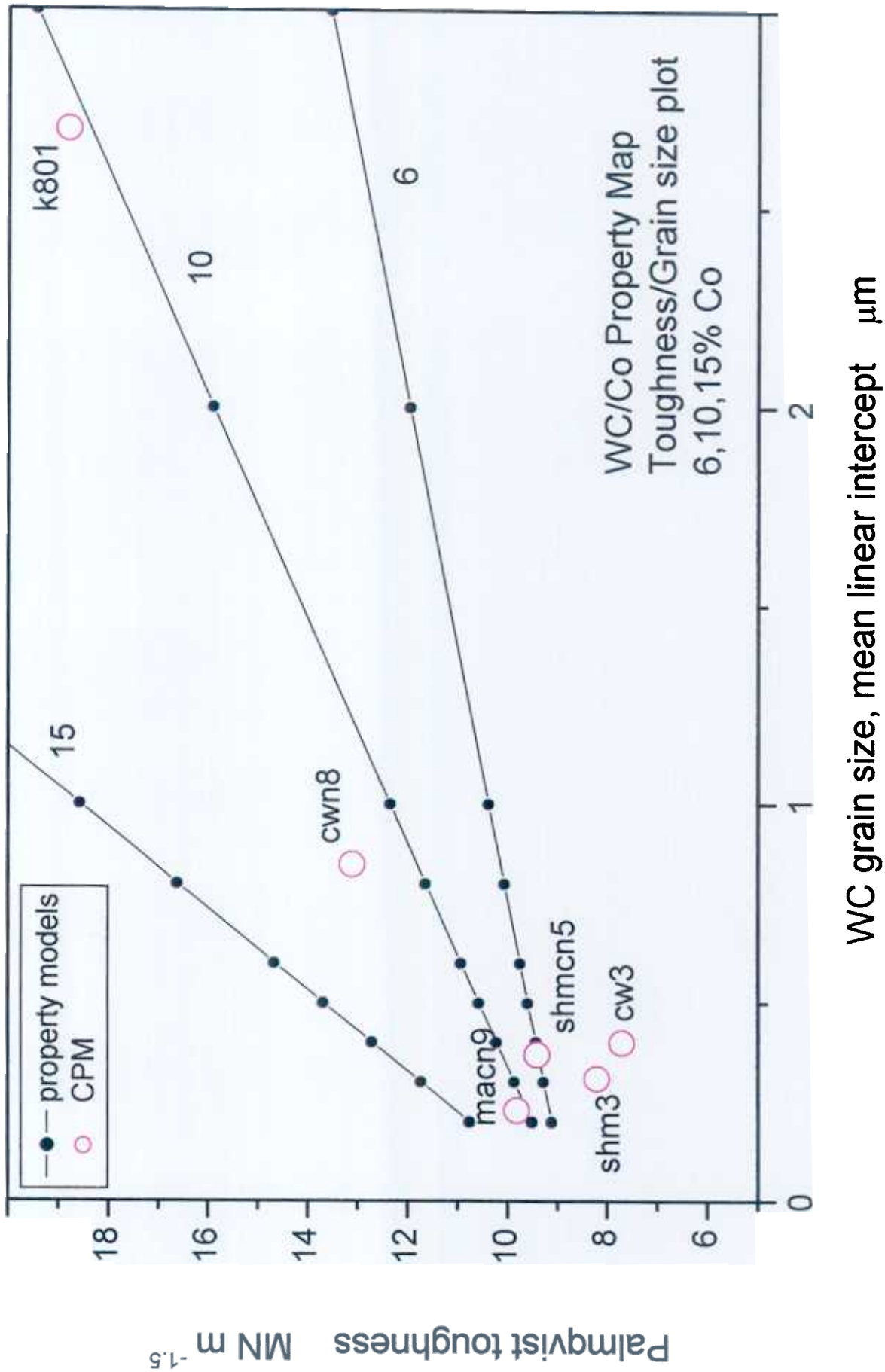


Fig 60 Palmqvist property map for non-standard CPM materials.

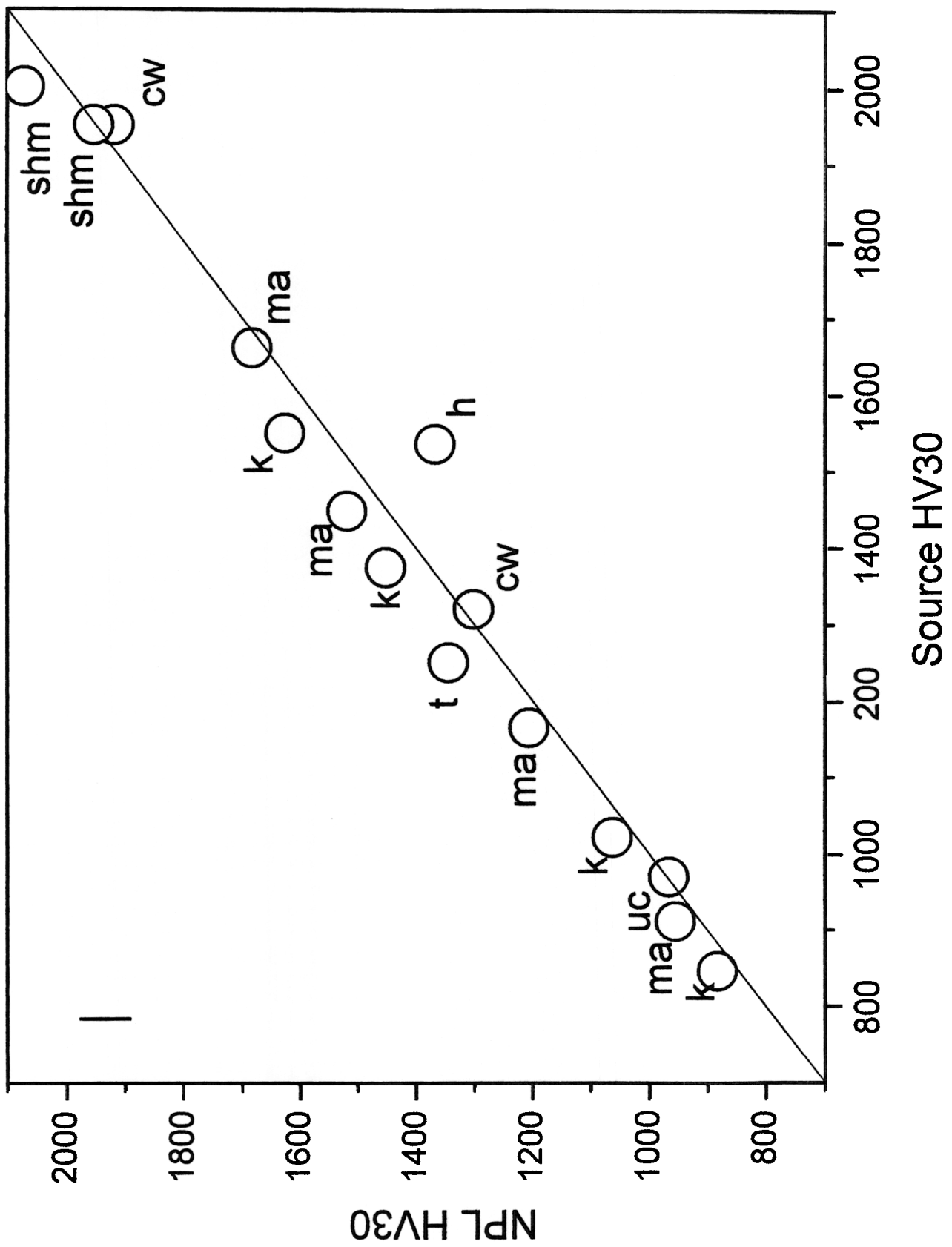
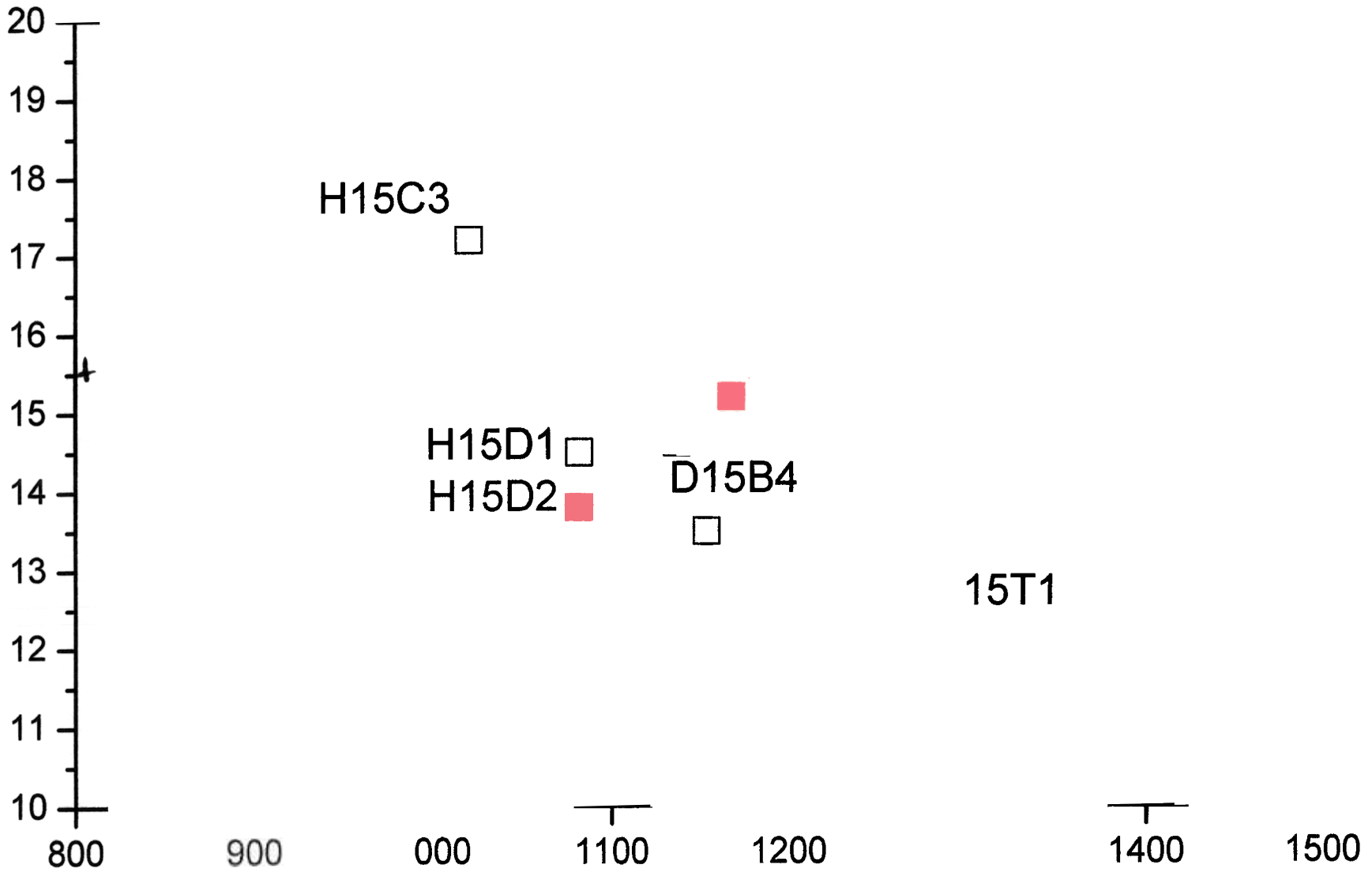
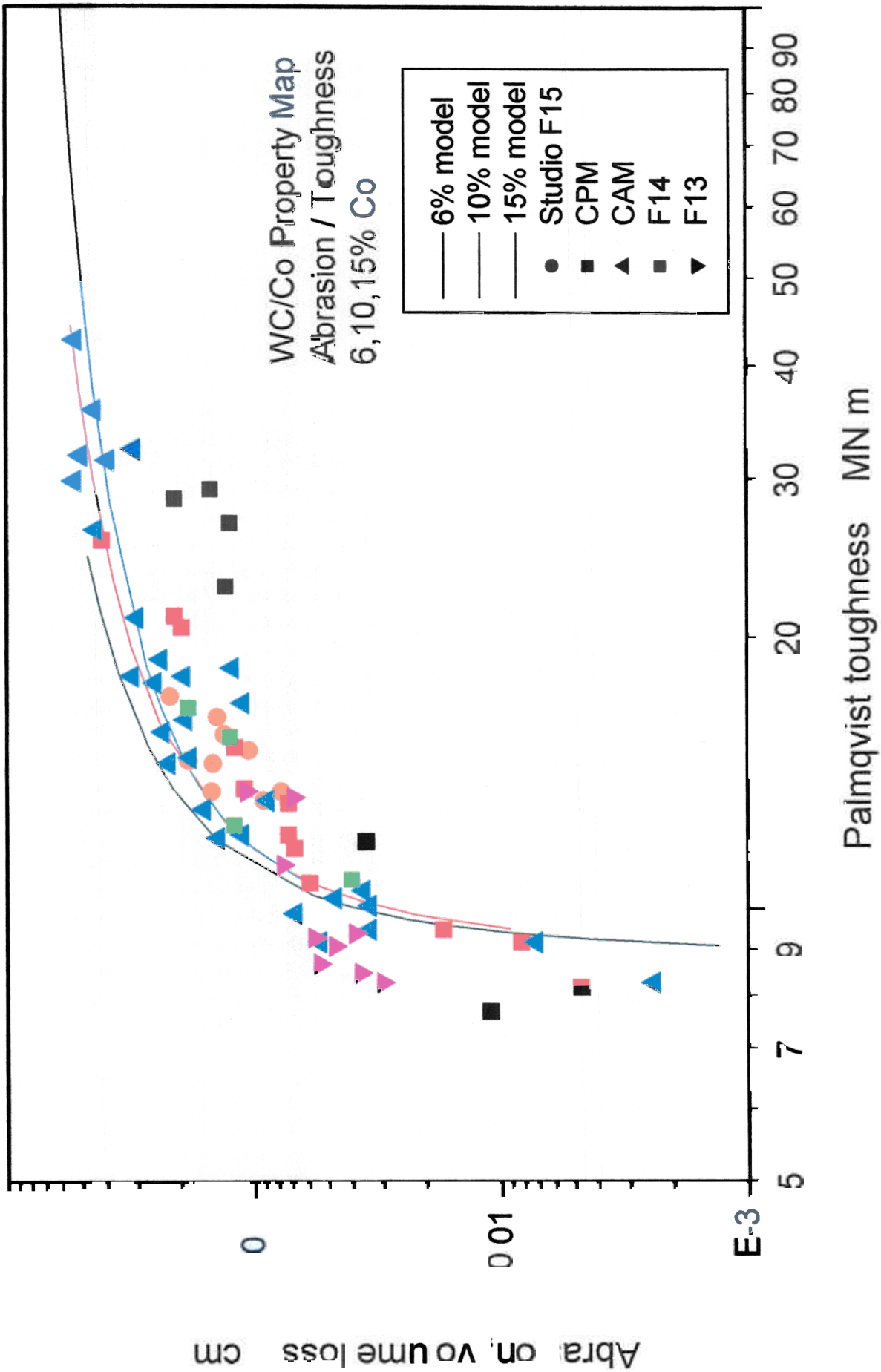


Fig 61 Comparison of NPL and source HV30 values



[Micro HM02/V1.7/BM]



F A asion/ hness property map base ine an wide gr ned hardmetal